

# A Survey on 5G Energy Efficiency: Massive MIMO, Lean Carrier Design, Sleep Modes, and Machine Learning

David López-Pérez, Antonio De Domenico, Nicola Piovesan, Harvey  
Baohongqiang, Geng Xinli, Song Qitao and Mérouane Debbah

## Abstract

Cellular networks have changed the world we are living in, and the fifth generation (5G) of radio technology is expected to further revolutionise our everyday lives, by enabling a high degree of automation, through its larger capacity, massive connectivity, and ultra-reliable low latency communications. In addition, the third generation partnership project (3GPP) new radio (NR) specification also provides tools to significantly decrease the energy consumption and the green house emissions of next generations networks, thus contributing towards information and communication technology (ICT) sustainability targets. In this survey paper, we thoroughly review the state-of-the-art on current energy efficiency research. We first categorise and carefully analyse the different power consumption models and energy efficiency metrics, which have helped to make progress on the understanding of green networks. Then, as a main contribution, we survey in detail—from a theoretical and a practical viewpoint—the main energy efficiency enabling features that 3GPP NR provides, together with their main benefits and challenges. Special attention is paid to four key technology features, i.e., massive multiple-input multiple-output (MIMO), lean carrier design, and advanced idle modes, together with the role of artificial intelligence capabilities. We dive into their implementation and operational details, and thoroughly discuss their optimal operation points and theoretical-trade-offs from an energy consumption perspective. This will help the reader to grasp the fundamentals of—and the status on—green networking. Finally, the areas of research where more effort is needed to make future networks greener are also discussed.

## I. INTRODUCTION

The living world is a unique and spectacular wonder. For 10,000 years, the average temperature of our planet has not increased or decreased by more than one degree Celsius [1]. The biodiversity

of the Holocene, together with this stationary climate, brought stability, settling the living world into a gentle, reliable rhythm —the seasons.

We invented farming, and with it, learnt how to master the seasons to produce large amounts of food crops. The history of all human civilization has followed, with each generation progressing with respect to its preceding one, mostly because the living world could be relied upon to deliver us the essentials we needed.

The industrial revolution and the automation of labour changed this natural rhythm of evolution, and since then, we have significantly transformed our living world [2]. After the Second World War, technology has developed faster than ever before. Automation is making our lives easier, and until very recently, it felt like nothing would limit our progress. However, we are starting to see the consequences of unsustainable progress now [3].

From 1937 to 2019, the world population has grown from 2.3 to 7.7 billions [4], and our modern transport, agricultural, manufacturing and life styles have sharply increased energy consumption. As a consequence, the amount of carbon in the atmosphere raised from 280 to 409 parts per millions in such time period [5], and the levels of greenhouse gas (GHG) emissions reached the historical record of 37.5 gigatonnes of carbon dioxide equivalent ( $\text{CO}_{2e}$ ) in 2018, —a 1.5 % increase with respect to 2008 [6]. If our societies do not significantly change the manner in which we consume energy, this level may reach 47.5 gigatonnes of  $\text{CO}_{2e}$  by 2030, and the outcomes could be catastrophic [7].

Indeed, this increase of GHG emissions, combined with current trends on deforestation, are contributing to global warming —the rise of the average Earth surface temperature [8]. This temperature rose 0.6 to 0.9 degrees Celsius between 1906 and 2005, and the rate of temperature increase has nearly doubled in the last 50 years [9] [10]. Alarming, an increase in the Earth's temperature of 1.5 to 2.0 degrees Celsius, above pre-industrial temperatures, has been estimated to be a threat to most natural ecosystems on Earth today, with the resulting dramatic effects on our planet, and in turn, on our everyday lives [11]–[14].

To address this challenge, international policymakers are targeting a dramatic increase in energy efficiency, and a sharp shift from fossil fuels to renewable sources of energy, such as solar, wind, and water. This will entail a completely new approach to the generation and use of energy, which must be adopted by every government, industry, business, and individual.

In the following, we review the important role that the fifth generation (5G) of mobile technology will play to revert the unsustainable energy consumption trend, and survey, in the rest

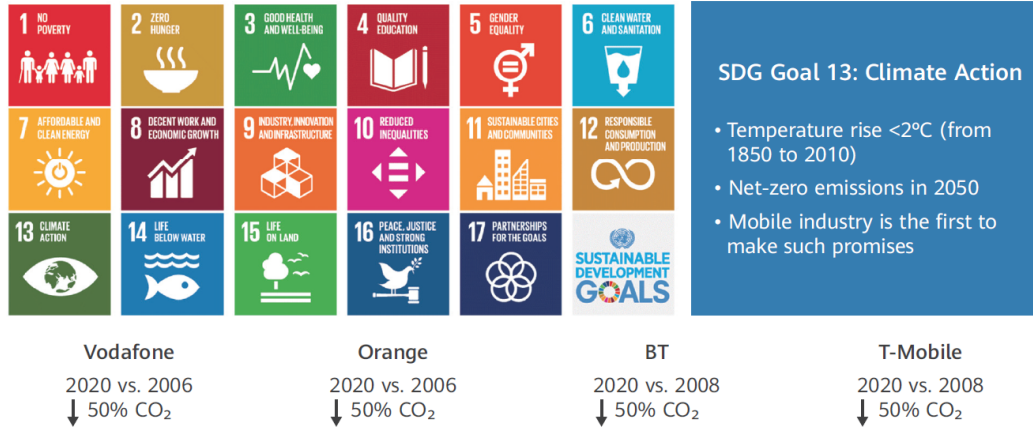


Figure 1. Wireless industry client action goals [15].

of the paper, the technical innovations that the third generation partnership project (3GPP) new radio (NR) specification brings in terms of energy efficiency—from a theoretical and practical viewpoint—with respect to previous ones to support such change.

#### A. The Enabling Role of 5G

Governments and industries have set—or are setting—ambitious targets to reduce their GHG emissions and help dealing with global warming. To date, 77 major economies have already establish a net-zero GHG emission target by 2050, and their industries are accordingly (re)defining their energy efficiency and consumption road maps. In this regard, the telecommunication sector has taken the lead—and an exemplary role—, setting stringent requirements for both the energy efficiency and consumption of their networks, together with a clear road map to achieve them (see Fig. 1) [15].

Enhancing the energy efficiency and reducing the energy consumption of 5G networks will help reducing GHG emissions. Their enabling effect, however, will be—without doubt—the most important contribution of the mobile industry to address the current climate change [16].

At a macro-scale level, the new 5G technology enables a new type of networking capability able to connect for the first time both everyone and everything together, including machines, objects, and devices, thanks to its higher capacity, lower latency, improved reliability, and larger number of supported connections Please refer to Fig. 2 for a comparison between 5G and fourth generation (4G) specification capabilities. These new 5G communication capabilities are

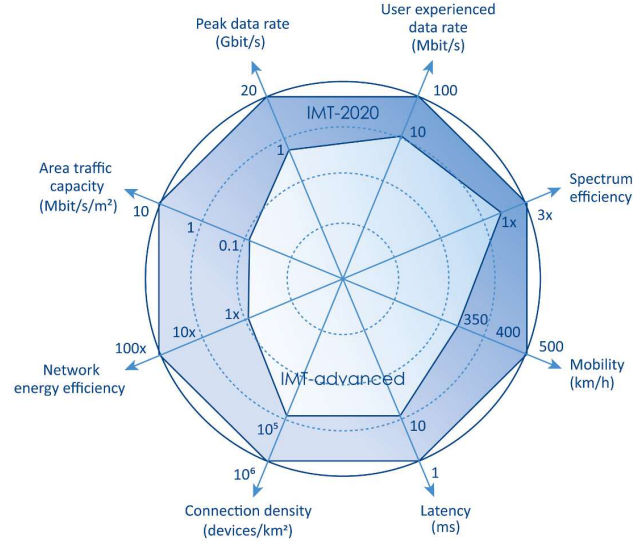


Figure 2. Comparison of key capabilities of IMT-Advanced (4G) with IMT-2020 (5G) according to [18].

already helping governments, current industries, and new forms of businesses to implement novel processes with improved effectiveness, by supporting a more flexible, tailored, and efficient use of resources.

Importantly, 5G has already become an integral part of governmental and industrial energy efficiency and consumption programs, as it is envisioned that an intelligent exploitation of resources will enable a significant decrease of GHG emissions through different avenues, for example *i)* an improved support for smart city and building energy management, *ii)* reduced requirements for office space and business travel, and *iii)* efficient just-in-time supply chains enabled by predictive analytics, to cite a few [17].

To give some idea of the magnitude and importance of this enabling effect, it should be noted that, according to the International Telecommunication Union (ITU) SMART 2020 report [19], the enabling effect of mobile communications alone was estimated to be around 2,135 million tones of CO<sub>2e</sub> in 2018, and that according to [20], the scale of it will increase in the 5G era, where the enabling effect across all the information and communication technology (ICT) sector was predicted to be equivalent to 15 % of all global emissions by the end of 2020.

Recent reports indicate that industries, such as transportation, health care, and manufacturing, are already significantly benefiting from such 5G enabling effect. For example, through smart city programs and 5G-related innovations, London, Berlin, and Madrid have already reduced GHG

emissions of motor vehicles by 30 % each from their peak rates, and Copenhagen by 61 % [21]. The ultra-reliable low-latency communication (URLLC) capabilities of 5G can also lead to autonomous driving, optimizing the route as well as the fuel and break control. which will further reduce the fuel consumption of vehicles [22]. In China, 5G-enabled remote computed tomography has eliminated the need for the road and/or air travel associated with expert consultation sessions, thus reducing by 99 % the GHG emissions of this health care sector [23]. Some smartphone manufactures, to give another example, are also using 5G-connected artificial intelligence (AI) cameras to perform quality inspections before smartphones are packaged, which has reduced by 6 % the energy consumption of the per-unit smartphone production [17].

To further assess the of breath and depth of the enabling effect of 5G networks, interested readers are refereed to [16], and references there in.

### *B. The 5G Energy Efficiency Challenge*

Unfortunately, the 5G enabling effect is no free lunch. In fact, it comes at the expense of a tremendous challenge for the telecommunication sector in terms of both carried data and energy consumption.

Allowing governments, industries, businesses, and individuals in general to increase their energy efficiencies and reduce their energy consumption through more flexible, tailored, and efficient operations via a telecommunication network entails

- a dramatic growth of data usage in some scenarios, and
- the need for more sophisticated networking to meet the required low-latency, high-reliability, and/or large volume of data connections in some others.

Confirming such challenge, recent studies already indicate that, by 2030, the number of connected devices is expected to grow to 100 billion [24], and that 5G networks may be supporting up to 1,000 times more data than 4G ones did in 2018 [17].

Importantly,

- to reach their established energy efficiency and consumption targets, and
- reduce their energy bills, up to 40 % by 2030 [17], to make their businesses profitable,

mobile network operators (MNOs) will need to meet the aforementioned more challenging traffic demands and requirements with significantly reduced GHG emissions with respect to those of today's 4G networks.

Considering these two aspects, the 3GPP NR stakeholders have already called for a 90 % reduction in energy consumption compared to 4G long term evolution (LTE) [25]. However, whether these gains can be realised or not in practical networks will not only depend on what the new specification can do and/or the energy performance of a single site, but also on how the actual network is deployed and operated as a whole.

In fact, to support the growing use of 5G connectivity and its more stringent requirements, while reducing energy consumption on a per-bit basis through an intelligent use of the network, changes are needed at all levels of it to achieve the maximum holistic effect. MNOs must thus embrace new approaches to network planning, deployment, management, and optimisation that have energy efficiency at heart, and are implemented end-to-end. Without energy efficiency driving future deployments, the study in [26] indicates that a 5G network, despite of its enhanced energy efficiency in bits per Joule due to its larger bandwidth and better spatial multiplexing capabilities, could typically consume over 140 % more energy than a 4G one, with similar coverage area. This unwanted energy consumption arises from 5G's greater density of base stations (BSs), antennas, cloud infrastructure, and user equipment (UE), among others.

To address this challenge, and better understand where the energy consumption could be meaningfully reduced in a 5G network, thus helping MNOs to take educated decisions, the authors of [17] put together an interesting analysis, reporting that the most consuming elements of the network in terms of energy are the BSs. They currently account for about 57 % of the total network energy consumption [27]. By 2025, that figure should be lower, as 5G becomes more prevalent, but the radio access network (RAN) will still be the biggest consumer of energy in the network, a 50.6 % according to [28] (see Fig. 3).

Within a BS itself, the radio frequency (RF) equipment i.e., the power amplifier plus the transceivers and cables, have been identified as the largest energy consumer, typically using about 65 % of the total BS energy. The cooling system, the digital signal and base band processing as well as the alternating current (AC)-direct current (DC) converters follow with an energy consumption of around 17.5 %, 10 %, and 7.5 %, respectively.

In this line, 5G can be —and has been— improved for a better energy efficiency. More efficient power amplifiers have been developed, renewable energy sources for powering on-grid and off-grid sites, including solar power, are starting to be widely adopted. Moreover, smart lithium batteries are becoming an integral part of any 5G site to enhance energy management, and liquid cooling is being implemented to reduce the need for air conditioning [17].

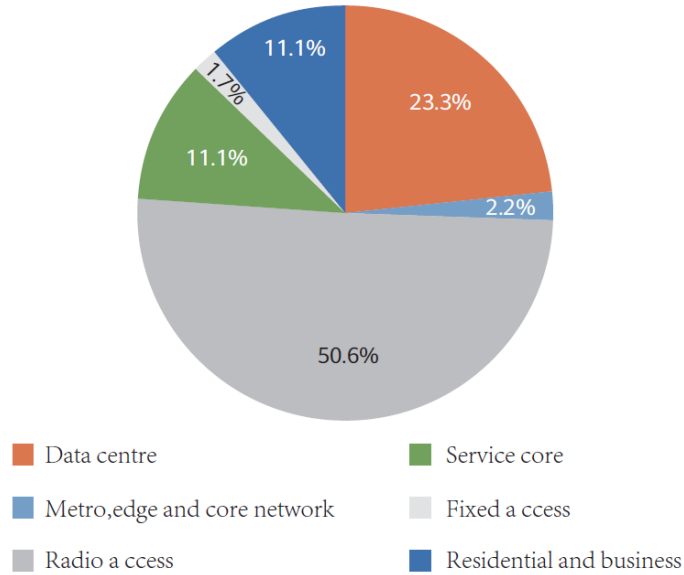


Figure 3. Energy consumption breakdown by network element in 2025 [28].

Importantly, since the BSs —and their RF equipment— consume most of the energy at a 5G network, we must advocate for a judicious networking [29]. BSs must thus only be active —and consume energy— when handling actual data. Plainly speaking, the Joules consumed should 'follow' the bits transmitted. As a result, and in contrast to 4G, the amount of always-on signalling in next generation networks must be greatly minimised at all cost. It is also equally necessary that data —and its related signalling— are transmitted to/received from the intended UEs while consuming the minimum possible energy to meet their required quality of experience (QoE) [30]. Avoiding the resource waste occasioned by the over-provisioning of QoE is essential to significantly reduce the GHG emissions of 5G networks.

To realise such network-wide energy efficient operation, the 3GPP NR specification [31] *i)* has been redesigned and developed using a new and more flexible user-centric principle [32], and *ii)* provides support for a number of new technology features that help reducing energy consumption at a network level. The unique 3GPP NR power saving technologies are:

- massive multiple-input multiple-output (mMIMO),
- lean carrier design,
- advanced sleep modes (ASMs), and
- artificial intelligence.

The good understanding of these features, how they enable energy efficiency and their optimal

operation points in such terms are the main focus of this survey.

### *C. Comparison to previous 5G Energy Efficiency Surveys*

Several surveys have been already published on energy efficiency and related aspects during the last 10 years. In the following, we describe the most relevant ones.

In [33], the authors have surveyed the goals set by the United Nations (UN) for sustainable development, where among others, urgent actions to combat climate change are called upon. Importantly, the wide variety of opportunities in the ICT sector for enabling energy efficiency have been highlighted, but although of relevance to understand the current scene, this survey did not touch on the particularities of wireless networks. The survey in [34], instead, has focused on green wireless networks, and has explained at a high level—and an introductory form—how different metrics such as energy efficiency, spectral efficiency, throughput, and delay relate to each other. The discussion has been organised around the open systems interconnection (OSI) layers, and has presented an exhaustive summary of the different frameworks and techniques that can be used to achieve optimal networking trade-offs in practical networks. Descriptions, however, are only qualitative, and lack of detail. For example, the paper has considered a simple power consumption model in most explanations, which only accounts for the transmit power, and has neglected the power consumption of equipment hardware. With a similar scope, the authors in [35] have surveyed the literature around the understanding of fundamental energy performance trade-offs, i.e., energy and deployment efficiency, energy and spectral efficiency, bandwidth and power as well as delay and power, this time, however, from a more focused cellular perspective, covering both 3GPP universal mobile telecommunication system (UMTS) and LTE aspects. Importantly, this paper has brought the attention to the importance of accurate BS power consumption models. Based on this work, the authors in [36] have further surveyed techniques to optimise the above mentioned four trade-offs, while putting the spotlight on the potential benefits of two features, i.e., multiple-input multiple-output (MIMO) and relay. With a more 3GPP LTE standard focus, the survey in [37] has provided an in-depth review on green aspects, discussing advancements in power amplifier technology, 3GPP LTE protocols for carrier shutdown and micro sleeps, as well as the potential benefits of small cell networks. On a forward looking note, the authors have also put forward cognitive radio and cooperative relaying as energy saving enabling technologies, and share the latest developments in these areas. Complementarily, the authors in [38] have surveyed the efforts of different academic and industry projects on energy efficiency,



emphasizing how to make use of daily network traffic variations and various quality of service (QoS) requirements to save energy at the network level. Several deployment strategies, such as cell-size, heterogeneous networks, cooperative communications and network coding, have been also discussed, together with their merits and challenges. On a similar note, in [39], a complete survey on 3GPP metrics and power consumption models for energy efficiency analysis can be found, with a detailed formulation of the most relevant energy efficiency trade-offs. An exhaustive—and critical discussion—on standardised features for energy-aware management in 3GPP LTE cellular networks from a broadband networking point of view has been also provided. In [40], the authors have turned the focus on the survey of efficient resource management schemes, which are capable of controlling how much of the network infrastructure is actually needed in a given space-time and which parts can be temporarily powered off to save energy. The survey includes both cellular- and Wi-Fi-based algorithms. Focusing on more modern applications, the work in [29] has overviewed the challenges brought by the big data era, describing issues and solutions around energy efficient data acquisition, communication, storage, computation, and analytics. Discussion on the necessity of avoiding radio resource waste to reduce energy consumption in wireless networks has been at the core of the survey, and four types of schemes have been surveyed in this line, i.e., power control, time-domain scheduling, spatial resource allocation, and spectrum sharing.

Unfortunately, it should be highlighted that any of the above mentioned surveys has gone into the specifics of 3GPP NR. They are either generic or 3GPP LTE focus, and as a result, they did not survey the assets of this new technology generation to harvest energy savings.

Giving a more related 5G perspective, the authors in [41] have provided guidelines for the development of energy efficient related features in 3GPP NR, and surveyed the literature around the user-centric concept of *no more cells*. This networking paradigm would enable energy efficiency through a flexible network comprised of heterogeneous cells, decoupled signal- and data-planes as well as downlink and uplink. A dynamic cloud radio access network (C-RAN)-based configuration has also been proposed to handle spatial and temporal mobile traffic variations without energy over-provisioning. In this paper, the potential of both mMIMO and full duplex features in 5G for power savings has been also surveyed, while considering hardware issues. In the same line, the work in [42] has provided an overview of the latest research on green 5G techniques. The authors have explored ultra-dense sub-6GHz and millimetre wave networks, unlicensed spectrum as well as device to device (D2D) and mMIMO communications, while

analysing their potential energy efficiency improvements, as well as circuit power consumption issues. As a main contribution, energy harvesting has been presented as fundamental to meet 5G green requirements, and the different lines of work in this have been discussed (e.g., renewable, RF energy harvesting). Taking a more theoretical and systematic approach, the authors in [43] have extended their work in [35], surveying energy efficient solutions for 5G networks using the aforementioned fundamental green trade-offs as a driver. This overview has been around three main pillars, i.e., non-orthogonal access, mMIMO, and heterogeneous networks. Importantly, the paper concludes that mMIMO is the most effective approach to enable high energy efficiencies, provided that issues around channel state information (CSI) acquisition, transceiver hardware impairments, and power inefficient components are addressed. A large number of references has been also provided around channel and carrier shutdown techniques for dense small cell networks, and the implications of centralised versus distributed network architectures have been discussed. With a more practical—but still vanilla—5G perspective, the authors in [44] provide a comprehensive survey on how machine learning (ML) can be used to address the energy efficiency challenges encountered in generic 5G networks. Finally, the recent survey in [45] has provided the most up-to-date overview on power saving techniques supported by the 3GPP NR standard, covering developments in Release 15 and 16, and the potential upcoming ones in Release 17. Such overview, however, has mainly focused on—and evaluated—UE power saving mechanisms, such as bandwidth parts, radio resource control (RRC) inactive state, discontinuous reception (DRX) mechanism, wake up signaling, cross-slot scheduling, and MIMO layer adaptation. At the network side, the lean carrier and discontinuous transmission (DTX) concepts together with that of dormant cells, have been only briefly touched upon.

As it can be derived from the previous summary, most of the existing energy efficiency surveys were written in a pre-5G era before the 3GPP NR existed/matured, or have a strong focus on the UE—and not on the network—side.

#### *D. Objective and Structure of this Paper*

In this survey paper, contrary to the previous ones, which speculatively discussed what 5G could be in terms of energy efficiency, we provide for the first time a detailed, up-to-date overview of the main practical 3GPP NR features that are currently used—or can be further leveraged—to increase the energy efficiency of practical 3GPP NR networks. The survey covers the role of mMIMO, the lean carrier design, ASMs, and ML in providing energy savings in macro

Table I  
SUMMARY AND COMPARISON OF THE MOST RELEVANT ENERGY EFFICIENCY SURVEYS.

Ref.	Year	Tech. era	Contribution/techniques	Gaps
[33]	2018	ICT	Surveys UN frameworks for sustainable development	No cellular or ML related.
[34]	2016	General wireless	Surveys green metrics and performance trade-offs.	No 5G or ML related.
[35]	2011	3G/4G	Surveys green metrics and performance trade-off.	No 5G or ML related.
[36]	2011	4G	Surveys green performance trade-off optimization. Explores MIMO and relay features.	No 5G or ML related.
[37]	2011	4G	Surveys 3GPP LTE green protocols. Focuses on carrier shutdown, and micro-sleep features. Explores cognitive radio, and cooperative relaying.	No 5G or ML related.
[38]	2013	4G	Surveys green academic and industry projects, and energy minimization under UE QoS constraints. Explores heterogeneous networks, cooperative communications, and network coding features.	No 5G or ML related.
[39]	2014	4G	Surveys 3GPP green metrics, power consumption models, and 3GPP LTE protocols. Detailed formulation of energy efficiency trade-offs.	No 5G or ML related.
[40]	2014	4G and Wi-Fi	Surveys energy efficient resource management schemes (with focus on Network and MAC layers).	No 5G or ML related.
[29]	2018	Big data era and 4G	Surveys the challenges brought by the big data era. With respect to cellular, surveys MAC layer power control, time-domain scheduling, spatial resource allocation, and spectrum sharing green protocols.	No 5G or ML related.
[41]	2014	Pre-5G	Surveys potential 5G energy efficiency features. Explores the user-centric concept, downlink and uplink split C-RAN, mMIMO, and full duplex features.	Guesses what 5G could be. No 3GPP NR or ML related.
[42]	2017	Pre-5G	Surveys research on green 5G techniques. Explores ultra-dense sub-6GHz and millimetre wave networks, unlicensed spectrum as well as D2D, mMIMO, and energy harvesting features.	Guesses what 5G could be. No 3GPP NR or ML related.
[43]	2017	Pre-5G	Surveys green metrics and performance trade-offs. Explores non-orthogonal access, mMIMO, and heterogeneous networks.	Guesses what 5G could be. No 3GPP NR or ML related.
[44]	2020	5G generic	Surveys how ML can be used to address 5G energy efficiency challenges.	No 3GPP NR focus. Lack of detail.
[45]	2020	5G	Surveys power saving techniques supported by the 3GPP NR standard (Rel.15/16) with focus on UE	Does not cover network aspects or ML techniques.

5G deployments, from both a theoretical and practical perspective, and highlights their still to be addressed challenges. Importantly, this survey provides detailed descriptions, including the formulation of BS power consumption models and energy efficiency metrics currently used for energy efficiency optimisation, as well as the bounds, the trade-offs, and the optimal operation points derived in the literature, making this a self-contained paper. The important role to be played by ML and data-driven in terms of energy efficiency is also surveyed for the first time. Areas of research which require further efforts are also discussed.

The rest of this survey paper is organised as follows (see Fig. 4):

- In Section II, we introduce mMIMO, the lean carrier design, ASMs and ML as energy efficiency enabling features in 3GPP NR;
- In Section III and Section IV, we present and discuss in detail existing BS power consumption models and metrics used for energy efficiency optimisation, respectively;
- In Section V, we overview the current theoretical understanding of mMIMO in terms of energy efficiency from a single and a multi-cell perspective and from a uplink and downlink viewpoint. Current bounds and trade-offs with other key performance indicators are formulated and explained, and the most relevant optimisation frameworks to enhance energy efficiency via mMIMO are surveyed;
- In Section VI, we dive into the details of the lean carrier design, and highlight the importance of ASMs and their optimisation at different levels (i.e., micro sleeps, carrier, and channel (antenna) shutdown);
- In Section VII, we highlight the potential of spatio-temporal traffic predictions and ML approaches to maximize energy efficiency, and overview the research in this area;
- Finally, in Section VIII and IX, we discuss future research directions and draw the conclusions, respectively.

## II. 3GPP NR ENERGY EFFICIENCY RELATED FEATURES

To reach the ambitious targets of 5G networks in terms of capacity, latency, reliability, number of supported connections, and energy efficiency, the 3GPP NR specification presents a paradigm shift with respect to any preceding cellular technology [32].

In comparison with 3GPP LTE and with regard to energy efficiency, 3GPP NR introduces a new beam-centric —or mMIMO-centric— design, which enables both

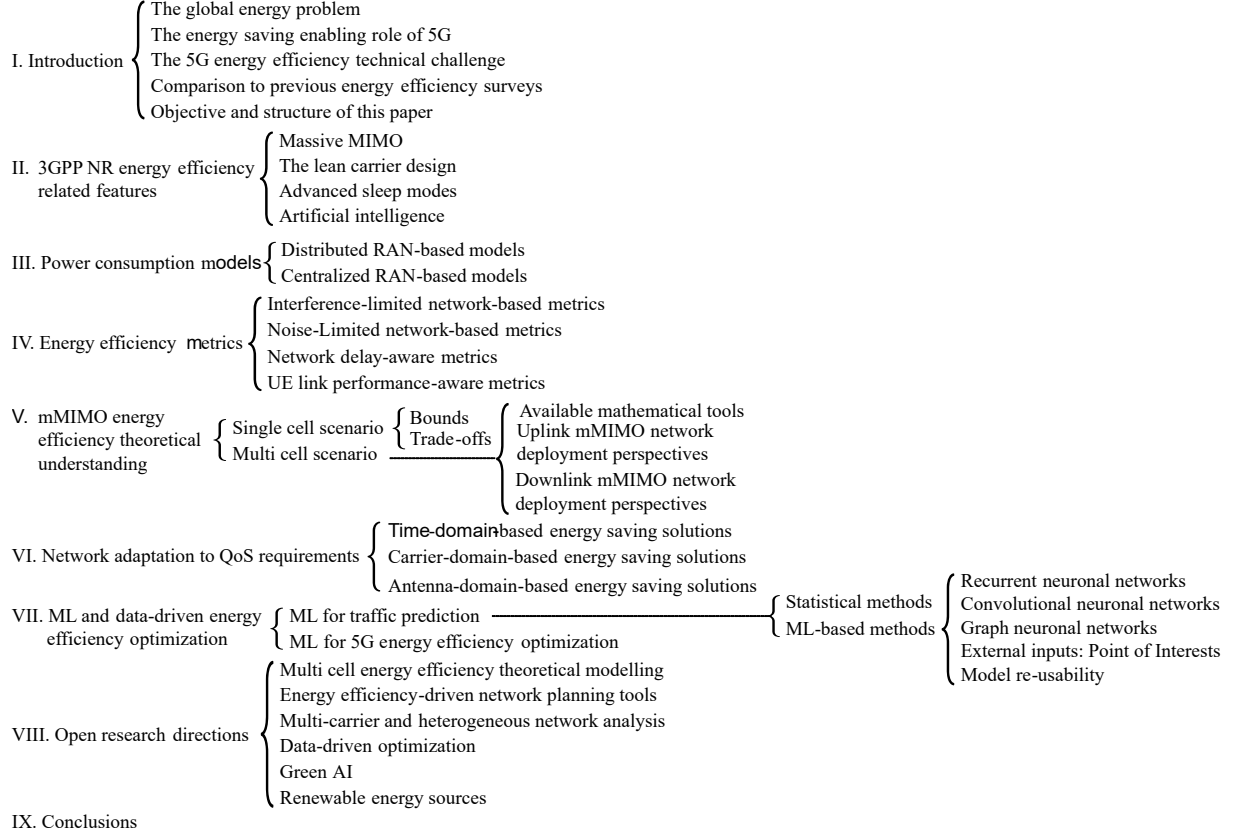


Figure 4. Outline and structure of this survey.

- an extensive use of beamforming through a massive number of antenna elements, not only for data transmissions, but also for control-plane procedures, such as the initial access [46], and
- a larger spatial multiplexing of information on a given time-frequency resource.

Such beamforming gains allow for a reduced transmit power to reach a given targeted distance and/or meet a given QoE at the UE, with the potential consequent benefits in terms of interference mitigation and energy savings [47].

Moreover, 3GPP NR follows a new ultra-lean design principle, in which control signals are not consistently transmitted in every radio frame, but on demand, based on traffic requirements [48]. This ultra-lean design allows for a more efficient operation of the mMIMO-centric design, and facilitates ASM support, i.e., BS wake-up/sleep, including symbol, channel, or carrier shutdown, which can significantly reduce energy consumption [49].

3GPP NR enhancements also allow for a more distributed architecture, which facilitates the

usage of AI to assist network optimisation through a centralised data gathering and processing—the mentioned required intelligence [50]. In this line, the current 3GPP NR architecture already introduces new functions in the core and the management domains, i.e., the network data analytics function (NWDAF) and the management data analytics function (MDAF), which can either run analytics on collected data or enhance the already supported network functions with statistics collection and prediction capabilities [51] [52]. Given the increased complexity of 5G networks, further leveraging 5G network data and ML will be necessary to derive optimum network-wide energy efficient operation policies [53].

In the following, we introduce the main concept behind these 3GPP NR features, whose proper optimisation will be key to minimise network energy consumption. We will further elaborate on their details and potential energy saving abilities in the rest of this paper.

#### A. *Massive MIMO*

Full dimension MIMO—generally refereed to as mMIMO—is probably one of the most important developments in 3GPP NR [46]. Plainly speaking, mMIMO refers to a technology feature where BSs are equipped with antenna arrays comprised of a large number of antenna elements [54]. At higher frequency bands, due to their more challenging propagation conditions, the large number of antenna elements are primarily used for beamforming to extend coverage. At lower frequency bands, the focus of this survey, in addition to leverage beamforming gains, the large number of antenna elements is readily used to enable extensive spatial multiplexing and interference mitigation by spatial separation [55] [56]. In more detail, the large mMIMO antenna array can excite a plurality of channel sub-spaces to support multiple simultaneous transmissions to—or receptions from—several UEs. In this way, the network capacity can potentially linearly grow with the number of spatial streams multiplexed. Due to the channel hardening effect, mMIMO is also more robust against wireless channel fluctuations, which simplifies its operation [57].

3GPP NR provides extensive support for mMIMO operation. Channels and signals, specially those used for control and synchronization, have been re-designed with respect to 3GPP LTE to natively use beamforming. The acquisition of CSI for the large number of antenna elements in a mMIMO BS is now supported through *i)* new UE CSI reports estimated over channel state information-reference signals (CSI-RS) in the downlink, or *ii)* channel measurements over

sounding reference signals (SRSs), exploiting channel reciprocity, in the uplink. Among others, 3GPP NR is also providing new functionalities to support analog beam-forming as well as digital precoding [58].

Although mMIMO was primarily designed with the objective of maximising achievable rates, studies have shown that mMIMO is also suited for maximising energy efficiency and minimising energy consumption. For example, the large number of antenna elements at mMIMO BSs can be used to increase the transmission rates, while keeping constant the transmit power at the mMIMO BS. This results in shorter active transmission periods, and is possible since the large number of antenna elements facilitates achieving unprecedented spatial resolutions, simultaneously diminishing harmful communication effects, such as the channel noise or the inter-user interference [47] [59]. Thanks to its beamforming gain, mMIMO is also able to minimise the transmit power required to achieve a given UE QoE, e.g., average UE throughput, at a given distance, which also reduces the BS energy consumption.

In Section V, we provide a detailed survey and analysis of the energy efficiency benefits and trade-offs of this important 5G feature —mMIMO— in both single- and multi-cell setups.

### *B. The Lean Carrier Design*

In previous generations, signals for BS detection, broadcast of system information, and channel estimation were always-active and transmitted over the air, regardless of whether the BS was serving UEs or not [60]. It is important to note that, while these always-active signals facilitate UE operations —as UEs always have signals to rely on—, they also

- result in a large overhead in dense deployments,
- introduce inter-cell interference to other cells, thus reducing the achievable throughput,
- reduce the battery lifetime of the UE, and
- worsen the energy efficiency,

thus, becoming a burden to efficient network operation.

In 3GPP NR, many of these procedures have been revisited, following a new lean carrier design [48]. In general, following the DTX concept [61], when the traffic load of a cell —or group of them— is low, or the mobility conditions of the UE allows, larger signaling cycles can be selected. This makes the carrier signalling transmission more sparse —leaner—, thus reducing overhead, mitigating interference, and saving energy. To accommodate for such longer

signalling cycles, cell search and association as well as CSI procedures at both the BS and UE side have been accordingly redesigned in the new specification.

In Section VI, together with the use of ASMs, we survey and discuss how the lean carrier benefits energy efficiency.

### *C. Advanced Sleep Modes*

Cellular networks are usually planned and deployed to meet certain requirements, where coping with the traffic needs at the peak hours usually leads to an over-dimensioning of the network for the less challenging traffic loads [62]. As the traffic pattern fluctuates over both time and space, underutilized BS resources can be dynamically turned off to save energy. The more network components that are shutdown and the longer the time that they are shutdown, the more energy can be saved [63].

Importantly, the less required always-active signalling of a lean carrier allows for longer micro-sleeps in the presence of bursty traffic. This micro-sleeps can last for hundreds of microseconds or even seconds, and when coupled with traffic shaping and efficient hardware at the BS able to power up and down in fractions of a millisecond, they can be leveraged to allow deeper sleep modes, further saving energy [64].

Most of the improvements that a network can achieve by appropriate management, however, do not lay on the micro-sleep space, as these sleep periods are only opportunistic and generally short. To enable longer BS resource deactivation times, and achieve larger energy consumption reductions, more advanced mechanisms are required, able to leverage knowledge on UE distributions and their requirements in terms of QoE.

Such tailored resource management according to the UE demands at a macro-time scale will avoid the resource waste emanating from the over-dimensioning of the network to meet peak hour needs. Provided with such UE-related information, not a single BS, but the entire network can be configured—and reconfigured—to operate with the minimum set of resources necessary to satisfy the active UEs' QoE on a semi-dynamic basis [65] [66].

In Section VI, together with the lean carrier design, we also survey and discuss how the advanced network functionalities can operate in time, carrier, and antenna domains to enhance energy efficiency.



#### *D. Artificial Intelligence*

The heterogeneous and stringent service requirements of 3GPP NR networks, together with their increasing complexity—a pinch of which has been depicted in previous sections—are making traditional approaches to network operation and optimization no longer adequate. Such methods use a significant level of expert knowledge and theoretical assumptions to characterize real environments. Thus, they do not scale well, and cannot handle the complexity of real scenarios with their many parameters and imperfections as well as stochastic and non-linear processes. To bridge this gap, and provide 3GPP NR networks with the intelligence required to strike optimum operation points, equipment vendors and MNOs have started to equip their products with ML-based functionalities [29] [50].

Fed by network measurements, supervised and unsupervised learning tools [67], two different branches of ML, are being extensively used nowadays to model 5G network behaviour first, and subsequently, take educated decisions and/or make predictions on complex scenarios [68]. This is particularly relevant to energy efficiency. As one can infer from the previous discussions, minimising 5G energy consumption is a large-scale network problem, which highly depends on complex BS and UE distributions, varying traffic demands and wireless channels as well as hidden network trade-offs. Thus, understanding and predicting UE behaviours and requirements, as well as their evolution in time and space, is critical to tailor the 5G network configuration—mMIMO, lean carrier, and advanced sleep modes—and address UE specific communications needs with the minimum possible energy consumption.

Additionally, due to the dynamic nature of wireless networks, and the lack of network measurements data for all network procedures and on all the possible configurations they can adopt, reinforcement learning (RL) [69] is also being widely explored to optimise 5G network performance in general, and energy efficiency in particular. For example, shutting down network elements is a combinatorial problem with a large number of variables. RL agents may be used to let the network interact with the environment, and learn optimum resource (de)activation policies to minimise the total network energy consumption. However, such learning may come at the expense of both *i)* an undesirably long exploration phase, where 5G network performance may be highly suboptimal, and *ii)* large computing powers and storage capabilities [70]. Moreover, continuously adapting an optimal policy, derived from and for a limited set of specific system configurations, to variations of network settings is a challenge.

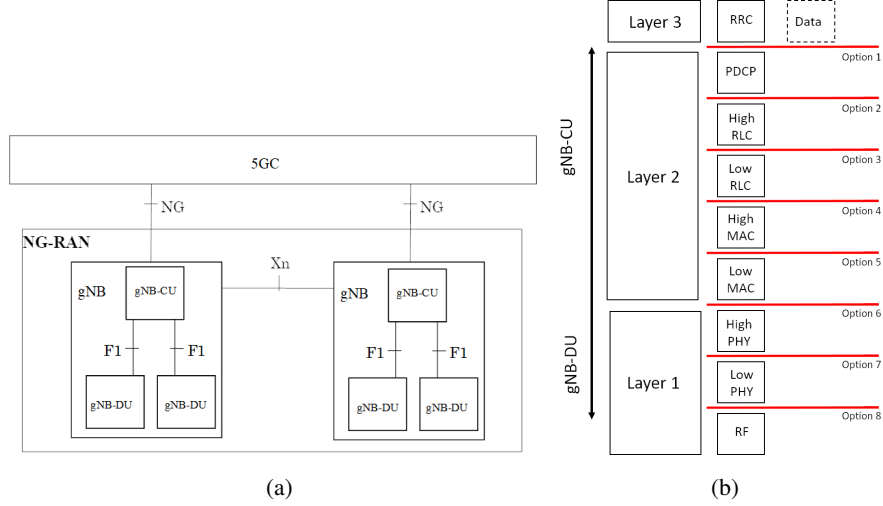


Figure 5. (a) NG-RAN overall architecture [72]; (b) 3GPP options for the function split between gNB-DUs and gNB-CU [71].

In Section VII, we will review how ML is being used to tackle the energy efficiency problem in 3GPP NR networks, and discuss both its benefits and main problems to tackle.

### III. POWER CONSUMPTION MODELS

To assess the impact of the different technology features presented earlier on the energy efficiency of a 5G network, it is necessary to define models that provide a good estimation of their energy consumption. Importantly, such energy consumption models need to offer the right balance between accuracy and tractability, while embracing different network and BS architectures, to empower 5G system performance characterisation and optimisation.

Fig. 5a shows the 3GPP NR RAN logical architecture. This architecture, denoted as next generation radio access network (NG-RAN) architecture, consists of a set of next generation NodeBs (gNBs) —the 3GPP NR BSs in the 3GPP terminology— connected *i)* amongst them through the  $X_n$  interface and *ii)* to the 5G Core Network (5GC) through the next generation (NG) interface. To take advantage of virtualization technologies and provide more implementation flexibility, a gNB may also consist of a central unit (CU) and multiple distributed units (DUs), connected to each other through the F1 interface. The 3GPP has studied eight functional split options between CU and DU (see Fig. 5b), and current RAN implementations are focusing on option 2 [71].

From an implementation perspective, each functional split corresponds to a distinct deployment option, which needs an appropriate power consumption characterisation. Specifically, it is

necessary to take into consideration both the power consumption of the sites where the DUs and CUs are deployed, as well as the transport network, also referred to as fronthaul, that connects the DUs and the CU. In addition, with the advent of Network Functions Virtualization (NFV), DUs and CUs functions can be implemented either through standard dedicated hardware or virtual network functions (VNFs) in a network cloud. Therefore, the overall RAN power consumption model may need to include the contribution of the cloud server, where the RAN VNFs are deployed. Accordingly, we can generally express the aggregated RAN power consumption of a 5G network as follows:

$$P_{\text{RAN}} = \sum_i P_{\text{BS}_i} + \sum_j P_{\text{FH}_j} + \sum_k P_{\text{VBBU}_k}, \quad (1)$$

where  $P_{\text{BS}_i}$ ,  $P_{\text{FH}_j}$ , and  $P_{\text{VBBU}_k}$  are the power consumption of the  $i$ -th gNB, the power consumption of the  $j$ -th fronthaul, and the power consumption of the  $k$ -th virtualized baseband unit (BBU), respectively. Depending on the specific RAN architecture, distributed or centralised, some of these components may not be considered.

In the following, we survey the most relevant power consumption models for both distributed and centralised RAN, while considering their most relevant characteristics.

#### A. Power Consumption Model for Distributed RAN

In case of a fully distributed radio access network (DRAN), the network power consumption can be modelled by taking into account only the BS contribution.

A widely used BS power consumption is that defined in [73], where the power consumption of a non-mMIMO BS is computed as a function of the power consumption of all its active antennas<sup>1</sup> in all its sectors, each one including a power amplifier (PA), an RF transceiver module, a BBU with a transmitter and a receiver section, a DC-DC power supply, an active cooling system and an AC-DC unit for connection to the electrical power grid. Such model is formulated as follows:

$$P_{\text{BS}} = N_{\text{TRX}} \frac{\frac{P_{\text{out}}}{\eta_{\text{PA}}} (1 - \sigma_{\text{feed}}) + P_{\text{RF}} + P_{\text{BB}}}{(1 - \sigma_{\text{DC}}) (1 - \sigma_{\text{MS}}) (1 - \sigma_{\text{cool}})}, \quad (2)$$

where  $N_{\text{TRX}}$  is the overall number of RF transceiver modules in a BS,  $P_{\text{out}}$  is the transmit power,  $P_{\text{RF}}$  and  $P_{\text{BB}}$  are the RF transceiver module and the BBU power consumption,  $\eta_{\text{PA}}$  is the PA

<sup>1</sup>Examples of active antennas are an antenna element, a dipole, or a macrocell column in a radome operated by a BBU.

power efficiency, and  $\sigma_{\text{DC}}$ ,  $\sigma_{\text{MS}}$  and  $\sigma_{\text{cool}}$  are the power losses in the DC-DC power supply, mains supply, and active cooling, respectively.

It should be noted that the model in eq. (2) is widely represented in the literature by a simplified version of it, which explicitly shows the linear relation between the BS power consumption,  $P_{\text{BS}}$ , and the transmit power,  $P_{\text{out}}$ , as follows:

$$P_{\text{BS}} = N_{\text{TRX}} \cdot (P_0 + \delta_p P_{\text{out}}), \quad (3)$$

where  $P_0$  and  $\delta_p$  are cell-type dependent parameters, which indicate the power consumption at the minimum non-zero output power and the slope of the load-dependent power consumption, respectively. Note that this model is general, and accommodates to macro, micro and small cells. For example, the parameters of eq. (3) for different types of small cells are provided in [73].

Importantly, in the last decade, in addition to appearance of the aforementioned smaller cells [74], two other main solutions have emerged as key enablers to boost the mobile network capacity, i.e., carrier aggregation (CA) (see Section VI-C) and mMIMO (see Section V). Accordingly, a number of works have evolved the previous presented model to capture the impact of these technology features on the BS power consumption.

*1) Carrier Aggregation Power Consumption Model:* CA is a 3GPP flagship feature primarily introduced to increase the cell throughput in 3GPP long term evolution advanced (LTE-A). The first version of CA allowed to aggregate up to 5 component carriers (CCs) of up to 20 MHz, and currently, in 3GPP NR, it has been extended to support up to 16 CCs and 1 GHz of bandwidth. The CA framework is flexible by design. It enables to use continuous or discontinuous intra-band CCs as well discontinuous inter-band CCs, which can be characterized by different bandwidth or coverage. It is also a key technology to enable licensed Assisted Access (LAA) [75], heterogeneous network (HetNet) deployments [76] and dual connectivity [77]. For each UE, a CC is defined as its primary cell (PCell) [78], which acts as the anchor CC, and is thus used for basic functionalities, including mobility support and radio link failure (RLF) monitoring. Additionally configured CCs are denoted as secondary cells (SCells), and they can be added, changed, or removed to optimise the BS performance.

When modelling the power consumption of a system using CA, it is necessary to take into account how the power consumption scales with the number of active CCs,  $N_{\text{CC}}$ . In this line,

the work in [79] has presented the following power consumption model for CA:

$$P_{BS} = \sum_{j=1}^{N_{CC}} \left( P_{TX_j} + B_j P_{CP_j}^{CA} \right) + P_{CP}^{CAi},$$

where  $P_{TX_j} = \frac{P_{out_j}}{\eta_{PA}}$ ,  $B_j$ , and  $P_{CP_j}^{CA}$  are the effective transmit power used by CC  $j$ , the bandwidth of CC  $j$ , and the variable circuit power consumption, which scales linearly with both the number of active CCs,  $N_{CC}$ , and their bandwidth,  $B_j$ , respectively, while as in the general model,  $P_{CP}^{CAi}$  is the load independent circuit power consumption of the CA system, i.e., of the hardware components shared by the distinct CCs.

Embracing the complexity of CA, the variables,  $P_{CP}^{CA}$  and  $P_{CP}^{CAi}$ , may take different values, depending on the specific CA implementation. For instance, contiguous CA can be realized with a single fast Fourier transform (FFT) and a single RF transceiver module for all CCs, while non-contiguous CA usually requires multiple of them [78]. In the worst case, each CC would require a fully dedicated hardware, and thus the load independent circuit power consumption of the CA system,  $P_{CP}^{CAi}$ , would scale linearly with the number of active CCs,  $N_{CC}$  [45].

2) *mMIMO Power Consumption Model:* With regard to mMIMO, and similarly as for the CA case, the linear power consumption model in eq. (3) has also been extended to take into consideration the large number of antenna elements and the new architecture of a mMIMO BS. In this line, the work in [80] proposed the following power consumption model for mMIMO:

$$P_{BS} = P_{TX} + N_{TRX}^A P_{CP}^A + P_{CP}^{li}, \quad (4)$$

where  $N_{TRX}^A$  is the number of RF mMIMO transceiver modules, which do not need to be necessarily equal and may be smaller than the number of antenna elements,  $P_{CP}^A$  is the power consumption of the RF and digital processing needed to support each RF mMIMO transceiver module, and  $P_{CP}^{li}$  is the load-independent circuit power consumption.

Importantly, it should be noted that  $N_{TRX}^A$  depends on the type of beamforming architecture implemented at the BS [81]. Digital beamforming provides high flexibility, but requires a large number of RF mMIMO transceiver modules. In contrast, analog beamforming decreases the power consumption by significantly reducing the number of RF mMIMO transceiver modules at the cost of a lower spatial resolution capability of the beamforming and a larger latency to select the proper beam weights/configuration. Hybrid beamforming combines the advantages of the two architectures.

The linear mMIMO power consumption model in eq. (4) provides a simple description of the relation between the number of RF mMIMO transceivers and the power consumption in a mMIMO system. However, more advanced works have highlighted that it is of paramount importance to also take into account the impact of multi-user scheduling. Specifically, the research in [82] has described the steps to derive a more complete model for mMIMO BSs, which accounts for both downlink and uplink communications, under the assumption of zero forcing (ZF) processing<sup>2</sup>. In more detail, the authors describe the mMIMO BS power consumption as the sum of the effective transmit power,  $P_{TX} = \frac{P_{out}}{\eta_{PA}}$ , and the circuit power,  $P_{CP}$ , as follows:

$$P_{BS} = P_{TX} + P_{CP}, \quad (5)$$

and then decomposed the latter term as:

$$P_{CP} = P_{FIX} + P_{TRX} + P_{CE} + P_{C/D} + P_{BH} + P_{SP} = P_{CP}^{li} + P_{CP}^{ld}, \quad (6)$$

where  $P_{FIX}$  is the fixed power required for site-cooling, control signalling, and load-independent backhaul and signal processors,  $P_{TRX}$ ,  $P_{CE}$ ,  $P_{C/D}$ ,  $P_{BH}$  and  $P_{SP}$  are the power consumption of the transceiver modules, the channel estimation process, the channel coding and decoding units, the load-dependent backhaul, and the beamforming processing, respectively. For clarity, let us denote by  $P_{CP}^{li}$  the sum of both the variable,  $P_{FIX}$ , and the load-independent part of the variable,  $P_{TRX}$ , and by  $P_{CP}^{ld}$  all the rest, i.e. the load-dependent part of the circuit power consumption,  $P_{CP}$ .

Accordingly, the mMIMO BS power consumption model in eq. (6) can be expressed as follows [83] [84]:

$$P_{BS} = \frac{K \cdot P_{UE}}{\eta_{PA}} + P_{CP}^{li} + \mathcal{C}_3 K^3 + \mathcal{D}_0 M + \mathcal{D}_1 M \cdot K + \mathcal{D}_2 M \cdot K^2 + \mathcal{A} K \cdot R_{UE}, \quad (7)$$

where  $K$  is the number of simultaneously multiplexed UEs at the BS,  $P_{UE}$  is the downlink output power per UE (i.e.,  $P_{out} = K \cdot P_{UE}$ ),  $\mathcal{C}_3$  is the part of the beamforming processing,  $P_{SP}$ , which scales linearly with  $K^3$ ,  $\mathcal{D}_0$  is the power consumed by the transceiver module attached to each antenna,  $\mathcal{D}_1$  is the part of the beamforming processing,  $P_{SP}$ , which scales linearly with  $M \cdot K$ ,  $\mathcal{D}_2$  is the sum of the contributions of the channel estimation process,  $P_{CE}$ , and the beamforming processing,  $P_{SP}$ , which scale linearly with  $M \cdot K^2$ ,  $R_{UE}$  is the UE throughput, and  $\mathcal{A}$  is the aggregated power consumption per bit of information required by the coding/decoding operations and by the load-dependent part of the backhaul. Table III describes typical values of the parameters in eq. (7).

<sup>2</sup>Models for other specific precoding and combining schemes are discussed in [56].

Table II  
TYPICAL VALUES FOR MMIMO POWER CONSUMPTION MODEL PARAMETERS [82] [83] [84].

Parameter	Value	Parameter	Value
$\eta_{\text{PA}}$	0.39	$P_{\text{CP}}^{\text{li}}$	20 [W]
$\mathcal{C}_3$	$10^{-7}$ [W]	$\mathcal{D}_0$	1 [W]
$\mathcal{D}_1$	$3 \cdot 10^{-3}$ [W]	$\mathcal{D}_2$	$9.4 \cdot 10^{-7}$ [W]
$\mathcal{A}$	1.15 [W/Gbps]		

### B. Power Consumption Model for Centralised RAN

Considering a more sophisticated RAN architecture, the work in [85] has studied the power consumption modelling of a centralized radio access network (CRAN) considering different functional splits between the gNB-DUs and the gNB-CU. In terms of energy efficiency, centralisation enables three main benefits with respect to a decentralised architecture: stacking gain, pooling gain, and cooling gain [85]. The stacking gain refers to the capability of deploying less processing units (in the central node) to serve the same amount of cells in a given area, while the pooling gain refers to the capability of using a limited amount of centralised resources to operate a large amount of cells, by exploiting the load variations in the network. The cooling gain appears due to the reduced amount of energy required to cool the cell site and the more advanced cooling solutions that can be implemented at the central node [86].

In this centralized architecture, the aggregated power consumption at the RAN can be computed as [85]:

$$\sum_i P_{\text{BS}_i} = \sum_i P_{\text{DU}_i} \left( 1 - \frac{P_{\text{co}_i} + P_{\text{NF}_i}}{100} \right) + P_{\text{BBU}}, \quad (8)$$

where  $P_{\text{DU}_i}$  is the power consumption of the site where the  $i$ -th DU is deployed, which can be computed as, e.g., eq. (7),  $P_{\text{BBU}}$  is the power consumption of the BBU host where the CU is located<sup>3</sup>,  $P_{\text{NF}_i}$  is the fraction of power consumption that corresponds to the Network Functions (NFs) moved to the CU, and  $P_{\text{co}_i}$  is the fraction of power consumption that corresponds to the cooling related to the  $i$ -th DU. Importantly, note that the higher the number of NFs moved to the

<sup>3</sup>This model can be easily generalised to the case where a larger network with multiple CUs is considered.

CU, the higher the values of both parameters,  $P_{\text{co}_i}$  and  $P_{\text{NF}_i}$ . Moreover, the power consumption of the BBU host,  $P_{\text{BBU}}$ , can be computed as:

$$P_{\text{BBU}} = \sum_i P_{\text{DU}_i} \left( \frac{1/G_{\text{co}}}{100} + \frac{P_{\text{NF}_i}/N_{\text{BS}}}{100} \left\lceil \frac{N_{\text{BS}}}{G_{\text{st}}G_{\text{po}}} \right\rceil P_{\text{add}} \right), \quad (9)$$

where  $G_{\text{st}}$ ,  $G_{\text{po}}$ ,  $G_{\text{co}}$ , and  $P_{\text{add}}$  are the stacking gain, the pooling gain, the cooling gain, and the additional power consumption in the BBU needed to enable resource pooling, respectively.

It is important to note that eq. (9) assumes that the CU is deployed on a dedicated hardware platform, which has a similar architecture to the one used for a single DU but with larger computational capacity. In the case of a virtualized radio access network (VRAN), the goal is to move the processing to general purpose processors (GPPs), which are capable to provide real-time processing to maintain the timing in the RAN protocols, while equipped with efficient and elastic resources —CPU, memory, and networking— to perform intensive digital processing. This approach promises further improved energy savings, which depend on the specifically used architecture [87]. One option is to use dedicated hardware (e.g., system on chip) for managing the layer 1 functions on dedicated hardware, while higher-layer functions are implemented in a software-based architecture. This solution may enable, however, limited additional energy savings with respect to CRAN. To reduce the power consumption and increase flexibility, an alternative option is to deploy only the most computationally-intensive functions on dedicated hardware, such as turbo decoding and encryption/decryption. As an extreme option, in the full GPP architecture, all the RAN functions are implemented in a virtual environment, which may enable large power savings at the expense, however, of performance if the GPPs and infrastructure around cannot cope with the workload.

Considering the GPP architecture, the work in [88] proposes a power consumption model for virtualized BBUs in a cloud node, which takes into account the impact of the cooling system, the workload dispatcher switch, and the GPPs as follows:

$$P_{\text{VBBU}} = P_{\text{Vco}} + P_{\text{Dis}} + \sum_i P_{\text{GPP}_i},$$

where  $P_{\text{Vco}}$ ,  $P_{\text{Dis}}$  and  $P_{\text{GPP}_i}$  are the power consumption contributions in the virtualized BBU due to the cooling system, the switch, and the  $i$ -th GPP, respectively.

To characterize the GPP power consumption, a linear power consumption model can be used [72] [89], i.e.,

$$P_{\text{GPP}} = P_{\text{GPP}_0} + \Delta_{\text{GPP}} P_{\text{GPP}_m} \rho_{\text{GPP}},$$



where  $P_{\text{GPP}_0}$  and  $P_{\text{GPP}_m}$  are the power consumption of the GPP when it is in sleep mode and at maximum load, respectively, and  $\Delta_{\text{GPP}}$  and  $\rho_{\text{GPP}}$  are the slope of the power consumption model, which is related to the specific GPP architecture, and the load of the GPP, respectively, where the latter depends on the GPP computational capacity and the computational resources required by the hosted VNFs.

To characterise of the GPP computational load, the work in [89] has used an experimental platform to infer the relationship between the downlink throughput and the percentage of central processing unit (CPU) usage at the BBU. Instead, the authors in [90] propose an analytical characterisation of the GPP computational load, which jointly depends on the functional split, the number of used transceiver modules/antennas, the bandwidth, the rate and the number of spatial MIMO-layers used at the virtualized BS. Importantly, the authors in [91] have further analytically investigated the computational complexity of lower layer functions in 3GPP NR, and this research has shown that, today, due to the form factor and power consumption of GPP, dedicated hardware is the only feasible option for deploying full 3GPP NR capabilities.

Complementing the above, the authors in [92] have also recently developed an empirical model to describe the computational requirements of the RAN NFs, focusing on the physical (PHY) layer, which includes the most computationally expensive functionalities. Their results highlight that NFs can be classified according to their complexity into three classes:

- PHY NFs, whose computational complexity only depends on the system configuration, and does not change with time (e.g., FFT),
- PHY NFs, whose computational complexity depends on both throughput requirements and channel quality (e.g., encoding/decoding), and
- higher layer NFs, whose computational complexity only depends on throughput requirements (e.g., packet scheduling).

Finally, to connect each DU to the CU, a fronthaul link, whose capacity fits the functional split throughput and latency requirements is needed. Therefore, the total power consumption of the fronthaul is a function of the transport network technology, its topology, the capacity required by each BS, and the number of BSs deployed in the RAN. For instance, when the fronthaul is based on optical dense wavelength division multiplexing with a ring architecture and optical switching, the power consumption of the network connecting the  $i$ -th DUs to the CU can be

modelled as [85]:

$$P_{FH_i} = \left\lceil \frac{C_{FS_i}}{R_{tr}} \right\rceil \left( 2 \cdot P_{tr} + \frac{P_W}{N_W} \right),$$

where  $C_{FS_i}$  is the transport capacity required by the functional split at the  $i$ -th gNB,  $P_W$  is the power consumption of a port used to interconnect access and metro rings in the transport network,  $N_W$  is the number of wavelengths per fiber, and  $R_{tr}$  and  $P_{tr}$  are the rate and the associate power consumption of the transport network nodes, respectively.

To provide a general view, and highlight the impact of the transport network on the overall system power consumption, we show in Fig. 6a the network power consumption with respect to the BS deployment density for a classic DRAN and different CRAN architectural options, using the parameters indicated in Table III. Moreover, Fig. 6b shows the impact of each contributor, i.e., DUs, fronthaul nodes, and BBU, with respect to the aggregated CRAN power consumption. Fig. 6a highlights that only a CRAN with functional split option 6 (see Fig. 5b) has similar power consumption to the classic DRAN. CRAN architectures with lower functional splits provide larger centralisation gains, but lead to higher power consumptions. In addition, Fig. 6b shows that the contribution from the transport network cannot be neglected in the overall power consumption characterisation, particularly when some architectures are adopted. Specifically, while for split option 6, it only amounts for around 2 % of the network power consumption, in split option 7 and 8, it contributes for around 30 % and 60 % of the network power consumption, respectively.

To conclude this section, let us also highlight that the research and industry communities have spent notable efforts to characterize the RAN power consumption —whether distributed or centralised— while considering the most relevant architectures. However, this is still an open research field. In particular, we argue that due to the large ecosystem of equipment vendors and their different implementation of solutions, there is a need for further data and experimentally driven research to validate the proposed models and find their appropriate parameters on real 3GPP NR equipment. In addition, further research is also needed to characterise CA and mMIMO BS power consumption in the presence of multiple configurations and more complex features, such as coordinated multi-point (CoMP), and the characterisation of the power consumption of sites where multiple radio access technologies (RATs) co-exist.

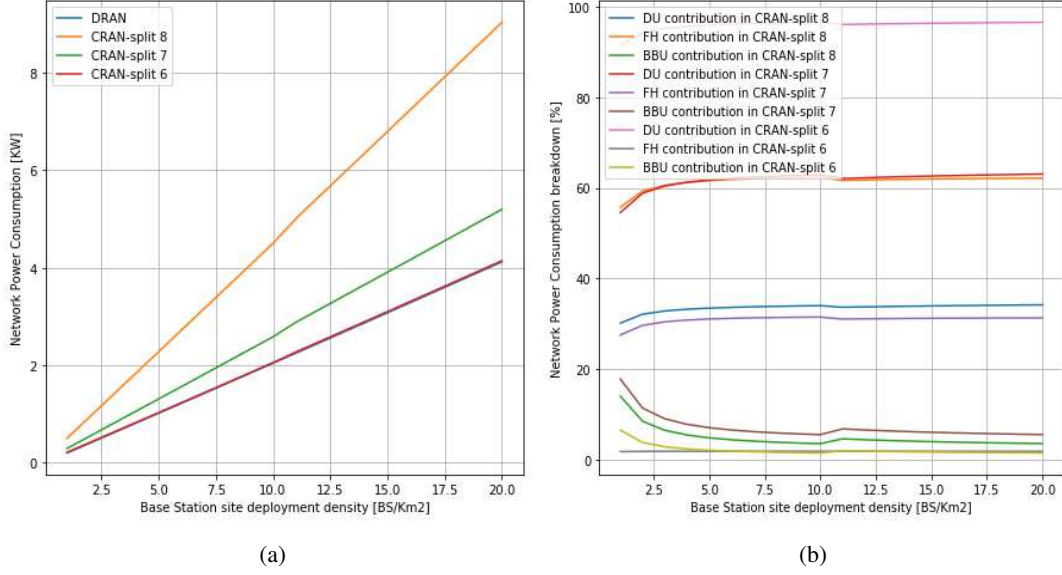


Figure 6. Network power consumption (a) and its breakdown (b) as a function of the BS deployment density for classic DRAN and different CRAN architectural options.

Table III  
CRAN POWER CONSUMPTION MODEL PARAMETERS [85] [93].

CRAN split 8	Value	CRAN split 7	Value	CRAN split 6	Value
$P_{co}$	10	$P_{co}$	10	$P_{co}$	0
$P_{NF}$	15	$P_{NF}$	10.5	$P_{NF}$	3
$G_{po}$	5	$G_{po}$	5	$G_{po}$	5
$G_{st}$	2	$G_{st}$	2	$G_{st}$	2
$P_{add}$	2	$P_{add}$	2	$P_{add}$	2
$G_{co}$	0.2	$G_{co}$	0.2	$G_{co}$	1
$C_{FS}$	3044 Gbps	$C_{FS}$	882 Gbps	$C_{FS}$	10 Gbps
$R_{tr}$	100 Gbps	$R_{tr}$	100 Gbps	$R_{tr}$	10 Gbps
$N_W$	40	$N_W$	40	$N_W$	80
$P_W$	2.2 W	$P_W$	2.2 W	$P_W$	2.2 W
$P_{tr}$	4.5 W	$P_{tr}$	4.5 W	$P_{tr}$	2 W

#### IV. ENERGY EFFICIENCY METRICS

To evaluate the impact of energy efficiency mechanisms on energy savings, energy efficiency metrics are as important as the used power consumption models. These metrics must be com-

prehensive, reliable and widely accepted to allow comparisons. In addition, they have to capture both the energy consumed by the system under investigation as well as the performance measured at network level (such as coverage, capacity, and delay).

To achieve these goals, the European Telecommunications Standards Institute (ETSI) Environmental Engineering technical committee, the ITU-T Study Group 5 and the 3GPP Technical Specification Group RAN have specified metrics to assess mobile network energy efficiency under different operating conditions. The contribution of these standard development organizations (SDOs) has mainly focused on global system performance, while considering different demographic areas, load scenarios, and radio access technologies. In contrast, the academic research community has contributed to this effort by proposing energy efficiency link-specific metrics, which enable a more tailored energy efficiency network optimisation [94].

In the following, we will first overview the contributions from different SDOs, considering both interference- and noise-limited scenarios, and then touch on energy-delay related metrics. Subsequently, we also describe alternative metrics proposed by the academic research community to drive energy efficiency optimisation problems, indicating the merits and the drawbacks of each one of them.

#### A. Energy Efficiency Metrics for Interference-Limited Networks

As one of the main targets of 5G networks to enhance energy efficiency is to adapt the system capacity —and the associated power consumption— to the network load, load-aware metrics are key for the next generation of green communication networks. In this context, ETSI has defined the mobile network data energy efficiency metric,  $EE_{DV}$  [bit/J] [95], which is the ratio between the data volume,  $DV$ , delivered in the network and the network energy consumption,  $EC$ , observed during the time period required to deliver such data, i.e.,

$$EE_{DV} = \frac{DV}{EC}, \quad (10)$$

where  $EC$  should be computed by integrating eq. (1) over an observation period that includes distinct load levels<sup>4</sup>. Note that the data volume,  $DV$ , includes both downlink and uplink traffic for both circuit switched services and packet switched services, and that this metric can be used to characterise a single or multiple BSs, operating in urban and/or dense-urban areas, in which the

<sup>4</sup>the 3GPP recommends that the performance should be evaluated considering at least 3 load levels [96].

network experiences highly variable loads, i.e. interference-limited scenarios. However, it is not appropriate for scenarios where the traffic load is low. Specifically, since the energy efficiency metric,  $EE_{DV}$ , is not weighted according to the global reference, a small energy saving in the low energy consumption region in a low load scenario may comparatively lead to apparently large energy efficiency gains. while a large energy saving in the high energy consumption region may comparatively result into limited energy efficiency gains.

To characterise the energy efficiency, while considering distinct deployment scenarios, e.g., dense-urban, urban, sub-urban, rural, or deep rural areas, ETSI has extended the previous metric to the total energy efficiency metric,  $EE_{Total}$  [bit/J] [95], which can be defined as the weighted sum of the energy efficiency in each deployment scenario, i.e.,

$$EE_{Total} = \frac{\sum_m PoPP_m \cdot EE_{DV_m}}{\sum_m PoPP_m},$$

where  $m$  is the index of the  $m$ -th scenario,  $EE_{DV_m}$  is the energy efficiency of the  $m$ -th scenario, and  $PoPP_m$  is the weight (percentage) representing the typicality of the  $m$ -th scenario in the network under test.

To jointly consider deployment scenarios and traffic loads, the 3GPP has further complemented the work from ETSI, introducing the network energy efficiency metric,  $EE_{global}$  [bit/J] [96], which can be defined as the sum of the energy efficiencies in multiple deployment scenarios and under different traffic loads, i.e.,

$$EE_{global} = \sum_m b_m \cdot EE_{DS_m} = \sum_m \sum_l b_m \cdot a_l \cdot EE_{DV_{m,l}},$$

where  $EE_{DV_l}$  is the energy efficiency of the network for an observed deployment scenario,  $m$ , and traffic load level,  $l$ , while  $b_m$  and  $a_l$  are the weights for the corresponding deployment scenario,  $m$ , and traffic load level,  $l$ , respectively. The 3GPP recommends to compute  $b_m$  considering the proportion amongst the different deployment scenarios in terms of *i*) power consumption, *ii*) traffic load, or *iii*) connection density [97]. With respect to  $a_l$ , and giving an example, if 10%, 30%, and 50% traffic load levels are investigated, the corresponding weights based on a daily traffic model could be 6/24, 10/24 and 8/24, respectively [97].

Although the above presented metrics provide a useful indication on how the energy consumption scales with the increase of the data rate requirements, it does not give any information about actual economic costs. To address this challenge, the work in [98] has introduced the

economical energy efficiency metric,  $E^3$  [bit/J], which is defined as the ratio of effective system throughput to the associated energy consumption, weighted by a cost coefficient, i.e.,

$$E^3 = \frac{\sum_{k \in \mathcal{K}} \alpha_k R_k}{\sum_{n \in \mathcal{N}} P_{Tn} + P_{0n} C_n},$$

where  $\mathcal{K}$  and  $\mathcal{N}$  are the sets of UEs and serving BSs, respectively,  $R_k$  is the effective throughput perceived by the  $k$ -th UE,  $\alpha_k$  is the priority weight related to the  $k$ -th UE,  $P_{0n}$  and  $P_{Tn}$  are the static and the load-dependent power consumption, respectively, and  $C_n$  is the cost coefficient of the  $n$ -th BS. Note that the cost coefficient,  $C_n$ , is calculated as the ratio of the corresponding device cost to a predefined benchmark cost, such that the metric,  $E^3$ , has the same unit as the energy efficiency. In scenarios where multiple access, fronthaul, computing, and other mechanisms coexist to provide efficient services to the end-users, this economical energy efficiency metric,  $E^3$ , is able to discriminate amongst solutions, not only in terms of provided network throughput and energy consumption, but also in terms of additional (deployment and operational) costs. This allows the analysis of advanced network deployment and resource management schemes.

#### B. Energy Efficiency Metrics for Noise-Limited Networks

To complement the energy efficiency metrics presented in the previous section and deal with scenarios with sustained low data volumes, in particular in rural or in deep rural areas, ETSI also introduced the mobile network coverage energy efficiency metric,  $EE_{MN,CoA}$  [m<sup>2</sup>/J] [95], which is the ratio between the area covered by the network, CoA, and the network energy consumption observed during one year, EC, i.e.,

$$EE_{CoA} = \frac{CoA}{EC}. \quad (11)$$

In addition to the above, the 3GPP has extended the coverage energy efficiency metric in eq. (11) to consider a global metric, the mobile network data energy efficiency metric,  $EE_{DV}$  [72], which, similarly as presented earlier, spans over distinct deployment scenarios, i.e.,

$$EE_{global, CoA} = \sum_i C_i \cdot EE_{CoA,i},$$

where  $C_i$  is the weight for each of the corresponding deployment scenarios, which is computed by taking into account the area covered per deployment scenario and the relevance of the scenario itself to the total power consumption, e.g., the percentage of power consumption in dense urban

areas to that in rural areas. The energy computation in the actual area under coverage—and how it is affected by a network feature—, however, can be complex to estimate, and it may require the collection of a large number of UE measurement reports. In this context, ETSI has defined a coverage quality factor, CoAQ [%] [95], to estimate the quality of the coverage and measure the amount of connection failures due to coverage issues, load congestion or significant interference effects, i.e.,

$$\text{CoAQ} = (1 - \text{FR}_{\text{RRC}})(1 - \text{FR}_{\text{RAB}_\text{S}})(1 - \text{FR}_{\text{RAB}_\text{R}}),$$

where  $\text{FR}_{\text{RRC}}$ ,  $\text{FR}_{\text{RAB}_\text{S}}$ , and  $\text{FR}_{\text{RAB}_\text{R}}$  are the radio resource control setup failure ratio, the radio access bearer setup failure ratio, and radio access bearer release failure ratio, respectively.

### C. Delay-aware Energy Efficiency Metrics

With respect to other important performance metrics, such as latency, which is also a key requirement of 5G systems due to the emergence of URLLC, ETSI has introduced the latency metric,  $\text{EE}_\text{L}$  [ $\text{s}^{-1}/\text{J}$ ] [95], to characterize 5G energy performance when these use cases are predominant. This metric is the inverse of the product between the end-to-end user-plane latency,  $T_{\text{e2e}}$ , and the energy consumption,  $\text{EC}$ , in the observation time period, i.e.,

$$\text{EE}_\text{L} = \frac{1}{T_{\text{e2e}} \cdot \text{EC}},$$

where  $T_{\text{e2e}}$  is the overall end-to-end latency between the transmitter side and the receiver side, including the delays due to, e.g. packet queuing, scheduling and the hybrid automatic repeat request (HARQ) process.

### D. Link-aware Energy Efficiency Metrics

As mentioned earlier, to aid a finer grain performance optimization, the research community has extended the network energy efficiency metric,  $\text{EE}_{\text{DV}}$ , presented in eq. (10) by taking into consideration the different requirements of its distinct links. In fact, since the energy efficiency metric,  $\text{EE}_{\text{DV}}$ , can be seen as the aggregated sum of the energy efficiencies of each network link, its optimisation through radio resource management may tend to favour the links that can provide the largest throughput, which may limit the QoS of e.g., cell edge UEs, and thus the network fairness.

To address this issue, and denoting by  $\mathcal{L}$  the set of links in the network, the weighted sum of the energy efficiencies (WSEE) metric, WSEE [bit/J] [94], is defined as the weighted mean of the different energy efficiencies measured at each link  $i \in \mathcal{L}$ , i.e.,

$$\text{WSEE} = \sum_{i \in \mathcal{L}} w_i \cdot \text{EE}_{\text{DV},i}, \quad (12)$$

where  $\text{EE}_{\text{DV},i}$  is the link energy efficiency, defined as in eq. (10), and  $w_i$  is the weight of  $i$ -th link. Importantly, note that the use of different weights for different links enables assigning them different priorities during the resource allocation to increase the system fairness.

To enable an even more fair resource allocation, researchers have also proposed the weighted product of the energy efficiencies (WPEE) metric, WPEE [bit/J] [94], which is defined as the exponentially weighted product of the different energy efficiencies measured at each link  $i \in \mathcal{L}$ , i.e.,

$$\text{WPEE} = \prod_{i \in \mathcal{L}} (\text{EE}_{\text{DV},i})^{w_i}.$$

In particular, the WPEE metric maximisation ensures that no link experiences a zero throughput, and has been shown to converge to the Nash Bargaining solution [99]. Following this approach, however, it is not possible to improve the energy efficiency of the  $i$ -th link,  $\text{EE}_{\text{DV},i}$ , without decreasing the energy efficiency of other link, e.g. the  $j$ -th link,  $\text{EE}_{\text{DV},j}$ .

To achieve a better trade-off among overall system performance and fairness, a max-min fair resource allocation policy can be adopted. An energy efficiency resource allocation scheme that is max-min fair can be designed by maximising the weighted minimum of the energy efficiencies (WMEE) metric, WMEE [bit/J], i.e.,

$$\text{WMEE} = \min_{\{i \in \mathcal{L}\}} (w_i \cdot \text{EE}_{\text{DV},i}).$$

Note that when the WMEE metric is optimised, the resource allocation achieves the same product,  $w_i \cdot \text{EE}_{\text{DV},i}$ , for all links  $i \in \mathcal{L}$ . Thus, if the weights are set equal, this max-min fair resource allocation will provide the same energy efficiency for each link.

To facilitate the reader's understanding, Fig. 7 provides a qualitative comparison of the performance achieved by a network with two links when optimising its energy efficiency using the WMEE, the WSEE and the WPEE metrics with respect to the Pareto boundaries. Each of the three approaches leads to a solution that belong to the energy efficient Pareto region. However, the WSEE and the WPEE metrics allocate more resources to the link 1, which is characterized by a better energy efficiency in order to get closer to the global optimum. In contrast, the WMEE



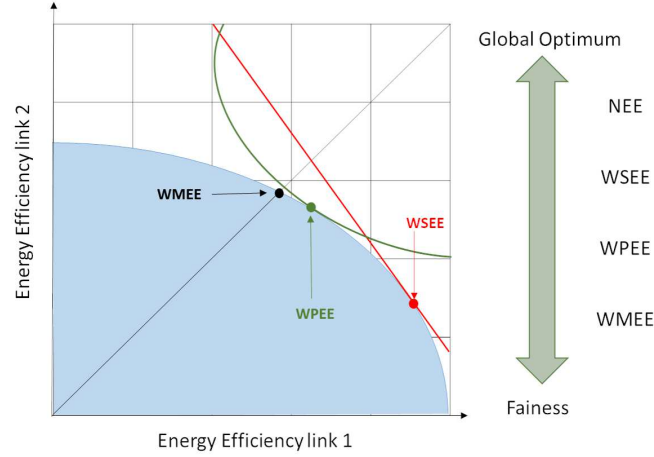


Figure 7. Operating regions of the energy efficient optimisation based on the NEE, the WMEE, the WPPE, and the WSEE metrics [94], where  $NEE = \sum_{i \in \mathcal{L}} EE_{DV,i}$ .

metric shares the resources between the two links such that they are characterized by the same energy efficiency.

To conclude this section, Table IV provides a summary of the most relevant energy efficiency metrics for 5G system optimisation, where it is important highlighting that these metrics have been mainly designed for assessing 4G networks, focusing on enhanced mobile broadband (eMBB) services, and considering only data rate, latency, and coverage requirement. In contrast, with respect to other 5G use cases, e.g. massive machine type communication (mMTC) and URLLC, there is a lack of specific and well understood metrics, and further research is needed in this area. mMTC applications call for energy efficiency metrics that takes into account the number of connection handled by the network in combination with the area covered by the network, e.g., an extension of the mobile network coverage energy efficiency metric,  $EE_{MN,CoA}$ . Similarly, URLLC applications require a metric able to capture the system reliability in combination with the end-to-end delay, e.g., an extension of the latency metric,  $EE_L$ .

## V. THEORETICAL UNDERSTANDING OF ENERGY EFFICIENCY: MASSIVE MIMO

3GPP NR networks are targeted at a 100 times higher energy efficiency with respect to previous generations (see Fig. 2), and mMIMO has been identified as a key technology to reach such target. As discussed in previous sections, by leveraging its extensive beamforming and spatial

Table IV  
SUMMARY OF EE METRICS.

Metric	Unit	Calculation	KPI	Pros	Cons
$EE_{DV}$ [95]	[bit/J]	$\frac{DV}{EC}$	Load-aware	It is a simple metric	Nothing to report
$EE_{Total}$ [95]	[bit/J]	$\frac{\sum_m PoPP_m \cdot EE_{DV,m}}{\sum_m PoPP_m}$	Load-aware	Appropriate for overall network assessment	It does not allow to tune the EE of each link
$EE_{global}$ [96]	[bit/J]	$\sum_m \sum_l b_m \cdot a_l \cdot EE_{DV,l}$	Load-aware	It captures multiple load scenarios	It does not allow to tune the EE of each link
$EE_{CoA}$ [95]	[m <sup>2</sup> /J]	$\frac{CoA}{EC}$	Coverage-aware	It can compare performance in cells with different size	The effective coverage is not well-defined
$EE_{global, CoA}$ [72]	[m <sup>2</sup> /J]	$\sum_i C_i \cdot EE_{CoA,i}$	Coverage-aware	It can capture multiple deployments	The effective coverage is not well-defined
$\frac{Power}{Subscriber}$ [100]	[W/UE]	$\frac{\sum_{k \leq N_{UE}} P_k}{N_{UE}}$	QoS-aware	It enable evolutionary comparison amongst systems	Need to model systems with a large UE number
$EE_L$ [95]	[s <sup>-1</sup> /J]	$\frac{1}{T_{ec} EC}$	Latency-aware	It is a simple metric	Nothing to report
$E^3$ [98]	[bit/J]	$\frac{\sum_{k \in \mathcal{K}} \alpha_k R_k}{\sum_{n \in \mathcal{N}} P_{T,n} + P_{0,n} C_n}$	Load & cost-aware	It can capture the cost of different solutions	The cost is not well-defined
$WSEE$ [94]	[bit/J]	$\sum_{i \in \mathcal{L}} w_i \cdot EE_{DV,i}$	Link & Load-aware	It captures link priorities	It cannot prevent links with zero throughput
$WPPE$ [94]	[bit/J]	$\prod_{i \in \mathcal{L}} (EE_{DV,i})^{w_i}$	Link & Load-aware	It prevent links with zero throughput	It cannot achieve max-min fairness
$WMEE$ [94]	[bit/J]	$\min_{\{i \in \mathcal{L}\}} (w_i \cdot EE_{DV,i})$	Load-aware	It leads to max-min fairness	Nothing to report

multiplexing capabilities, mMIMO can significantly reduce the transmit power required at the BS to achieve a targeted capacity, given a frequency band of operation and coverage area. However, running such larger number of antennas at the BS, together with the more signal processing required to handle the larger capacity in a mMIMO cell, also increases the energy consumption of the BS, and in turn, that of the network.

Multiple studies have set out to fundamentally understand the challenges of mMIMO networks in general, and the above presented energy efficiency trade-off in particular. Mainly concentrating on providing insights for network design, a large body of research has focused on deriving theoretical bounds on the capacity and the energy consumption of mMIMO systems, as well as the interplay between different network parameters. More practical research, on the other hand, has tackled mMIMO-based network design, BS deployment, as well as radio resource management and optimisation problems, while taking into account more realistic QoS constraints.

One of the main challenges faced in these fundamental studies is around the accuracy and the tractability of the models used to characterise performance at the network-level. mMIMO capacity and rates, for instance, significantly degrade in the presence of channel correlation and/or pilot contamination, which is a function, among others, of the BS and the UE distributions, the scenario topology and the wireless channel, as well as independent BS scheduling decisions and the resulting interference. However, this is hard to capture in tractable models. Same issues also revolve around the accuracy and complexity of the power consumption models, as discussed in Section III.

In light of these tractability issues, most theoretical findings on energy efficiency related to mMIMO networks are limited to single-cell scenarios, where model simplifications can be easily justified. In contrast, the estimation of energy efficiency metrics and trade-offs in multi-cell scenarios tends to be addressed through computer aided numerical evaluations.

In the following, we provide an overview of fundamental studies addressing the problem of energy efficiency in the context of mMIMO systems, in both single- and multi-cell scenarios. We focus on the relevant findings with regard to the energy efficiency bounds and its trade-off with respect to the spectral efficiency, and discuss the assumptions taken to extract such knowledge. We also summarize useful insights for an energy efficient mMIMO network design and deployment.

#### A. Single-cell scenario

In this section, we focus —and survey— energy efficiency bounds and trade-offs when considering a single-cell mMIMO scenario, of which there is a good understating in the literature. Explicit closed-form expressions are available, and the impact of different mMIMO parameters into energy efficiency and power consumption has been carefully analyzed.

1) *Bounds:* To understand the energy efficiency scaling law with respect to the system bandwidth, the work in [101] considered a single-cell MIMO case —not a mMIMO one— with a single UE, where both the transmitter and the receiver were equipped with  $M$  antennas. The channels were assumed to be deterministic, and as consequence, perfect CSI was available at both the transmitter and the receiver. The adopted BS power consumption model included

- the BS transmit power,  $P_{\text{TX}}$ ,
- a term which corresponds to the power consumption of processing  $M$  parallel signals at the transmitter and the receiver, and

- a term which relates to the power consumption of encoding and decoding the corresponding information.

The results of such analysis showed that the energy efficiency of this single-cell MIMO is maximized for a non-zero finite ratio of the BS transmit power,  $P_{\text{TX}}$ , to the bandwidth,  $B$ , which typically corresponds to a low signal to noise ratio (SNR). Importantly, the optimal mentioned ratio depends on the propagation characteristics and the transceiver hardware, but not on the power consumption of encoding and decoding information. The latter only affects the quantitative maximum value of the energy efficiency, but not the optimal operating point in terms of the BS transmit power,  $P_{\text{TX}}$ , and the bandwidth,  $B$ . Given such optimal ratio, any bandwidth,  $B$ , can thus be selected to achieve any data rate. In other words, there is no trade-off between the energy efficiency and the data rate when the BS transmit power,  $P_{\text{TX}}$ , and the bandwidth,  $B$ , are not constrained by external factors. This is an important insight, which may also apply to the mMIMO case. However, it is important to note that both the BS transmit power,  $P_{\text{TX}}$ , and the bandwidth,  $B$ , are scarce resources, which cannot be infinitely abused, and usually more complex hardware is generally needed to handle more bandwidth. Turning the attention to mMIMO systems, where data rates can be scaled up by the usage of more antennas, the pioneering work in [102]–[104] provided a first analysis of the energy efficiency in a single-cell scenario, mostly based on the assumption of perfect CSI being available at the BS. The research in [102] showed that the performance of a mMIMO system with  $M$  antennas at the BS and a BS transmit power,  $P_{\text{TX}}/M$ , is equal to the performance of a single input single output (SISO) system with a BS transmit power,  $P_{\text{TX}}$ , without any intra-cell interference. This result indicated that, by using a large number,  $M$ , of BS antennas the BS transmit power,  $P_{\text{TX}}$ , can be proportionally scaled down by a factor,  $1/M$ . This work also suggested that the spectral efficiency in a mMIMO system can be increased by a factor,  $K$ , when serving  $K$  UEs in the same time-frequency resource. The findings in [103], [104] also resonated with these conclusions, reporting that a power reduction proportional to  $1/M$  can be achieved in time division duplexing (TDD) systems<sup>5</sup>, while maintaining non-zero rates, as the number,  $M$ , of antennas grows to infinity. In this way, the energy efficiency of the system can be monotonically increased with the number,  $M$ , of antennas, without any trade-off. This was a promising result, but it is important to mention that it was obtained with significant assumptions in the BS power consumption model.

<sup>5</sup>The power reduction is proportional to  $1/\sqrt{M}$  in the case of imperfect CSI.

Soon after, further developments in this area of research showed that the energy efficiency bounds in mMIMO systems are hidden behind more complex BS power consumption models, and that inaccuracies and/or oversimplifications, not reflecting the essence of mMIMO hardware implementations, can lead to misleading practical insights. For example, when not considering the circuit power consumption related to running a larger number of antennas, as it was the case in [102]–[104], one can be let to believe that an unbounded energy efficiency can be achieved by adding more and more antennas. Deploying more and more antennas, however, requires additional circuitry, incurring a larger power consumption, which needs to be accurately captured by the analysis to draw the appropriate conclusions. In this line, the pioneering work in [82] considered a more sophisticated—and realistic—mMIMO BS power consumption model, and in turn, found significantly different conclusions to the previously stated ones. Since this paper has become a landmark on the subject, let us explore it further in the following, and analyse the theoretical bounds derived.

Using the more detailed BS power consumption model developed by the authors in [82], and already presented in eq. (6), the total energy efficiency of the uplink (UL) and downlink (DL) in a single-cell mMIMO network was analyzed in such work with respect to

- the total transmit power,  $P_{\text{TX}}^{\text{tot}}$ , accounting for the downlink and the uplink transmit powers,
- the number,  $K$ , of simultaneously multiplexed UEs, and
- the number,  $M$ , of antennas, where  $M \geq K + 1$ .

Remarkably, closed-form expressions for the energy efficiency optimal operating point with respect to each of these parameters, when the other are fixed, were provided for the case where both ZF processing and perfect CSI knowledge are considered. In particular, the authors considered a TDD system, in which the pilot signaling occupies  $\tau^{(\text{ul})}K$  and  $\tau^{(\text{dl})}K$  symbols in the uplink and downlink, respectively, where the inequality,  $\tau^{(\text{dl})}, \tau^{(\text{ul})} \geq 1$ , must be true to enable orthogonal pilot sequences among UEs, and with this model, they provided a formulation of the gross downlink rate, expressed in bit per second, as follows:

$$\bar{R} = B \log(1 + \rho(M - K)), \quad (13)$$

where  $\rho$  is a design parameter proportional to the received SNR. Following such formulation, the total transmit power,  $P_{\text{TX}}^{\text{tot}}$ , required to serve each UE with a gross rate,  $\bar{R}$ , was shown to be:

$$P_{\text{TX}}^{\text{tot}} = \frac{B\sigma^2\rho\mathcal{S}_{\text{x}}}{\eta}K, \quad (14)$$

where  $\sigma^2$  is the channel noise power,  $\mathcal{S}_x$  is a term that accounts for the UE distribution and propagation environment, and  $\eta$  is a term that accounts for the efficiency of the PAs.

From the above formulation, it is important to restate that the value of the design parameter,  $\rho$ , is proportional to the UE SNR, which in turn, is directly proportional to the total transmit power,  $P_{\text{TX}}^{\text{tot}}$ , when considering ZF processing. Thus, finding the optimal total transmit power,  $P_{\text{TX}}^{\text{tot}*}$ , which maximizes the joint UL and DL energy efficiency involves deriving the optimal design parameter,  $\rho^*$ . After some manipulations, in [82], the authors showed that the optimal design parameter,  $\rho^*$ , is lower bounded by:

$$\rho^* \geq \frac{\frac{\eta(\mathcal{C}' + M\mathcal{D}')}{B\sigma^2\mathcal{S}_x} - \frac{\ln\left(\frac{\eta(M-K)(\mathcal{C}' + M\mathcal{D}')}{B\sigma^2\mathcal{S}_x} - 1\right)}{M-K}}{\ln\left(\frac{\eta(M-K)(\mathcal{C}' + M\mathcal{D}')}{B\sigma^2\mathcal{S}_x} - 1\right) - 1}, \quad (15)$$

with

$$\mathcal{C}' = \frac{\sum_{i=1}^3 \mathcal{C}_i K^i + P_{\text{CP}}^{\text{li}}}{K} \text{ and } \mathcal{D}' = \frac{\sum_{i=0}^2 \mathcal{D}_i K^i}{K}, \quad (16)$$

where the terms  $\mathcal{C}_3$ ,  $P_{\text{CP}}^{\text{li}}$ , and  $\mathcal{D}_{i,i \in \{0,1,2\}}$  are BS power consumption model coefficients, defined as in Section III-A, whereas  $\mathcal{C}_1$  and  $\mathcal{C}_2$  are UE power consumption model coefficients. More specifically,  $\mathcal{C}_1$  is the power required by all the circuit components of each single-antenna UE, and  $\mathcal{C}_2$  is the term that accounts for the linear processing at the UE. The bound in eq. (15) shows that the optimal total transmit power,  $P_{\text{TX}}^{\text{tot}*}$ , increases with the load-independent circuit power consumption,  $P_{\text{CP}}^{\text{li}}$ , the power required by all the circuit components of each single-antenna UE,  $\mathcal{C}_1$ , and the power consumed by the transceiver module attached to each antenna,  $\mathcal{D}_0$ . In fact, if the circuit power consumption,  $P_{\text{CP}}$ , is large, then higher total transmit powers,  $P_{\text{TX}}^{\text{tot}}$ , —and in turn, higher UE rates— can be afforded in the system, since the total transmit power,  $P_{\text{TX}}^{\text{tot}}$ , has a small impact on the overall power consumption. This indicates that the optimal strategy to improve the energy efficiency is to increase the total transmit power,  $P_{\text{TX}}^{\text{tot}}$ , with the number,  $M$ , of antennas, not in an arbitrary manner, but while considering the circuit power consumption,  $P_{\text{CP}}$ .

These conclusions are in stark contrast with those in [102]–[104], which as depicted earlier, concluded instead that the BS transmit power,  $P_{\text{TX}}$ , —the downlink part of the total transmit power,  $P_{\text{TX}}^{\text{tot}}$ — can be decreased with the increase of the number,  $M$ , of antennas, while remaining energy efficient, thus implying a linear increase of the energy efficiency with the number,  $M$ , of antennas. This optimistic finding only applies, however, in the idealistic case where the circuit power consumption,  $P_{\text{CP}}$ , plays no —or a negligible role— in the overall power consumption.

Importantly, the analysis in [82] showed that, for a moderate and/or large number,  $M$ , of antennas, the optimal value of the parameter,  $\rho^*$ , can be approximated by:

$$\rho^* \approx \frac{\eta \mathcal{D}'}{2B\sigma^2 \mathcal{S}_x} \frac{M}{\ln(M)}, \quad (17)$$

which shows a quasi-linear relation between the number,  $M$ , of antennas and the total transmit power,  $P_{\text{TX}}^{\text{tot}}$ . This more clearly indicates that, since the circuit power consumption,  $P_{\text{CP}}$ , grows with the number,  $M$ , of antennas, the total transmit power,  $P_{\text{TX}}^{\text{tot}}$ , can be increased to improve the UE rates up to a given extend, before it becomes the limiting factor of the energy efficiency.

Moreover, the study on the optimal number,  $K^*$ , of multiplexed UEs, provided in [82], highlights that, if the power consumption for the beamforming processing,  $P_{\text{SP}}$ , and channel estimation,  $P_{\text{CE}}$ , are negligible, then the optimal number,  $K^*$ , of multiplexed UEs can be approximated as follows:

$$K^* \approx \left\lfloor \left( \mu \sqrt{1 + \frac{U}{(\tau^{(\text{ul})} + \tau^{(\text{dl})}) \mu}} - 1 \right) \right\rfloor, \quad (18)$$

where  $U$  is the channel coherence time (in symbols), and

$$\mu = \frac{P_{\text{CP}}^{\text{li}} + \frac{B\sigma^2 \mathcal{S}_x}{\eta} \rho K}{\mathcal{C}_1 + \bar{\beta} \mathcal{D}_0}, \quad (19)$$

where  $\bar{\beta}$  is the ratio of the number,  $M$ , of antennas to the number,  $K$ , of multiplexed UEs, (i.e.,  $\bar{\beta} = M/K$ ),

From eq. (18), we see that the optimal number,  $K^*$ , of multiplexed UEs decreases with the power required by all the circuit components of each single-antenna UE,  $\mathcal{C}_1$ , and the power consumed by the transceiver module attached to each antenna,  $\mathcal{D}_0$ . On the contrary, the optimal number,  $K^*$ , of multiplexed UEs increases with the load-independent circuit power consumption,  $P_{\text{CP}}^{\text{li}}$ , the total transmit power  $P_{\text{TX}}^{\text{tot}}$  (proportional to  $\rho$ ), the noise power,  $\sigma^2$ , and the parameter,  $\mathcal{S}_x$ . Note that this last term,  $\mathcal{S}_x$ , increases proportionally with the coverage radius of the cell, meaning that a larger number,  $K$ , of multiplexed UEs must be served when the coverage area increases in order to maximize the energy efficiency.

In addition, the study on the optimal number,  $M^*$ , of antennas, provided in [82], also indicates that such number,  $M^*$ , is lower bounded by:

$$M^* \geq \frac{\frac{B\sigma^2 \mathcal{S}_x}{\eta \mathcal{D}'} \rho + \frac{\mathcal{C}'}{\mathcal{D}'} + K - \frac{1}{\rho}}{\ln(\rho) + \ln\left(\frac{B\sigma^2 \mathcal{S}_x}{\eta \mathcal{D}'} \rho + \frac{\mathcal{C}'}{\mathcal{D}'} + K - \frac{1}{\rho}\right) - 1} - \frac{1}{\rho}. \quad (20)$$

This bound indicates that the optimal number,  $M^*$ , of antennas increases with the load-independent circuit power consumption,  $P_{\text{CP}}^{\text{li}}$ , and the power required by all the circuit components of each single-antenna UE,  $\mathcal{C}_1$ , whereas it decreases with the power consumed by the transceiver module attached to each antenna,  $\mathcal{D}_0$ .

Importantly, when the design parameter,  $\rho$ , becomes large, the lower bound given in eq. (20) can be approximated as:

$$M^* \approx \frac{B\sigma^2\mathcal{S}_x}{2\eta\mathcal{D}'} \frac{\rho}{\ln(\rho)}, \quad (21)$$

which shows that there is an almost linear scaling law of the optimal number,  $M^*$ , of antennas with respect to the design parameter,  $\rho$ , in its high value regime, and thus with respect to the total transmit power,  $P_{\text{TX}}^{\text{tot}}$ .

It should also be noted the linear dependence of the optimal number,  $M^*$ , of antennas with the UE distribution and propagation environment, captured by the variable,  $\mathcal{S}_x$ , which implies that a larger optimal number,  $M^*$ , of antennas is needed, as the size of the coverage area increases, since the variable,  $\mathcal{S}_x$ , increases with the cell radius.

For the sake of clarity, Fig. 8 shows the achievable energy efficiency for four different values of the number,  $M$ , of antennas, when varying the number,  $K$ , of multiplexed UEs. Note that the energy efficiency curves are characterized by a concave shape in all the considered antenna configurations, and that the maximum achievable values are highlighted in red. This plot highlights that the optimal number,  $K^*$ , of multiplexed UEs increases sub-linearly with the number,  $M$ , of antennas.

In a similar way, Fig. 9 shows the achievable energy efficiency for different values of the number,  $K$ , of multiplexed UEs, when varying the number,  $M$ , of antennas. The energy efficiency curves have, in this case, a quasi-concave shape, and the maximum achievable values are also highlighted in red. These results confirm that, for a given value of the number,  $K$ , of multiplexed UEs, augmenting the number,  $M$ , of antennas increases the energy efficiency up to a maximum energy efficiency value, where the UE rate gain due to the further increasing the number,  $M$ , of antennas is not sufficient anymore to counterbalance the cost incurred by their associated power consumption.

Finally, it should be noted from Fig. 8 and Fig. 9 that deploying hundreds of antennas to serve a large number of UEs is the optimal solution from an energy efficiency perspective, confirming the energy efficiency-enabler role of mMIMO.



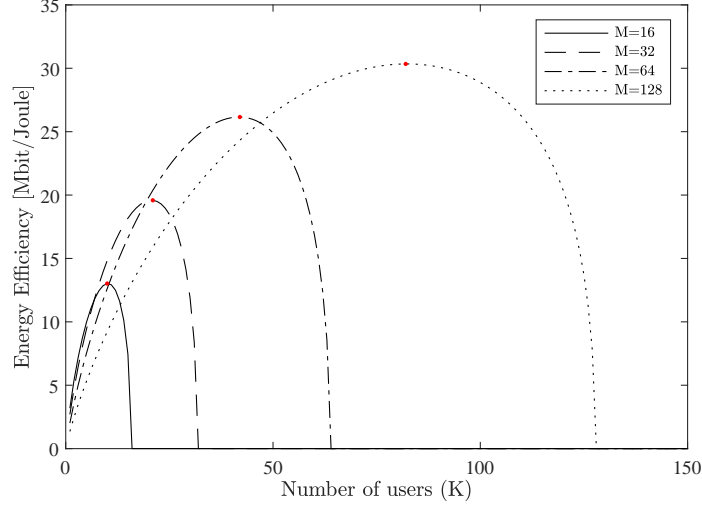


Figure 8. Energy efficiency with respect to the number,  $K$ , of multiplexed UEs for a given number,  $M$ , of antennas. The maximum energy efficiency values are highlighted in red.

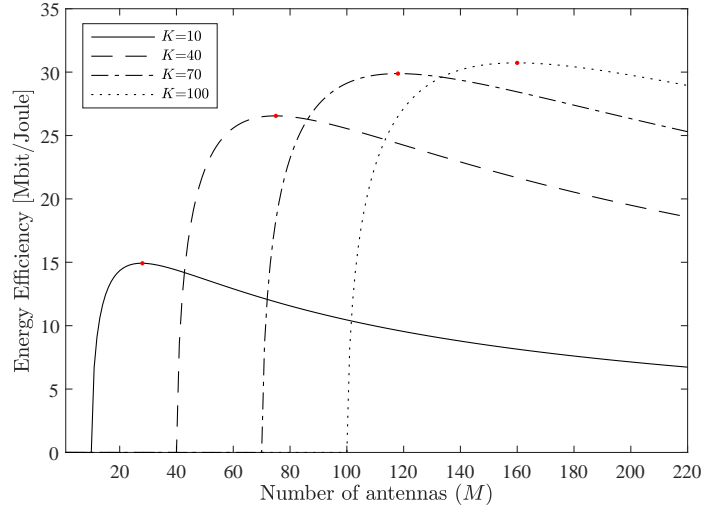


Figure 9. Energy efficiency with respect to the number,  $M$ , of antennas for a given number,  $K$  of multiplexed UEs. The maximum energy efficiency values are highlighted in red.

2) *Trade-offs*: The spectral efficiency, defined as the system throughput per unit of bandwidth, has been historically adopted as the key optimisation metric to optimise mobile network deployments. As energy efficiency has become a new important key performance indicator (KPI) to the operation of 5G networks, the relation between these two metrics is thus of fundamental importance. How much spectral efficiency is trade to realize some energy efficiency gain?

Early works in the literature, not accounting for the circuit power consumption,  $P_{CP}$ , in the

BS power consumption model, concluded that a 10x spectral efficiency improvement could be achieved for a given BS transmit power,  $P_{\text{TX}}$ , when adopting hundreds of antennas at the BS [54]. In this idealized scenario, since the energy efficiency grows proportionally to the number,  $M$ , of antennas, the corresponding energy-spectral efficiency curve is pushed outwards, meaning that both metrics can be simultaneously maximized. However, this insight is not practical, since the circuit power consumption,  $P_{\text{CP}}$ , plays a major role today, as already discussed.

Indeed, as shown earlier, the circuit power consumption,  $P_{\text{CP}}$ , linearly grows with the number,  $M$ , of antennas, and when this number is large, it dominates the BS overall power consumption, implying that the energy efficiency cannot be enhanced, unless the efficiency of the BS hardware is improved accordingly [82]. In this way, the circuit power consumption,  $P_{\text{CP}}$ , breaks the monotonic relation between energy efficiency and spectral efficiency, and makes these two metrics not consistent and conflicting with each other. For this reason, their trade-off must be carefully analyzed, and proper network optimisation techniques need to be developed to strike the right balance between these two metrics.

Studies on such energy and spectral trade-off are often carried out based on optimisation problems, aiming at maximizing the energy efficiency given a spectral efficiency requirement. However, in some more sophisticated approaches, the balance between the energy and the spectral efficiency is achieved by maximizing the resource efficiency (RE) metric [105], where this metric is defined as the weighted sum of the energy efficiency and spectral efficiency, and the weights assigned to the two terms allows to give more or less importance to any of them. It is important to highlight, however, that all such frameworks do not generally provide explicit equations for the energy-spectral efficiency trade-off. Instead, they mostly built on the top of results obtained from tailored optimisation algorithms aimed at solving such problem, which usually turns out to be intricate [106]–[109].

In this line, the fundamental trade-off between the energy and the spectral efficiency has been carefully studied in [109], when considering a single-cell mMIMO system with linear precoding, i.e. ZF and Maximum Ratio Transmission (MRT), and transmit antenna selection. In particular, the BS transmit power,  $P_{\text{TX}}$ , and the number,  $M_a < M$ , of active antennas are jointly considered as a resource to balance the energy and the spectral efficiency, and the adopted BS power consumption model is equivalent to the one introduced in eq. (6). Note, however, that this study has not taken into account the impact of the number,  $K$ , of multiplexed UEs, which may have a significant influence to the trade-off. Importantly, this study has shown that different

number,  $M_a$ , of active antennas leads to different energy efficiency-spectral efficiency curves. In more details, for a given number,  $M_a$ , of active antennas, the energy efficiency is a quasi-concave function with respect to the spectral efficiency, which confirms that the existence a clear trade-off between these two metrics. Their numerical results have also shown that in the low SNR region, which corresponds to a low spectral efficiency, MRT achieves a higher energy efficiency than ZF due to its lower complexity. In the high spectral efficiency regime, ZF outperforms MRT in terms of spectral efficiency, for a given energy efficiency, owing to its ability of canceling intra-cell interference.

As briefly mentioned when discussing the single-cell mMIMO energy efficiency bounds in the previous section, most of the works in literature assume spatially uncorrelated channels and perfect knowledge of the CSI due to tractability reasons, as in the aforementioned study. However, in practical scenarios, spatial channel correlation is likely to appear, favouring more some spatial directions than others due to the propagation environment. In this case, the CSI knowledge at the transmitter becomes fundamental. However, its acquisition is challenging, especially when dealing with the large antenna arrays in the mMIMO case. In TDD systems, the acquisition of downlink CSI can be performed via uplink training by taking advantage of the channel reciprocity. However, the CSI may still be inaccurate due to practical hardware limitations, such as calibration errors in the transceivers [110], and in high mobility scenarios, it can quickly become outdated.

Tackling this challenge, the authors in [107], [108] have explored this problem, and provided analyses of the energy and the spectral efficiency trade-off, considering the knowledge of statistical CSI, instead of an instantaneous one. This type of feedback has the advantage of being stable during longer time periods and to be more easily obtainable by the BS, through long-term feedback or covariance extrapolation at the expense of a lower network capacity.

Particularly, the work in [108] has analysed the single-cell mMIMO downlink case, where one BS with  $M$  antennas simultaneously transmits signals to  $K$  UEs, the channel spatial correlation is modelled using a jointly correlated Rayleigh fading model [111], statistical CSI is available at the transmitter, and the considered BS power consumption model accounts for the BS transmit power,  $P_{TX}$ , and the static circuit power consumption,  $P_{CP}$ . The energy-spectral efficiency trade-off has been investigated by maximizing the RE metric [105], which strikes for a energy-spectral efficiency balance.

Fig. 10 shows the derived trade-off when considering different values of the BS transmit

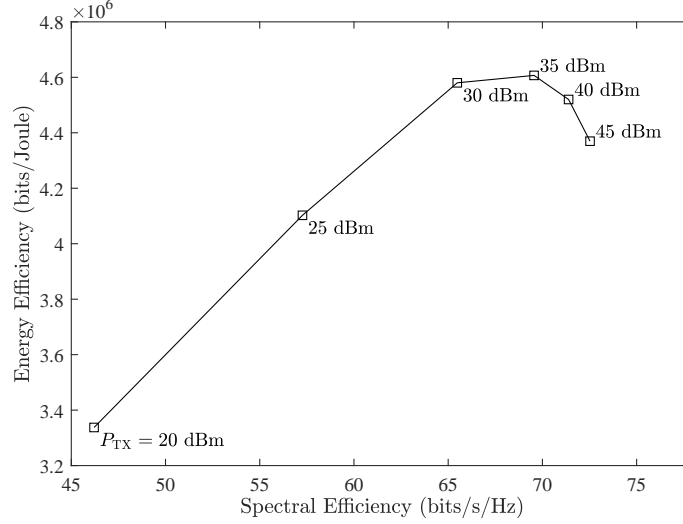


Figure 10. Trade-off between energy efficiency and spectral efficiency for different values of the BS transmit power,  $P_{TX}$

power,  $P_{TX}$ . Note that the energy-spectral efficiency curve is characterized by a concave shape. In particular, the energy and the spectral efficiency can be jointly augmented by increasing the BS transmit power,  $P_{TX}$ , until reaching, in this case, the optimal energy-spectral efficiency point with a BS transmit power,  $P_{TX} = 35$  dBm. After reaching such optimal point, which corresponds to the maximum achievable values of both energy and spectral efficiency, the BS transmit power,  $P_{TX}$ , becomes the dominating consuming factor. Thus, increasing the BS transmit power,  $P_{TX}$ , allows to increase the spectral efficiency only at the expense of a reduced energy efficiency.

Table V

SUMMARY OF SINGLE-CELL ENERGY EFFICIENCY BOUND AND TRADE-OFFS LITERATURE

Paper	Type	KPI	Parameters
[101]	bound	EE	bandwidth, BS transmit power
[82]	bound	EE	transmitting antennas, multiplexed UEs, BS transmit power
[109]	trade-off	EE-SE	transmitting antennas, BS transmit power
[108]	trade-off	RE	BS transmit power
[107]	trade-off	RE	BS transmit power

Finally, before concluding this section, it should be noted that large research efforts have also being spent on the understanding of both practical precoding and UE scheduling techniques, while considering single-cell scenarios, to enhance the energy efficiency of mMIMO systems. The optimal precoding to achieve optimal energy efficiency under ideal and known channel conditions has

been derived in [112]. Optimal energy efficient precoding schemes, while considering imperfect CSI at the transmitter, have also been studied in [113]. UE scheduling algorithms that take channel orthogonality into account, avoiding to schedule two *nearby* UEs, have been proposed in [114]–[117]. Other more experimental approaches considered to increase energy efficiency have been modulation diversity [118], cognitive radios [119], and spatial modulation [120].

### B. Multi-cell scenario

In this section, we focus —and survey— the latest most representative developments on the understating of the energy efficiency in large-scale multi-cell mMIMO networks, introducing the most relevant tools used to carry the analyses out and differentiating among the uplink and downlink case. In contrast to the single-cell mMIMO case, it should be noted that the multi-cell mMIMO one is not so well understood as of today, due to its much higher complexity. Large-scale networks are in general hard to model (see Fig. 11), due to their

- complex topology,
- evolving UE distributions,
- dynamic traffic demands,
- fluctuating wireless channels,
- sophisticated protocols and algorithms, and
- large number of parameters to tune.

This poses a real challenge on their theoretical comprehension. As a result, there are no available explicit —and general— closed-form expressions that describe the energy efficiency bounds and trade-offs of a multi-cell mMIMO network in a holistic manner. Instead, the research is scattered and focused on particular aspects of the system, which together with some of the assumptions taken, have helped to increase the tractability of the problem, and derive some initial insights on the energy efficiency problem. Further research on the topic is needed.

*1) Available Mathematical Tools:* Given that the comprehension of the power consumption of a mMIMO BS has reached some degree of maturity (see Sections III and V-A), one of the main difficulties to unlock a fundamental understanding of the energy efficiency in multi-cell mMIMO networks is the derivation of its capacity. Stochastic geometry [121], the state-of-the-art tool for the theoretical analysis of multi-cell networks, particularly small cell ones [122]–[125], has been recently started to be used to address this issue.

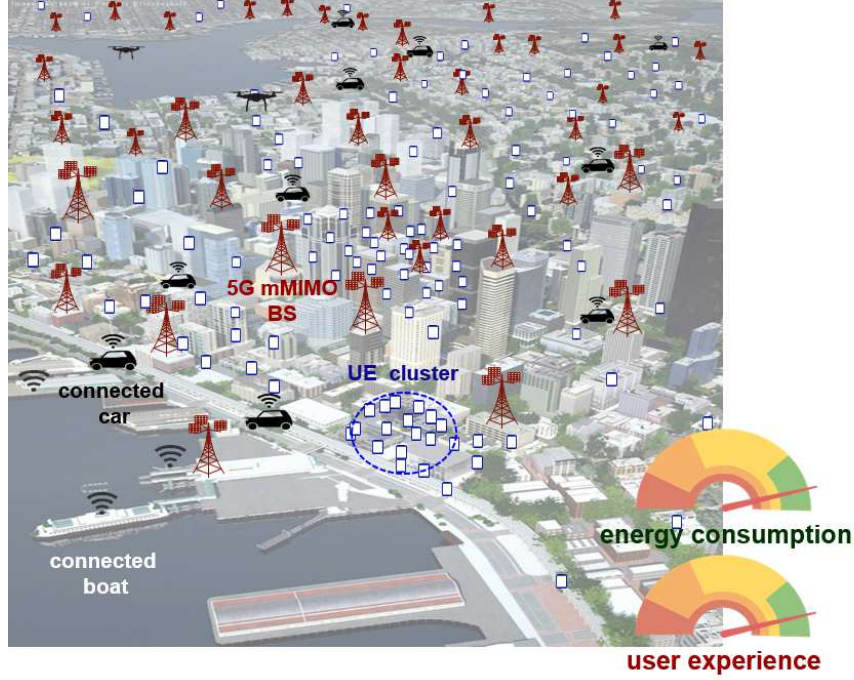


Figure 11. Example of a large-scale multi-cell mMIMO network.

Embracing the randomness of today's deployments, the work in [126] has analysed the uplink mMIMO performance, considering a large-scale multi-cell network and the pilot contamination problem. This paper has presented a mMIMO network capacity scaling law as a function of the number of antennas and multiplexed UEs per BS, and investigated the performance gains attainable through a practical fractional uplink pilot reuse, used to mitigate pilot contamination. It is important to note, however, that significant assumptions were taken for tractability reasons. The study assumed that there was a large number of UEs in each BS at all times, and thus that all BSs in the network were active and that all uplink pilots available were in use in all BSs. This makes it difficult to study off-peak hours where energy savings are more likely to be harvested. Moreover, a pure non-line-of-sight (NLoS) path loss model with Rayleigh multi-path was considered, which cannot capture the important effect of channel directionality on mMIMO performance, as described in the previous section. Unfortunately, even though these important assumptions and simplifications, the resulting expressions are still not tractable, requiring few folds of integrals, making difficult to infer relationships among system parameters. This is particularly true when capacity expressions need to be coupled with complex BS power consumption models, as those presented in Section III.

Using similar stochastic geometry tools, the authors in [127] studied the downlink mMIMO performance, while considering a heterogeneous network comprised of mMIMO macrocells and single-antenna small cells, together with the effect of line-of-sight (LoS) and NLoS transmissions, pilot contamination, and cross-tier interference. However, similar as in the previous case, a fully loaded network is considered with all uplink pilots at use, which significantly affects the pilot contamination, and does not allow to analyse low and medium traffic load scenarios. In addition, important assumptions also revolve around the use of Rayleigh fading for the LoS transmissions. Some of these issues have been recently addressed by the research in [128], where pilot allocation schemes are considered with the objective of reducing the pilot contamination. However, the expressions are still too complex to infer parameter relationships without a numerical evaluation.

2) *Uplink mMIMO network deployment perspectives:* Aware of such complexities, the authors in [129] proposed a tractable stochastic geometry-based analysis of the energy efficiency of a TDD multi-cell mMIMO network subject to QoS constraints, while using a simplified but yet complete system model. In more detail, the authors targeted at maximizing the uplink energy efficiency of such multi-cell mMIMO network, while ensuring a minimum uplink spectral efficiency to the average UEs, and used this formulation to obtain some practical insights into the problem. The adopted homogeneous Poisson point process (HPPP)-based system model<sup>6</sup> accounted for

- the BS density,  $\lambda$ ,
- the number,  $M$ , of antennas per BS,
- the number,  $K$ , of multiplexed UEs per transmission time interval (TTI) at each BS,
- an idealised uplink fractional power control,
- imperfect channel estimation through pilot contamination<sup>7</sup>,
- hardware impairments, modelled as a reduction of the signal power by a factor,  $1 - \epsilon^2$ ,
- maximal ratio combining (MRC) received filters at the BS,
- single-antenna UEs, and
- an uplink pilot reuse scheme.

<sup>6</sup>It should be also noted that this general system model allows to compare mMIMO setups, with few BSs and many antennas per BS, to small cell ones, with many BSs and few antennas per BSs, thus providing guidance on the design of future green wireless networks, from the uplink perspective.

<sup>7</sup>Rayleigh fading was still assumed, and thus the effect of spatial correlation was ignored in this analysis.

Importantly, the complexity of calculating the average spectral efficiency of the network as the sum of the spectral efficiencies of all UEs through this framework was acknowledged, indicating the need for heavy numerical evaluations of integrals. To address this issue, and obtain explicit expressions, the authors focused on the performance of the average UE instead, and derived the following tractable —but yet tight— lower bound for its uplink signal to interference plus noise ratio (SINR):

$$\text{SINR}_{\text{UL}} = \frac{M(1 - \epsilon^2)^2}{(K + \frac{\sigma^2}{\zeta})(1 + \frac{2}{\beta(\alpha-2)} + \frac{\sigma^2}{\zeta}) + \frac{2K}{\alpha-2}(1 + \frac{\sigma^2}{\zeta}) + \frac{K}{\beta}(\frac{4}{(\alpha-2)^2} + \frac{1}{\alpha-1}) + M(1 - \epsilon^2)(\frac{1}{\beta(\alpha-1)} + \epsilon^2)}, \quad (22)$$

where  $\alpha$  is the path loss exponent,  $\beta$  is the pilot reuse factor,  $\zeta$  is the path loss compensation power control coefficient, and  $\sigma^2$  is the noise power.

Leveraging this expression, the authors formulated the uplink average UE spectral efficiency and the resulting uplink area spectral efficiency (ASE), and with that, they derived the uplink area power consumption (APC) of the multi-cell mMIMO network, using a linear version of the BS power consumption model presented in (7), i.e.,

$$\text{APC}_{\text{UL}} = \lambda \left( \left( 1 - \frac{\beta K - 1}{S} \right) \frac{\zeta \omega \Gamma(\frac{\alpha}{2} + 1)}{\eta (\pi \lambda)^{(\frac{\alpha}{2})}} K + P_{\text{CP}}^{\text{li}} + \mathcal{C}_1 K + \mathcal{D}_0 M + \mathcal{D}_1 M K \right) + \mathcal{A} \cdot \text{ASE}, \quad (23)$$

where  $S$  is coherent block length, which is related to the channel coherence time,  $U$ , in eq. (18),  $\eta$  is the PA power efficiency,  $\Gamma()$  is the Gamma function, and ASE is the area spectral efficiency.

With these formulations, the authors defined an optimisation problem to find the most uplink energy efficient network deployment, while provisioning the average UE with a minimum SINR. Through some mathematical manipulations detailed in [129], the authors derived

- the uplink spectral efficiency feasibility,
- the optimal uplink pilot reuse factor,  $\beta^*$ ,
- the optimal BS density,  $\lambda^*$ ,
- the optimal number,  $K^*$ , of multiplexed UEs per TTI at each BS, subject to a given ratio,  $\frac{M}{K}$ , of the number,  $M$ , of antennas to the number,  $K$ , of multiplexed UEs, and
- the optimal number,  $M^*$ , of antennas per BS, subject to a given number,  $K$ , of multiplexed UEs,

and demonstrated that reducing the cell size is beneficial for energy efficiency, but that such positive effect —increasing the BS density— saturates when the circuit power consumption dominates over the transmission power. Their results also showed that adding antennas to the



BS to bring it to the mMIMO regime also enhances the energy efficiency<sup>8</sup>. In more detail, their numerical examples on a typical scenario resulted in the maximum energy efficiency when having 91 antennas and 10 UEs multiplexed per BS, which resembles a mMIMO —and not a small cell— setup. It should be noted that the energy efficiency gains, in this case, mostly came from the intra-cell interference suppression provided by mMIMO, and by sharing the circuit power costs among the multiple multiplexed UEs. Moreover, the analysis showed that a large pilot reuse factor can be used to protect the network against inter-cell interference, and that it can be tailored to guarantee a certain average UE spectral efficiency.

Using a different modelling tool than stochastic geometry, based on numerical evaluations, but also focusing on the uplink energy efficiency, the authors in [130] provided an analysis of the area energy efficiency (AEE) and the ASE trade-off for different system parameters, such as the pilot reuse ratio and number of antennas and multiplexed UEs per BS. Importantly, even if this work does not focus on minimising power consumption, but maximising the AEE, it reaches similar general conclusions than those of [129]. The multi-cell mMIMO network always performs better in terms of ASE with an increasing number of antennas. However, adding more antennas or multiplexed UEs might not achieve the optimal AEE. The reason is that the power consumed by the transceiver module attached to each antenna and the related signal detection and processing have a non-negligible effect on the total BS power consumption. In more detail, their results have shown that, when considering smaller ASE targets, a lower number of antennas (see Fig. 12a) and multiplexed UEs (see Fig. 12b) at the BS suffices to achieve the optimal AEE. However, more antennas and multiplexed UEs are required to satisfy higher ASE requirements, which makes the network less energy efficient, resulting in a smaller AEE, as soon as the transmit power dominates the circuit and processing power consumption. Finally, in this work, the authors have derived the pilot-to-data power ratio that maximizes the AEE, and studied how such parameters affects the AEE and the ASE trade-off (see Fig. 12c). The study has also shown that in relevant scenarios, the optimal number of multiplexed UEs for maximizing the AEE is much smaller than half of the coherent clock length, as it is for maximizing the ASE [54].

<sup>8</sup>These conclusion are inline with that presented in the analysis of the single-cell mMIMO case in the previous sections, indicating that the optimal strategy to improve the energy efficiency is to increase the total transmit power,  $P_{\text{TX}}^{\text{tot}}$ , with the number,  $M$ , of antennas, not in an arbitrary manner, but while considering the circuit power consumption,  $P_{\text{CP}}$ .

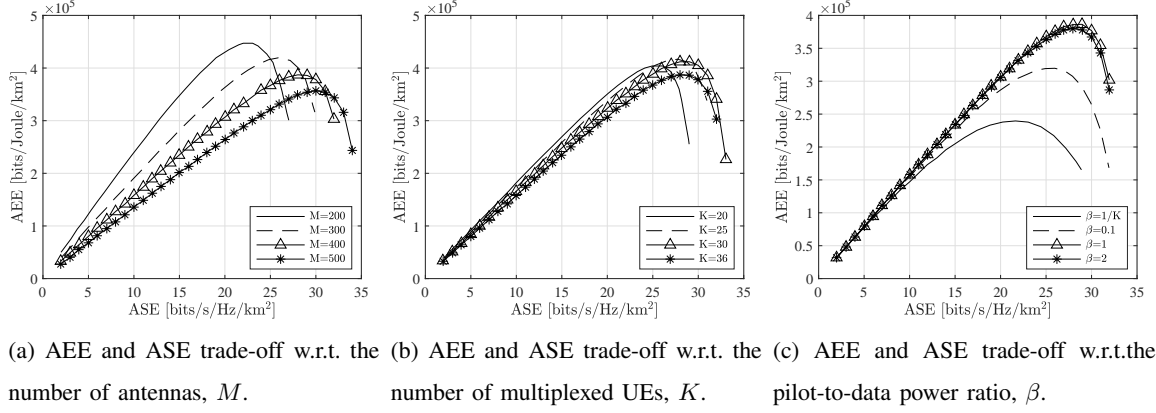


Figure 12. Multi-cell AEE and ASE trade-offs

3) *Downlink mMIMO network deployment perspectives:* Using a similar stochastic geometry approach and BS power consumption model as in [129], the authors in [131] extended the previous work to the downlink case, aiming at optimising the downlink energy efficiency of a TDD multi-cell mMIMO network, while providing a minimum spectral efficiency to the average UE. It is important to note that perfect CSI was assumed in this case due to the complexity of modelling in the same framework both the channel estimation phase in the uplink and the data transmission phase in the downlink<sup>9</sup>. As a result, the effect of pilot contamination was neglected, decreasing the accuracy of the model. ZF precoders at the BS and single-antenna UEs were considered. Importantly, it should be noted that embracing the same methodology as in [129], the authors also focused their analysis on the performance of the average UE, and derived the following tractable lower bound for its downlink SINR:

$$\text{SINR}_{\text{DL}} = \frac{(1 - \epsilon^2)(M - K)}{\frac{2K}{(\alpha-2)} + \epsilon^2(M - K) + \frac{\Gamma(\alpha/2+1)}{(\pi\lambda^2)} \frac{\omega\sigma^2}{\rho}}, \quad (24)$$

where  $\rho$  now represents the downlink transmit power allocated by the BS to the average UE.

With such expression, and using the corresponding downlink APC model, shown in the following for the sake of clarity:

$$\text{APC}_{\text{DL}} = \lambda \left( \frac{K\rho}{\eta} + P_{\text{CP}}^{\text{li}} + \mathcal{C}_1 K + \mathcal{D}_0 M + \mathcal{D}_1 MK \right) + \mathcal{A} \cdot \text{ASE}, \quad (25)$$

<sup>9</sup>Such downlink dependency on the uplink is the main reason why the theoretical downlink energy efficiency of mMIMO networks has been less rigorous studied.

the authors derived the following optimal operation points by following similar steps as in the uplink counterpart work, i.e.,

- the optimal downlink transmit power per UE,  $\rho^*$
- the optimal BS density,  $\lambda^*$ ,
- the optimal number,  $K^*$ , of multiplexed UEs per TTI at each BS, subject to a given ratio,  $\frac{M}{K}$ , of the number,  $M$ , of antennas to the number,  $K$ , of multiplexed UEs, and
- the optimal number,  $M^*$ , of antennas per BS, subject to a given number,  $K$ , of multiplexed UEs.

The analysis of the obtained closed-form expressions showed that the same conclusions obtained from the uplink analysis apply to the downlink one. The optimal energy efficiency is achieved by a mMIMO-like deployment, where in their particular example, the optimum number of antennas and multiplexed UEs per BS are 193 and 21, respectively. Note that the results for the downlink case in the section and those for the uplink one in the previous section differ due to the different network requirements and power consumption values.

These uplink and downlink results advocate for mMIMO deployments and their dimensioning optimisation, according to end-users' QoS, as an important tool to increase energy efficiency in 5G networks. Using an inadequate number of BS or antennas per BS to meet a given end-users' QoS can result in highlight suboptimal energy efficiency performances. In the following section, we provide more details on how antenna selection and advanced sleep modes can be also be further leveraged to increase energy efficiency in a large-scale network.

Finally, before concluding this section, it is important to highlight that, from an optimisation perspective, a large body of research exists on the development of power control algorithms for energy efficiency maximization in multi-cell mMIMO networks. In [94], systematic approaches to solve energy efficiency maximization problems are extensively discussed. In this regard, the framework presented in [132] has provided network- and UE-centric downlink power control algorithms, where minimum rate constraints are imposed and the SINR takes a general form, able to deal with complex mMIMO systems/configurations. Centralised algorithms are also developed, which are guaranteed to converge, with affordable computational complexity, to a Karush–Kuhn–Tucker point of the considered non-convex optimisation problem. Building on such framework, the work in [133] has proposed a framework to compute suboptimal power control strategies with even more affordable complexity. This is achieved by jointly using

fractional programming and sequential optimisation. Numerical evidence has shown that such sequential fractional programming framework achieves global optimality in several practical communication scenarios.

## VI. NETWORK ADAPTATION TO QoS REQUIREMENTS

As motivated previously, future wireless communication systems require efficient hardware and mechanisms that enable the adaption of the network functionalities and parameters to the load variations in an on-line manner in order to avoid excessive energy consumption, while ensuring end-users' QoS. These enabling technologies can be classified, for example, by observing the time-scale and the domain in which they operate, e.g., time, frequency, or spatial (antenna) domains. Time-domain mechanisms refer to those solutions that operate in the time scale of the 3GPP NR frame, and take advantage of its lean carrier design, to rapidly (de)activate the hardware components of the BS according to the absence or not of traffic. Frequency domain mechanisms include solutions that adjust the status of the cell —or the number of CCs— to match the cell capacity with the slow variations of the traffic across the day. Finally, considering the abilities of the new energy efficiency enabler in 3GPP NR, i.e., mMIMO, spatial domain solutions can be used to adapt the number of active antenna elements and channels as well as the associated hardware to the cell load.

### A. Time-domain energy saving solutions

In this section, we focus on the energy savings that can be harvested by considering the short-term traffic load variations in a cell, which depend on several factors, such as the number of active UEs, the traffic types, and the interference. To realise such savings, fast adaptation mechanisms, which operate in the 3GPP NR frame time scale, are thus required to dynamically meet the momentary rate requirement with the minimum energy consumption.

In 3GPP LTE, cell DTX can be used for deactivating BS hardware components, such as the PA, when transmissions are absent in a given frame [61]. The benefits of cell DTX are, however, limited by the control signalling required by 3GPP LTE to drive UE cell camping procedures, even in the absence of traffic. In more detail, the 3GPP LTE frame lasts 10 ms, and it is composed by 10 sub-frames, each one including 14 orthogonal frequency division multiplexing (OFDM) symbols with a duration of  $71.4 \mu\text{s}$ . In the unicast mode, cell-specific reference symbols (CRSs) are transmitted in every sub-frame, primary synchronisation channels (PSSs) and secondary

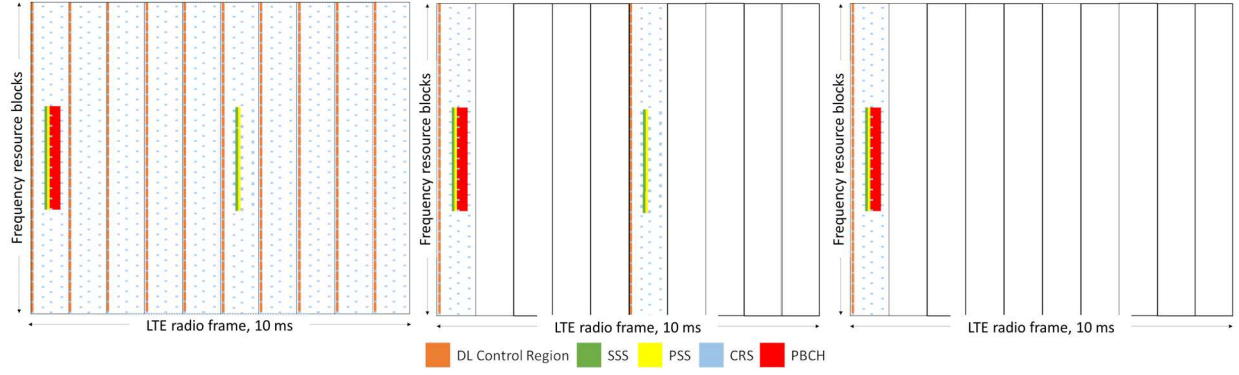


Figure 13. LTE frame for (left) unicast cell; (middle) Rel. 14 MBSFN-dedicated cell; (right) Rel. 14 FeMBMS/unicast-mixed cell.

synchronisation channels (SSSs) every 5 ms, and broadcast channels (BCHs) are repeated in every first sub-frame of a frame (see the left side of Fig. 13). Therefore, the BS is only able to sleep for a few of the OFDM symbols, and needs to wake-up one OFDM symbol before the transmission of any control signal. In this case, cell DTX can achieve at most a 33% sleep ratio at zero load [64].

To allow longer sleep periods in 3GPP LTE, the use of the MBSFN frame was proposed, which is a feature introduced to enable mobile television broadcasting, characterized by the need of less frequent signalling. To standardise such feature, the 3GPP evaluated in [134] both the sleep ratio (at symbol level and sub-frame level) and the sleep duration, when using

- Rel. 14 FeMBMS/unicast-mixed cells, in which two out of ten sub-frames, i.e. sub-frames 0 and 5, contain unicast control signaling (see the central plot in Fig. 13), and
- LTE Rel. 14 MBSFN-dedicated cells, where only one non-MBSFN sub-frame with standard unicast signaling is transmitted every 40 ms (see the right side of Fig. 13).

The results from the 3GPP studies showed that, in FeMBMS/unicast-mixed mode, a BS can stay in energy saving mode for up to 4 ms, which leads to an 80% sleep ratio. Importantly, in MBSFN-dedicated mode, a BS can sleep even further up to 39 ms, which results into a 93.75% sleep ratio.

As discussed in Section II-B, in contrast to 3GPP LTE, 3GPP NR is characterized by a user/data-specific signalling instead of a cell-specific one —the lean carrier (see Fig. 14). Specifically,

- The CRS is not used anymore in 3GPP NR, and a synchronization signal (SS) burst set,

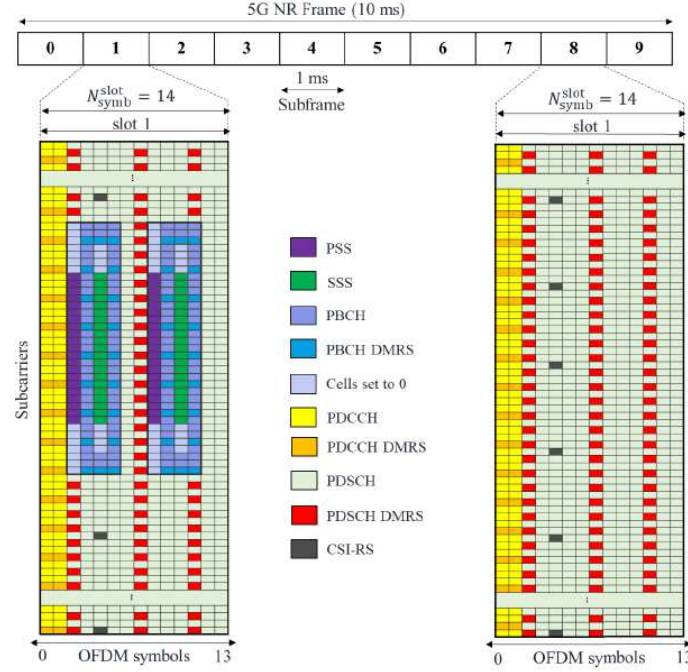


Figure 14. NR frame structure example [49].

including one or multiple SS block(s) —each one of them in turn comprised of PSS, SSS, and BCH— is transmitted to support UE cell (re)selection and handover procedures with a larger periodicity, i.e., 5, 10, 20, 40, 80, and 160 ms [32].

- Since the CRS is not used, CSI acquisition procedures has also been redesigned, and on demand CSI-RSs are reused —and further extended— to provide support for beam and mobility management as a complement to the SS-block.
- The minimum required system information (SI) broadcast in 3GPP NR has also been reduced with respect to 3GPP LTE, and the part not strictly necessary for network entry is transmitted on-demand now [135].
- Moreover, in 3GPP NR, a single-antenna port can be used to transmit the mandatory control signals, while, in LTE, all the antenna ports are used to transmit such mandatory control signals [64].

This lean carrier design enables both longer sleeping periods and larger sleep ratios, whose particular values depend on the specific system numerology, i.e., subcarrier spacing, the number of SS blocks per SS burst set, and the SS burst set periodicity. In more detail, when considering a subcarrier spacing of 15 KHz and two SS blocks per SS burst set, a 3GPP NR cell can stay

in sleep mode up to 19 ms, which leads to a sleeping ratio of 95% for a SS burst set periodicity of 20 ms. Importantly, when the SS burst set periodicity is maximised to 160 ms, a 3GPP NR cell can stay in sleep mode up to 159 ms, which leads to a sleeping ratio of 99.38% [134].

It is important to note that when a BS enters in long sleeping periods, larger energy savings can be achieved, also because more hardware components can be switched off. According to [136], multiple BS sleep states can be defined in this line, where each sleep mode is associated to a given sleeping period duration. As a rule of thumb, all the hardware elements that can enter and exit the sleep mode fast enough with respect to the sleep mode duration can be easily deactivated in such period, while the components having a longer latency need to remain active. In more detail, and to give an example,

- in sleep mode 1 (i.e., cell DTX [61]), characterized by a duration (deactivation plus reactivation time) of  $71 \mu\text{s}$ , the PA and some components of the digital BBU and the analog front-end (FE) are deactivated.
- In sleep mode 2, which has a minimum duration of 1 ms, additional components of the analog FE are switched off.
- In sleep mode 3, which has a minimum duration of 10 ms, the BS additionally deactivates the PA, all the digital BBU processing, and almost all the analog FE (except the clock generator).
- Finally, in sleep mode 4, which has a minimum duration of 1 s, only the wake-up functionalities are maintained [137].

Interested readers should note that the complete list of BS elements that can be switched off for each sleep mode can be found in [138].

To assess the positive impact of such different sleep modes on energy efficiency, a new BS power consumption model was proposed in [139], i.e.,

$$P_{\text{BS}} = \begin{cases} P_{\text{TX}} + P_{\text{CP}}, & \text{if } P_{\text{TX}} > 0, \\ \delta_s P_{\text{CP}}^{\text{li}}, & \text{if } P_{\text{TX}} = 0 \text{ and sleep mode is active,} \end{cases} \quad (26)$$

where  $P_{\text{TX}}$ ,  $P_{\text{CP}}$ , and  $P_{\text{CP}}^{\text{li}}$  are the transmit power, the circuit power, and the load independent part of the circuit power consumption, respectively, and  $\delta_s$  is the fraction of the load-independent circuit power consumption,  $P_{\text{CP}}^{\text{li}}$ , required by the cell in sleep mode. In this case, the authors assume that the fraction,  $\delta_s$ , is equal to 0.84, 0.69, and 0.29 for sleep mode 1, sleep mode 2, and sleep mode 3, respectively. For sleep mode 4, the fraction,  $\delta_s$ , can be lower than 0.1 [136].

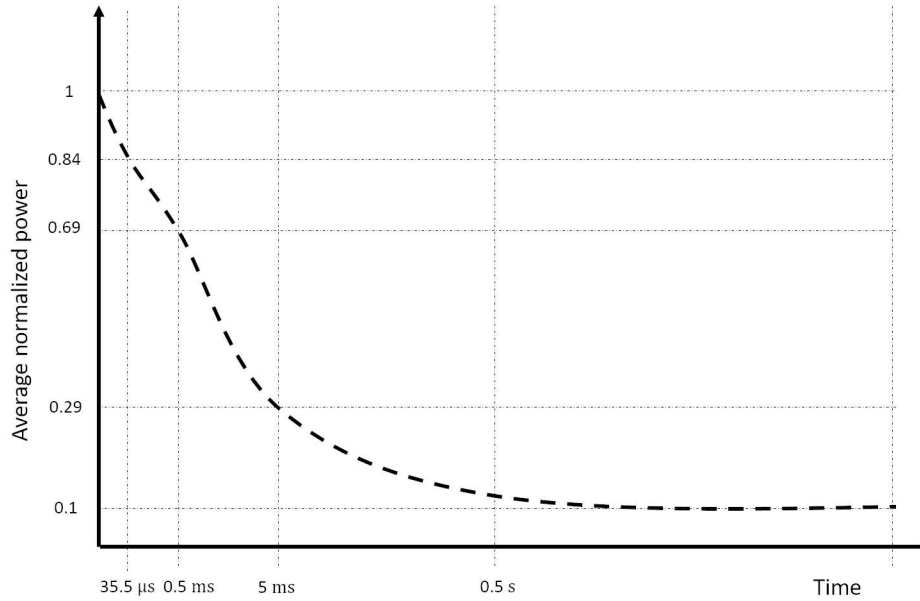


Figure 15. Power consumption trend as the BS enters in successive sleep modes [136]. Activation time is assumed to be equal to the half of the minimum sleep duration [137].

However, current 3GPP NR implementation cannot realise this mode of operation, as it requires one second of continuous sleeping period.

In periods with absence of traffic, a BS can go through the presented sleep modes subsequently to reduce its energy consumption. This process is often referred as ASM (see Fig. 15). When the cell load rises and UE traffic appears, such UE traffic is buffered, and the BS has to immediately switch on its functionalities, and serve the required data to satisfy the end-user QoS requirements. However, it should be noted that, since hardware activation and deactivation times are not negligible, and their lengths increase with the number of involved hardware components [137], ASM may increase the UE perceived latency, and this can accordingly affects the UE throughput [140] [141]. Therefore, there is the need for optimising the path between different sleep modes, and proactively activate the BS components in order to limit performance losses.

The work in [141] has proposed the use of dedicated timers to control when to deactivate components and go into deeper sleep modes. The authors have highlighted that these timers should depend on the type of traffic carried out by each single BS, and to make a more flexible usage of the ASM, they have designed a RL model, based on Q-Learning, to optimise the



duration of each sleep state. Energy savings and experienced delay are balanced using this technique, using as enabler the average packet inter-arrival time. Importantly, their results have shown that it is possible to implement ASM and achieve significant energy savings, even with stringent delay constraints, for medium and low load scenarios. In more detail, up to 80% energy savings can be obtained when replacing 3GPP LTE with 3GPP NR technology and using the proposed ASM.

Nevertheless, it should be noted that this type of scheme relies on a continuous exchange of network signalling, and may impact, e.g., the performance of cell (re)selection processes [142]. More work is thus needed in this direction to understand of how ASM impacts the network load distribution, the resulting inter-cell interference, the related radio resource management (RRM) procedures, and finally the end-users' QoS.

### *B. Carrier-domain energy saving solutions*

In this section, in contrast to the previous one, we focus on the energy savings that can be harvested by considering the long-term traffic load variations in the network. For example, in most of the cells, the traffic daily profile shows a regular trend, with low load periods early in the morning, medium loads during the work-hours and high data rate in the late evening (see Fig. 16). Weekends may be characterized by lower traffic demands with respect to workdays. As a result, since mobile networks are sized to satisfy peak time traffic, energy may be wasted during low and medium load periods, and thus energy saving mechanisms able to adapt, the network configuration to this long-term traffic load variations are necessary.

Overall, to realise these longer-term energy saving mechanisms, different approaches may be considered, i.e. intra-site, Inter-site, and Inter-RAT energy saving me [143], which are further discussed in the following.

*1) Intra-site energy saving mechanisms:* In the first case, intra-site energy saving, a BS may activate energy saving mechanisms to locally adapt its capacity to traffic requirements. At this level, one possibility is to control the number of active cells/sectors [144], the number of CCs active in each sector, if CA is implemented [79], and/or the transmission bandwidth [145].

The work in [144] has investigated the impact of cell-level and sector-level switch off patterns on the network performance, considering hexagonal tri-sectorial cell layouts and UEs uniformly distributed in the network, according to a Binomial point process. Specifically, the authors have compared the performance of different switch off patterns in terms of number of served UEs,

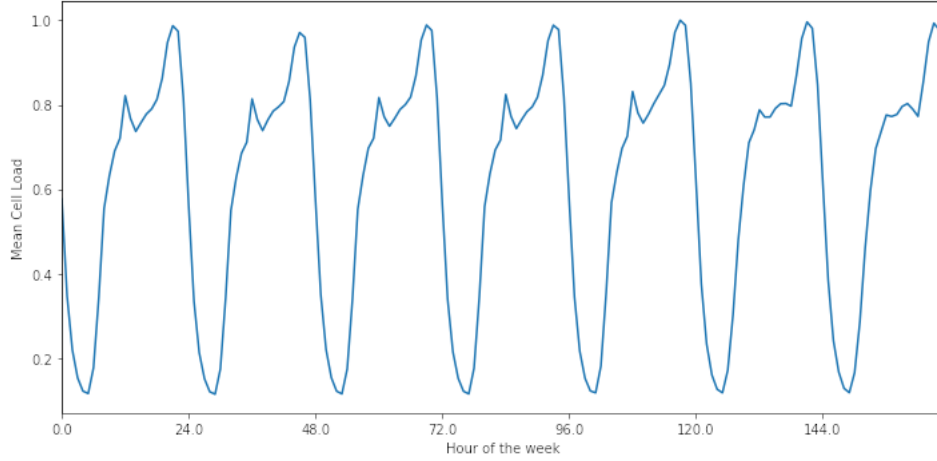


Figure 16. Normalized weekly load for a typical cell in a dense urban scenario.

spectral efficiency, and energy efficiency. Results indicate that the energy savings of sector-level patterns importantly depend on the hardware shared among the sectors of each site, such as cooling and BBU processing equipment. The authors' analysis has shown that, out of the twenty-six investigated patterns, those that activate only one out of three sectors are particularly beneficial.

To improve the system energy efficiency, besides switching off the overall cell—or one or more sectors—it is also important to dynamically control the number of active CCs, if CA is available. As discussed in Section III-A1, CA is a 3GPP flagship feature introduced in 3GPP LTE-A, which allows a BS to simultaneously operate on different bands. In 3GPP NR Rel. 15, the dormant state was introduced in CA, such that (de)activation delay for SCells could be reduced, and the set of active CCs could be rapidly adapted to match UEs requirements [45]. In addition, the concept of Bandwidth Part (BWP) was also introduced in Rel. 15 [146]. With this mechanism, when the cell load is reduced, the BS can configure only a part of a given CC for actual transmission/reception, which is referred to as a BWP<sup>10</sup>. Importantly, control and data signalling only occur within this part of the spectrum, enabling thus a reduced power consumption at both the BS and UE sides, as they need to handle/monitor smaller bandwidths. BWP can be (de)activated by a timer, downlink control information (DCI), and/or RRC signalling, which can enable faster bandwidth adaptation with respect to the CA framework. In this context,

<sup>10</sup>For each CC, at most four BWPs can be defined for the downlink and the uplink communications.

the work in [79] investigated the optimal transmit power and CA configuration to optimise the WSEE metric (see eq. (12) in Section III), while satisfying the downlink and the uplink UEs requirements.

It should be noted, however, that these intra-site energy saving mechanisms —whether cell, sector, or CC (de)activation— may have unwanted network side effects. This is because, while reducing energy consumption, they may significantly impact the network layout (i.e., coverage) as well as the load and interference distributions across the network [147]. Turning off a BS, for example, may leave some UE without coverage, and increase the traffic loads of multiple neighbouring BSs. If these BSs operate on the same spectrum band, BS (de)activation will also impact the inter-cell interference pattern, which will also have important consequences on the rank and the modulation and coding scheme (MCS) selection, and thus on packet success rate. To provide a proper network-wide optimisation, and ensure the satisfaction of the end-users' QoS, it is necessary to take these effects into account when adjusting a BS configuration.

2) *Inter-site energy saving mechanisms*: Inter-site mechanisms serve this purpose, operating over multiple neighbouring BSs, in a centralised or a distributed manner, to jointly optimise the use of radio resources and provide energy savings without affecting end-users' QoS. This resource management problem is typically challenging, as it involves multiple network functionalities and complex mathematical formulations. For instance, the authors of [148] investigated how to optimise the network energy efficiency by jointly managing BS activity, UE association and power control in a HetNet with mMIMO capabilities. They modelled this problem using mixed-integer programming, and to address complexity, proposed a sub-optimal centralised scheme where the integer variables (i.e., the cell (de)activation and the UE association variables) are relaxed, and *ii*) the BS activity, UE association, and power control problems are iteratively solved. Since their centralised solution was still characterized by a large complexity, they also proposed a distributed solution based on game theory, which provided lower performance, but it is proven to converge to the Nash equilibrium.

In addition to affect the network performance, energy saving mechanisms can have a detrimental effect on the BS hardware life-time. Specifically, deep and frequent transients between different status lead to large temperature gradients in the involved hardware components, which increase their failure rates, thus augmenting the maintenance costs to fix or replace the BS. The impact due to these long-term energy saving mechanisms can be measured as the acceleration factor, which is defined as the ratio between the failure rate observed by applying such mecha-

nisms over time and the one experience when keeping the BS always active. Recently, the work in [149] has modelled hardware failure rate due to cell switch on/off, and proposed a heuristic to control the statuses of BSs, which minimises the acceleration factor growth over time, while satisfying the end-users' QoS requirements. In contrast to baseline solutions, which maximize the power saving at the cost of increasing the BS failure rate over time, the proposed approach achieves around a 30% of power savings in a 3GPP LTE scenario, while keeping the acceleration factor close to one.

To further avoid excessively frequent status changes of the BSs and associated network performance losses, the BS control policy in charge of (de)activation decisions could consider the load distribution and the manner in which it varies in time and space. To this end, load can either be characterized statistically or using data-driven approaches. For instance, the authors of [150] have considered a dense HetNet, where small cells and UEs are randomly deployed, following a HPPP distribution, and packets arrive to the transmission buffers according to an exponential distribution. Using this model, they have characterized the probability density function of the cell load using a gamma distribution, and used this information to elaborate multiple (de)activation strategies, comparing them in terms of complexity, blocking rate probability, throughput, and energy efficiency.

In the same line, the authors of [151] have proposed a stochastic game, where distinct BS instances in a CRAN platform take advantage of spatial correlation, and jointly estimate the network traffic, exploiting past observations. The CRAN then uses these estimates to decide the status of the remote radio heads (RRHs) in the network, distribute the UEs among the cells, control the RRHs transmit power, and setup cooperative transmission schemes to guarantee that coverage requirements are satisfied. The authors also demonstrated, through a CRAN experimental platform, that the proposed solution using traffic estimations leads to large energy savings with respect to a dynamic BS switching solution [66], which is not aware of the traffic evolution.

Cell zooming has also become a popular inter-cell energy saving mechanism, which consists in reducing the cell coverage of lightly loaded cells, while simultaneously increasing the area covered by neighbouring compensating ones [152] (see Fig. 17). When using this mechanism, topology changes should be smoothly implemented to limit service outage [153]. To face this challenge, the work in [154] has proposed a data-driven approach to optimise the cell zooming mechanism. Specifically, this framework has represented the network through a graph, and used a BS connectivity metric related to user-level data to construct the graph adjacency matrix.

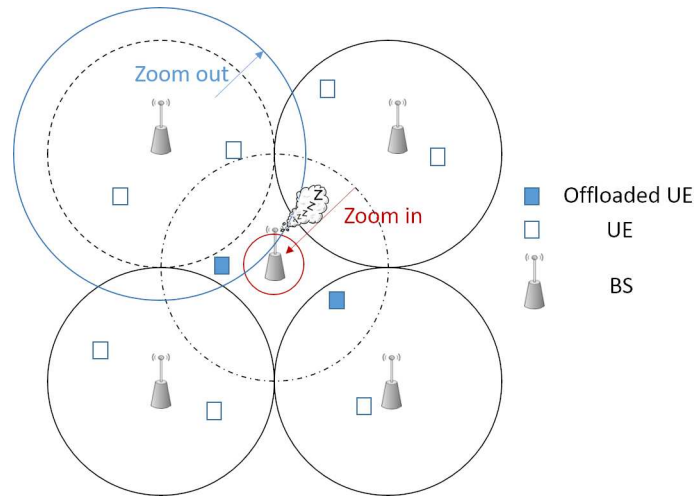


Figure 17. Cell zooming procedure [154].

The authors have run a Markov process on the graph to identify network communities on which implementing the cell zooming. This process is realized through two steps. The first step consists on using a polynomial model to predict the expected community traffic load in the next hour, and the second step operates the cell zooming to identify the BSs to deactivate and how to distribute the load among the active BSs. With respect to baseline solutions based on the knowledge of instantaneous traffic [66], [152], the authors have highlighted that the proposed solution leads to 20% energy saving gains at the cost of increasing the blocking rate only by 0.1%. They have also shown that the achieved blocking rate is greatly affected by the large prediction noise, which results in inaccurate forecasts.

To make the prediction more robust, researchers have also designed more complex frameworks than the previous one based on artificial neural networks (ANNs). The work in [155] has investigated multiple prediction models and evaluated how their errors affect the (de)activation control. In particular, they have considered ANN and long short term memory cell (LSTM) together with other simpler models. Their results have highlighted that the considered models achieve energy savings close to the ideal strategy, which is aware of future traffic trends, leading to a blocking rate lower than 5%. The authors have also noted that prediction errors affect the network QoS only at the time of the day when the (de)activation control is activated. Accordingly, average errors may lead to misleading conclusions at this important time periods, indicating that prediction frameworks should be designed considering the specifically implemented energy

saving algorithm.

3) *Inter-RAT energy saving mechanisms*: It should also be noted that, in the early stage of 5G deployments, 3GPP NR BSs are not uniformly distributed across a city area, and thus there is a need for a tight inter-working between the 3GPP NR network and the underlying 3GPP LTE one. As previously mentioned, 3GPP NR BSs are characterized by a larger power consumption with respect to 3GPP LTE ones, as they integrate more complex hardware to operate on a wider bandwidth and use a larger number of antennas and transceiver modules (due to mMIMO). Therefore, the wireless community is also currently developing inter-RAT energy saving solutions to switch off capacity booster cells i.e., 3GPP NR cells, when the traffic demand is low [156]. In its simpler form, the 3GPP NR cell can autonomously decide to switch off based on its own load. However, as highlighted earlier, this process would allow better coordination across 3GPP NR and LTE BSs to perform mobility management and reactivate capacity booster cells on a need basis [157]. More research is needed in this area.

### C. Antenna-domain energy saving solutions

While the mMIMO frameworks presented Section V have provided general important insights on the deployment of energy-efficient mMIMO networks in both the uplink and the downlink, it should be noted that, once the network is deployed, different approaches can be used to minimise energy consumption. When the traffic load is low, the energy consumption of a mMIMO system may be reduced by using only a subset of the available BS antennas and/or transceiver modules, according to traffic requirements and avoiding resource waste. This type of approaches are referred to as antenna selection or channel shutdown [158], [159].

A number of frameworks have investigated channel shutdown subject to QoE constraints on the basis of multi-path fast fading variations, i.e., activating those BS antennas with favorable channel conditions at each —or a small number of— TTIs [160]–[165]. However, in wideband systems such as 5G with many subcarriers per carrier, it is unlikely that a BS antenna is simultaneously not selected on all such subcarriers. Moreover, antenna selection based on multi-path fast fading also requires all antennas to be activated at least for channel estimation, thus limiting their sleeping time.

Taking a more practical approach, the authors in [166] investigated the antenna selection problem in the downlink based on large-scale fading instead, targeting at finding both the optimal number of BS antennas and their transmit powers to minimise the downlink power consumption

of a mMIMO network. QoS constraints were also considered in the form of a minimum SINR per UE. Both the single-cell and multi-cell scenarios were analysed, where the system model in the latter accounted for multiple BSs, a number of antennas and simultaneously multiplexed UE per BS, and imperfect channel estimation through pilot contamination. It should be noted, however, that the authors adopted a basic BS power consumption model, which depends on the PA efficiency, and is only linear with the number of BS antennas. Signal processing power consumption, for example, as a function of the number of simultaneously multiplexed UEs in each TTI is not considered. For the single-cell case, the work derived the optimal number of BS antennas and their transmit powers in closed-form. Importantly, these expressions prove that, only when the circuit power consumption per BS antenna is small, the minimum BS power consumption can be attained by activating all the BS antennas. Otherwise, the BS can save energy by deactivating some of them. For the multi-cell case, and contrary to the single-cell one, since pilot contamination was considered, a coherent interference term appeared in the SINR formulation, which scales with the number of BS antennas in the pilot-sharing cells, thus limiting the achievable SINRs of UEs. As a consequence, the results indicated that increasing the number of BS antennas still leads to lower transmit powers, but this is not necessarily the optimal to minimise the BS power consumption, as there is a cost associated with using such BS antennas. Unfortunately, the authors concluded that it is hard to obtain closed-form expressions for the optimal number of BS antennas and their transmit powers for this more complex multi-cell case. Instead, they showed that the joint optimisation problem can be relaxed as a geometric programming problem that can be solved efficiently, and suggested that their algorithm can be used to optimally (de)activate antennas depending on the traffic load variations.

The work in [83] has extended these studies investigating how to solve the antenna selection problem, while considering daily load variations in multi-cell mMIMO networks. The authors have computed the distribution of the active UEs in a cell for different network loads using queuing theory. They have then modelled the distributed daily energy efficiency maximization problem, using the active number of BS antennas in each cell as a variable, and solved it through a game theory framework. As a result, a best response algorithm has been proposed, where each BS iteratively selects the strategy that produces its most favorable outcome given other BS strategies. This *selfish* approach has not achieved the global optimum, but lead to a Nash equilibrium without the need for coordination across cells. It should be noted that the authors have not considered specific UE rate requirements. Therefore, their analysis have shown

that, at low loads, their adaptive antenna selection scheme can achieve around 250% of energy savings at the expense, however, of around 50% reduction of the average UE data rate.

Considering both rate and latency requirements, the work in [167] has also recently investigated the power consumption minimisation problem in multi-cell mMIMO networks, by implementing cell DTX (see Section VI-A) in conjunction with precoding and antenna selection. The authors have considered a multiple frame optimisation window, and have proposed a strategy to select the proper precoding technique for each transmission frame such that the total transmission time and latency are minimised. Moreover, they authors have proposed a technique to trade the UE latency for additional energy savings, by reducing the number of active BS antennas used in each frame. Numerical results have highlighted that the proposed adaptive system provides large energy efficiency gains in lightly loaded scenarios without impacting the end-users' QoS.

## VII. MACHINE LEARNING AND DATA-DRIVEN ENERGY EFFICIENCY OPTIMIZATION

As previously discussed in Section II-D, energy efficiency optimisation highly depends on the accuracy of the embraced models, and unfortunately, many of the current models are rigid, mostly the theoretical ones, unable to adapt to specific channel characteristics, technology features, or environment changes. This may yield a considerable theory to practice gap. Instead, data-driven optimisation may be able to close this gap, learning the practical state of the network and inferring optimum network operation policies by means of AI to enhance the energy efficiency of mobile networks [29]. In this line, recently, several works in the literature are aiming at improving energy efficiency by exploiting state-of-the-art ML algorithms.

In Fig. 18, we illustrate the relationships between the main concepts developed in the framework of AI and ML [168]. Specifically, today, within the AI world, ML comprises the family of algorithms which uses data to develop intelligent systems. We can identify three main models: supervised learning, unsupervised learning, and RL.

Supervised and unsupervised learning models have been investigated to characterise and forecast network traffic and predict 5G network behaviour, leveraging rich data-sets. These models are, for example, becoming increasingly popular to define new solutions for PHY layer functions [169]. In contrast to supervised and unsupervised learning, the essence of RL concerns learning to make online decisions through interactions with the environment to control network operations. Therefore, ML models are key to enable an intelligent mobile network able to



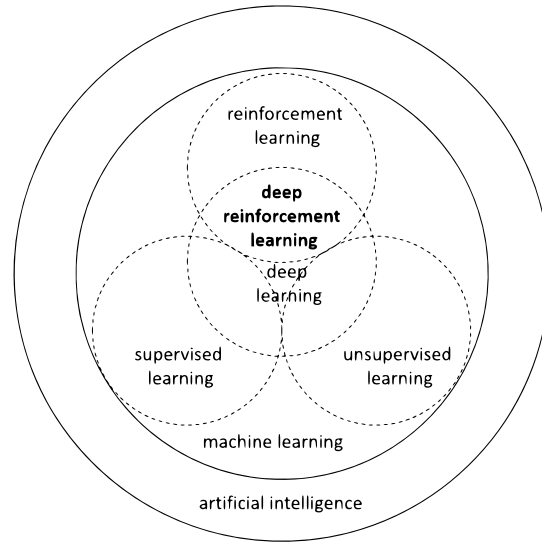


Figure 18. Relationships among deep reinforcement learning, deep learning, reinforcement learning, supervised learning, unsupervised learning, machine learning, and AI.

characterize its environment, predict system changes in time and space, and react accordingly in a real time manner.

In the following, we review the literature related to the use of ML techniques for traffic prediction and network optimization in green 5G networks.

#### A. ML for Traffic Prediction

One of the fundamental challenges along the path to enable full network adaptation to end-users' QoS requirements is the accurate forecasting of the network traffic. Such data forecasting can help driving energy efficient network decisions, e.g., carrier shutdown and others, as it will be shown in the next section.

The forecasting of the network traffic presents, however, important challenges:

- End-users have different QoS requirements at different moments of the day and in different places. Therefore, traffic demands change in time and space, making the prediction task difficult.
- The mobility of UEs introduces spatial dependencies among neighboring cells. Moreover, spatial dependencies can occur between distant cell towers, as efficient urban transportation systems easily enable UEs to travel across cities within half an hour.

- The spatial distribution of UEs at the urban scale is further influenced by many factors, including land use, population, holidays, and various social activities. These further complicate the spatio-temporal dependencies among traffic in distinct cell towers.
- The prediction time scale should match the decision periodicity of the energy saving mechanism. For instance, when adjusting every hour the number of active carriers, the forecasting model should provide predictions of the cell load every hour. In contrast, if the mechanism works on a daily basis, a longer prediction, i.e., 24 hours, is required, making the task more challenging.

The studies in the literature aiming at predicting the network traffic can be differentiated into two groups, according to the adopted methods, i.e., statistical-based and ML-based approaches.

1) *Statistical-based methods*: Statistical-based methods rely on capturing the statistics of the network traffic. One of the most popular statistical approaches when predicting network traffic is autoregressive integrated moving average (ARIMA) [170], which originates from three models: the auto-regressive model, the moving average model, and their combination (ARMA). The predictions performed by this model are based on considering the lagged values of a given time-series, while accommodating for non-stationarity. The main limitation of ARIMA is its inability to capture the seasonality—a time series with a repeating cycle—of network traffic. To overcome such limitation, an extension of this algorithm, named seasonal autoregressive integrated moving average (SARIMA), has been proposed [171]. SARIMA adds three new hyper-parameters to specify the auto-regression, the moving average, and the differencing for the seasonal component of the series, as well as an additional parameter for the period of the seasonality.

Statistical methods like this, however, are not able to capture rapid traffic variations, since they rely on the mean value of the historical data. Moreover, they are mainly linear, and it has become clear that they cannot provide high accuracy when predicting network traffic, especially when considering complex network traffic behaviors observed in real scenarios [172].

2) *ML-based methods*: In contrast to statistical methods, data-driven approaches based on ML have been recently investigated as a solution for network traffic prediction, as they allow to model non-linearities, while taking advantage of the big amounts of data currently being collected by the BSs.

Traditional ML algorithms such as  $k$ -nearest neighbours (KNN) [173] and support vector regression (SVR) [174] are able to model non-linear relationships. However, they require well-tuned parameters to achieve accurate prediction results. Moreover, these methods are known

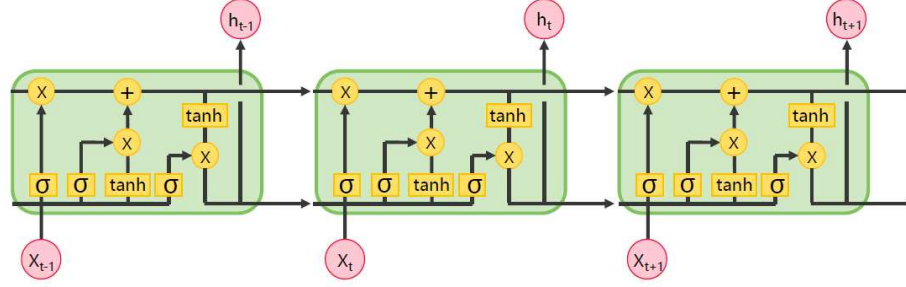


Figure 19. Example of RNN composed of three stacked LSTM units. The terms  $x_t$  and  $h_t$  are respectively the input and the output at time  $t$ . Moreover, the sigmoid and hyperbolic tangent activation functions are represented by the  $\sigma$  and  $\tanh$  symbols, respectively.

to have short memory due to their limited parameter set and inefficient computing, which is detrimental for improving the prediction accuracy.

*a) Recurrent Neuronal Networks:* Research has then moved into recurrent neural networks (RNNs) to model more complicated nonlinear sequence patterns, which has provided promising results in many fields, such as speech recognition, image caption, and natural language processing. In particular, LSTM has been proposed as a solution to the problem of vanishing gradient in traditional RNNs [175]. This neural network architecture allows to learn long-term dependencies from the time series provided in the input. A LSTM unit is characterised by three gates, i.e., input gate, forget gate, and output gate. These gates control the unit operations by considering three inputs, i.e., the input vector, the memory of the previous time-step, and the output of the previous time-step. The non-linearity is modeled through a sigmoid unit and a hyperbolic tangent unit, which implement the respective functions. As an example, Figure 19 shows a neural network architecture composed of three stacked LSTM units.

Based on such initial definition, the authors in [176] improved the LSTM state-of-the-art with an LSTM architecture using an encoder-decoder model based on gated dilated causal convolution. In the encoder, the long-range memory capacity is enhanced by gated dilated convolutions without increasing the number of model parameters in order to learn a vector representation of the input sequence. Subsequently, different temporal-independent and temporal-depended features, such as the daytime, holidays, weather, are fused with the representation vector. This allows to provide to the model additional relevant information with respect to the network traffic time series. In the decoder, the model applies a RNN with multiple LSTM units to map the fused vector

representation back to the variable-length target sequence.

Attention mechanisms are also often used when adopting a LSTM architectures to weight the importance of previous observations [177]. However, experiments have highlighted that simply using lagged inputs (i.e., data points from one year ago, half a year ago, and a quarter before) allows reaching better prediction accuracy than using complex attention mechanisms due to the strong periodicity characterizing the network traffic time series.

It should be noted, however, that the aforementioned LSTM methods do not take into consideration the spatial dependencies between the traffic experienced by different BSs, although it has become apparent that capturing this information may be fundamental to provide accurate forecasting of network traffic [178]. Different extensions of the previous presented approaches have been proposed in this direction.

The authors in [179] have, for example, proposed a novel prediction model to forecast traffic congestion, such that the uplink to downlink resource ratio can be adjusted to improve networking efficiency. The proposed model is composed of a tree-based deep model, followed by an LSTM. This tree-based model uses convolutional layers, which are useful to capture spatial information. Moreover, using a deep model allows to reduce the computational cost, because the convolution operations are performed in parallel in a tree-like structure.

In [180], a hybrid deep learning model for spatio-temporal prediction is proposed instead to incorporate spatial correlation, in which the temporal dependence is captured by a LSTM, whereas the spatial dependence is encapsulated by auto-encoders. Specifically, an auto-encoder is a neural network architecture used in unsupervised learning to represent a set of data, while reducing its dimensionality [181]. The auto-encoder learns to compress data from the input layer into a short code, i.e., the embedding, and then decompresses that code into a data structure that closely matches the original data i.e., the output layer. With this architecture, the auto-encoders are used to model historical information from the neighboring BSs, and capture spatial dependencies.

Even though the aforementioned attempts to capture spatial information, LSTM is not fundamentally adequate for it. In particular, the gates that characterize this model are usually fully connected, and as a consequence, the number of parameters is large, requiring high memory and computation time for training the model. This model is thus highly complex and frequently turns overfitted.

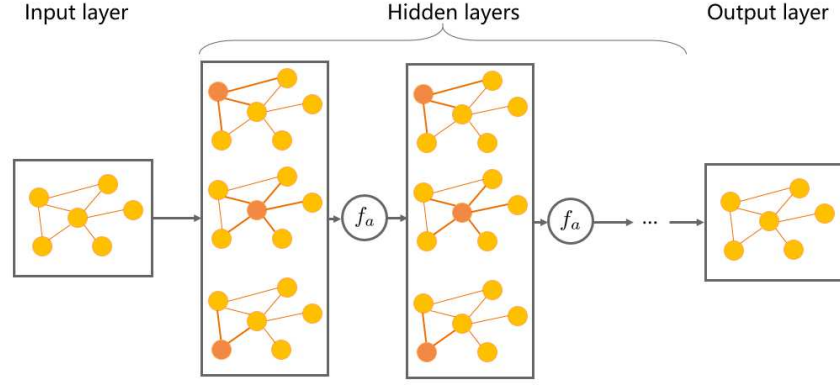


Figure 20. Example of a GNN architecture. The activation function unit is indicated by the  $f_a$  symbol.

*b) Convolutional Neuronal Networks:* An evolution of LSTM, named Convolutional LSTM (ConvLSTM) has been proposed to solve this problem, by replacing the inner dense connections with convolution operations [182]. This architecture significantly reduces the number of parameters, and enhances the ability of capturing spatio-temporal information. Indeed, convolutional neural networks (CNNs) are widely adopted now to deal with image classification problems, and capture spatial information. Similarly, when considering the network traffic prediction case, network traffic data is treated as images, where the geographical space is modeled by a matrix, and the traffic distribution in different areas of the city is described by the elements of such matrix.

As a good example, the authors in [183] provide a traffic prediction architecture, in which spatio-temporal dependencies are captured by utilizing densely connected CNNs. In a similar way, the authors in [184] have proposed a prediction algorithm, which can model both temporal and long-distance spatial dependencies. The proposed model follows an encoder-decoder paradigm, where a stack of ConvLSTM and CNN elements are combined.

A main limitation of this type of approaches, however, is that they only work with regular grid-based region partitions, which are not practical for cellular networks, and limits the prediction performance.

*c) Graph Neuronal Networks:* To overcome this limitation, an architecture based on graph neural network (GNN) has recently been proposed to model the network traffic spatio-temporal dependencies using a graph representation. In particular, given a direct graph, each BS is modeled as a vertex, and each edge defines the spatial relations between adjacent BSs.

The authors in [178] have adopted such GNN-based architecture, and decompose the total data traffic volume into in-tower traffic and inter-tower traffic, which corresponds, respectively, to the traffic serviced to the UEs residing within the coverage of a BS and the traffic serviced to the UEs moving among areas covered by different BSs. In the proposed architecture, each edge has a weight that depends on the total data traffic moving from the corresponding BSs vertexes. Importantly, it should be noted that complete directed graphs can contain a huge amount of edges, which hinder the efficient learning of model parameters. Therefore, low weights are treated as noise, and the corresponding edges are pruned by defining a threshold that allows to balance prediction accuracy and computing efficiency. The presented numerical results have highlighted that the traffic mobility induced by the roaming of humans plays a large role in the prediction accuracy, and showed that a combination of in-tower and inter-tower traffic patterns can be applied for network or social event forecasting.

*d) External inputs: Point of Interests:* While the aforementioned research has mainly focused on the network traffic itself, it is also well understood that external factors, such as the point of interest (POI) distribution, may influence the demand of network traffic. In particular, the analysis provided in [185] reveals that the dynamic urban network traffic usage exhibits five basic time domain patterns, which are correlated to the city functional zones, e.g., residential, transport, office.

In this line, the work in [186] has targeted network traffic prediction by exploiting cross-domain data. Specifically, three types of data sets are considered, i.e., BSs location, POIs distribution, and social activity level. In particular, the latter contains information generated by the end-users when using social networks, such as location and keywords, which may allow to better capture particular social events, such as concerts and football matches. The correlation between these data sets and the network traffic is analyzed and used to improve the prediction accuracy. A novel deep learning based traffic prediction architecture is then proposed. This architecture can fuse the cross-domain data sets into a unified representation. Spatial, temporal, and external factors are then captured and processed by ConvLSTMs. In order to consider the pattern diversity and similarity of the network traffic of different city functional zones, the authors have also proposed an algorithm for grouping city areas into different clusters. Then, inter-cluster transfer learning is proposed to capture regional similarities and differences. The achieved results have shown that cross-domain data sets have high correlation with the network traffic, and thus the introduction of the aforementioned data sets benefits the prediction accuracy.

*e) Model re-usability:* Another important issue related to traffic prediction is that of re-usability. Prediction algorithms generally lack of re-usability, which require them to be re-trained to learn a new representation of the spatio-temporal information, when adopted in a new —or dramatically changing— scenario. The generalization problem of prediction algorithms has been recently discussed in [187], where the authors have proposed a model based on auto-encoders, which learns the embedding of BSs based on raw data. In this framework, the embeddings are vectors, which contain spatio-temporal information of the BSs, and their size is much smaller than the raw data, which allows to improve the generalisation capabilities of the prediction algorithm, while also reducing its computational cost. The architecture is composed of three main modules: an encoder, a spatial adder and a decoder. In more detail, the encoder is designed to extract information from the BS, and infer its embedding. The spatial adder is in charge of building the relation among different BSs, whereas the decoder restores original data from the embeddings. In this way, the training phase makes the encoder learn how to generate an embedding that conforms to the spatial relation with neighboring BSs. After training the model, the encoder is able to use the raw data from the BS itself to infer its embedding, which contains information about how this BS influence other BSs. Numerical results have shown that this approach helps temporal models to achieve similar performance as spatio-temporal ones, at the cost of a small increase in the training time.

### *B. ML for 5G Energy Efficiency Optimisation*

The wireless network environment is complex and stochastic by nature as already discussed earlier, and in more detail, traffic requirements, user mobility, interference and channel variations in time and space make system-wide optimisation a hard problem. In the past, most of solutions proposed in the literature to configure mobile network parameters have not considered the dynamic nature of wireless networks. More specifically, state-of-the-art algorithms, as many of the once already surveyed, are typically based on perfect —or partial— knowledge of the instantaneous system conditions, which requires to re-compute the solution of a problem whenever a notable change has occurred in the environment. With the complexity carried by such approaches, they may lead to significant computation and signaling overhead. Thus, there is an urgent need for more light-weight, flexible and adaptive solutions with respect to environment dynamics to minimise the energy consumption of practical networks.

In the last decade, RL, and more recently deep reinforcement learning (DRL), have emerged as potential tools to pave the way for artificial intelligence driven optimisation in 5G systems and beyond. For more details on the motivation, refer to [188] and [67] and the references therein. Given their importance, in this section, we provide an overview of RL, highlighting its benefits and drawbacks, and emphasizing how the combination of deep neural network (DNN) and RL, i.e., DRL, is leading to continuous breakthroughs in multiple research domains, with distinct challenges. We also present several class of algorithms, and show relevant applications in the energy efficiency optimisation domain.

*1) RL Framework Overview:* In RL, the environment is often modelled as a markov decision process (MDP), which consists of [189]:

- a set of states,  $\mathcal{S}$ ,
- a set of actions,  $\mathcal{A}$ ,
- transition probabilities;  $\mathcal{T}(s_{t+1}|s_t, a_t)$ , which map a state-action pair at time  $t$  to a distribution of states at time  $t + 1$ ;
- a reward function,  $\mathcal{R}(s_t, a_t)$ , and
- a discount factor,  $\gamma \in [0; 1)$ .

The sequence of received rewards leads to the definition of the cumulative discounted reward, i.e.,

$$R_t = \sum_{k=0}^{\infty} r_{t+k} \gamma^k.$$

where  $r_{t+k}$  is the expected reward at time  $t + k$ .

In an MDP, a decision-maker, i.e., the agent, attempts to find the optimal policy,  $\pi^*$ , which maps the optimal action to each state, such that the cumulative discounted reward,  $R_t$ , is maximized. Specifically, in literature, two functions are defined to characterise the expected value of a policy, and find the strategy that optimises the system behaviour:

- the state-value function,  $V_{\pi}(s) = \mathbb{E}[R_t | s_t = s]$ , and
- the state-action value,  $Q_{\pi}(s, a) = \mathbb{E}[R_t | s_t = s, a_t = a]$ ,

where  $V_{\pi}(s) = \max_a Q_{\pi}(s, a)$  [69].

Fig. 21 describes the agent interactions and learning process in a MDP. This problem is characterised by multiple challenges. For instance, the environment is typically partially observable, i.e., an agent does not have full knowledge of the system state, but only a partial observation. In the context of wireless network optimisation, this is very likely, and it can represent the case where



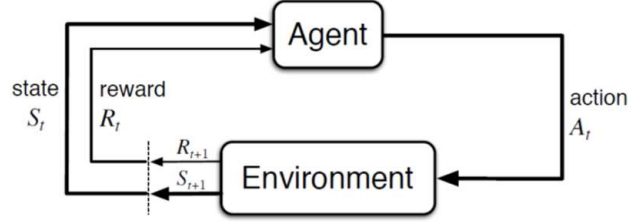


Figure 21. The perception-action-learning loop.

a BS is not aware of the load of other BSs. Moreover, the perception of the reward related to a state-action pair is often delayed, which makes hard to evaluate the effect of an action, and thus to learn the optimal policy. This effect is known as the temporal credit assignment problem [69]. Similarly, in a multi-agent system, a perceived reward depends on the actions of multiple agents behaving independently from each other, i.e., a cell throughput depends on how each neighbouring BS schedules its own resources. In addition, the environment transition probabilities are likely to be unknown, as the system is too complex to be modelled.

When the environment can be fully modelled, dynamic programming can be used to solve the learning problem through algorithms whose complexity is polynomial in the size of the set of states,  $\mathcal{S}$  [69]. In RL, an agent tries to achieve a full characterisation of the transition probabilities,  $\mathcal{T}$ , and the reward function,  $\mathcal{R}$ , through continuous interactions with the environment. Through this learning by interaction loop, a exploration-exploitation trade-off arises, i.e., exploiting the information collected so far to benefit the locally optimal decision, or exploring for achieving a better characterisation of the environment and achieve higher long-term gains.

2) *RL and Energy Efficiency*: Recently, in the context of energy efficiency, new RL schemes have been proposed to manage ASMs in 5G BSs. In [137], the authors have mapped the time-domain ASM control —see Section VI-A— as a decision making problem in which a BS sequentially sets the sleeping level length. Specifically, when the cell becomes idle, this approach first puts the BS in the deepest level of sleep, and then gradually switches it on. At each stage, the BS decides the number of slots during which the current sleep mode status will be kept. If a UE request arrives during a sleep period, the associated data is saved in a buffer until the BS wakes up. Accordingly, the state set includes the possible states in which a BS can operate, i.e., idle, active, or one of the sleep modes enabling energy saving. The action set includes the values of the possible number of time slots that can be associated to a given sleep mode. The reward

is defined as the weighted sum of the energy saving gain due to the ASM and the additional latency experienced at the UEs due to the buffering of their traffic. In this way, different ASM policies can be defined according to whether the operator wants to trade end-users' QoS for energy savings. The authors have used a popular RL scheme, named as Q-Learning, to find the optimal policy. This scheme is a model-free algorithm, which uses transition experiences to iteratively construct an estimate,  $\hat{Q}(s, a)$ , of the optimal state-action value function,  $Q^*(s, a)$ , also referred to as Q-function, as follows:

$$\hat{Q}(s_t, a_t) = \hat{Q}(s_t, a_t) + \alpha \left( r_t + \gamma \max_{a' \in \mathcal{A}} \hat{Q}(s_{t+1}, a') - \hat{Q}(s_t, a_t) \right), \quad (27)$$

where  $\left( r_t + \gamma \max_{a' \in \mathcal{A}} \hat{Q}(s_{t+1}, a') - \hat{Q}(s_t, a_t) \right)$  is the temporal difference (TD) error between the predicted Q-value,  $r_t + \gamma \max_{a' \in \mathcal{A}} \hat{Q}(s_{t+1}, a')$ , and its current value,  $\hat{Q}(s_t, a_t)$ , and  $\alpha$  is a learning-rate parameter, which controls how new estimates are iteratively blended together over time. If each state-action pair is visited infinitely often, and the learning rate is decreased over time, the estimate,  $\hat{Q}(s, a)$ , converges to the optimal value,  $Q^*(s, a)$  [190]. Note that the optimal state-action pairs are stored into a look-up-table. The results in [137] have shown that if delay is critical, ASM should not be activated for a cell load larger than 30%. In contrast, for very low loads, up to 55% of energy savings can be achieved, even when prioritizing the end-users' QoS.

A well known problem of RL algorithms is the so-called curse of dimensionality, meaning that their computational requirements grow exponentially with the size of the state and action spaces [69]. To deal with this challenge, function approximation can be used to approximate the state-action value function when the state and/or action spaces are large or continuous, i.e.,  $\hat{Q}_\pi(s, a, \mathbf{w}) \approx Q_\pi(s, a)$ , where  $\mathbf{w}$  is a set of parameters defined by the function approximators. Multiple function approximation methods have been investigated in the literature for RL, e.g., linear functions or ANNs.

In [191], the authors proposed a fuzzy Q-learning model to deal with complexity, where a network controller jointly optimises the DTX of the underlying cells and backhaul nodes to minimise the energy consumption and satisfy the end-users' QoS. Specifically, to reduce complexity, the controller maintains a distinct model for each cell. The state space of each cell characterises its buffer state in terms of rate and latency requirements, the BS capacity, and the estimated spectral efficiency loss due to the interference of the nearby BSs, which are expected to be active. Then, in each time slot, the controller observes individually each state

space, and decides in a distributed manner which cells (and associated backhaul nodes) to keep in energy saving mode or activate. The authors have associated to each state-action pair a cost function, which models the weighted sum of the BS power consumption and the packet lost, either due to latency constraints or interference. As the state space is composed by continuous variables, this would prevent a classic RL algorithm to converge to an optimal policy in a finite time. Accordingly, the authors have integrated a fuzzy inference system (FIS) to their framework, and reduced the state space by mapping the state representation in fuzzy sets [192]. The authors have shown that the proposed framework is able to coordinate the activation and deactivation of neighbouring BSs, thus limiting the inter-cell interference. Moreover, this scheme takes advantage of the latency-energy trade-off, and achieves up to 38% of energy savings with respect to a baseline DTX, which does not exploit data buffering.

To manage curse of dimensionality, DNNs are currently widely used as a powerful global function approximator, where a neural network is used to compress the Q-table [193]. However, the combination of DNN and RL, i.e., DRL can lead to instability, and even divergence during the training process [189]. To address these issues, recently, the authors of [193] have proposed a deep Q-learning (DQL) framework that leverages two main ideas, i.e., the usage of experience replay, and the introduction of the target network. Experience replay consists in the usage of a buffer, where tuples of experiences (i.e., interactions with the environment) are saved and continuously replayed to break the correlation across subsequent observations during training. Moreover, during training, two distinct deep networks are used. One that is continuously updated, and another one, updated less frequently, which represents the target network on which the TD error is computed (see eq. (27)). These modifications make the algorithm training more stable.

These enhancements have led to continuous research innovations and DRL architectures that can successfully deal with problems that were previously considered intractable. For instance, the authors of [194] have proposed a DQL model to dynamically (de)activate BSs based on traffic requests. This framework has introduced few enhancements with respect to the baseline DQL in [193]. First, they have observed that non-stationary traffic leads to oscillation between waking- and sleeping-dominating regimes. To break this correlated sequence of actions, the authors propose an *action-wise* experience replay, where experiences related to different actions are saved into distinct buffers, which are uniformly sampled during the training process.

In the literature, other mechanisms have been proposed to improve the effectiveness of the experience replay process, e.g., the well know prioritized experience replay [195]. Moreover,

and although the reward is clipped to  $[-1; 1]$  in classic DQL, to capture the strong variations characterising the wireless environment, this work has also proposed an adapting reward re-scaling scheme, which consists into dividing the instantaneous reward by a positive adapting scaling factor, and summing a saturation penalty to the DQL loss function, i.e., the square of the TD error in (27). In addition, the authors of this work have also used an interrupted Poisson process to model the traffic requests, and generate additional pseudo experiences, which, using the DynaQ framework [69], are periodically stored into the replay memory along with real experiences, and used indiscriminately for training. Empowered by these innovations, their DQL algorithm attempts to learn the optimal policy that control the BS status, based on a reward that takes into account the served requests, the queued or re-transmitted requests, and the failed ones. The reward considers the cost to wake up the BS and the one for changing the BS status. Their experiments have shown that modelling the traffic requests and generating pseudo experiences does not lead to large gains. In contrast, action-wise experience replay and adaptive reward scaling improve the stability and adaptability of the proposed framework. Overall, the proposed scheme achieves large gains with respect to a baseline Q-learning approach, in terms of energy saving and QoS.

Similarly, the authors of [196] have proposed a DRL model to control the small cell (de)activation in dense HetNets. In this framework, the system state comprises the status of each small cell and the estimate of its traffic arrival rate, while the action set includes the (de)activation actions. The cost function provides a qualitative description of the small cell network power consumption, the additional latency experienced due to deactivating BSs, and the switching cost due to the change of status of the small cells (i.e., from off to on and vice-versa). This work has improved the state-of-the-art solutions by considering an actor-critic DRL scheme. In the actor-critic algorithm, the actor selects the action given the state of the environment, and the critic estimates the value function, given the state and the action. Then, it delivers a feedback to the actor (see Fig. 22). Importantly, it should be noted that this type of DRL based on actor-critic has emerged as a powerful solution to deal with continuous action spaces [197]. Conventionally, the actor provides a probability distribution of the possible actions at a given state. In [196], the action space has the size,  $2^{N_{SC}}$ , where  $N_{SC}$  is the number of small cells in the network. Therefore, the output of the actor is defined as a single vector of continuous values. To compensate for the lack of exploration in the actor's side, this work proposed to add noise to the output action vector. The noisy vector is then converted in a hard decision (i.e., the proto-action), and then, the algorithm

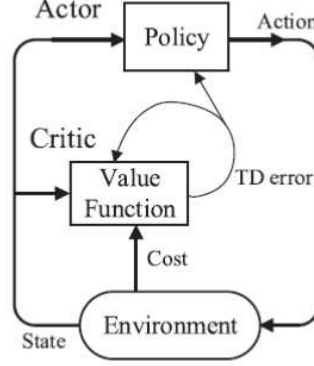


Figure 22. The actor-critic framework.

explores the set of actions close to the proto-action, and selects the action with the minimum estimated cost. For training the proposed model, the authors have used a deep deterministic policy gradient framework, in which the policy and value function are both approximated by DNNs. The authors have shown for that this approach limits the cumulative network cost over time with respect to baseline RL algorithms, achieving up to 30% of gain with respect to a Q-learning model, and provides larger stability in case of non-stationary traffic. Moreover, they have indicated that the proposed action exploration method reduces the convergence time.

To conclude this section, let us highlight that, although DRL has allowed great progresses in the context of system optimization in a stochastic environment, many challenges are still opened, such as enabling distributed optimization in the context of multiple competitive or collaborative agents, or designing fast and low complex methods to update the learned policy after notable change in the system, which have not been observed during the training phase. More challenges faced by RL with respect to the energy efficiency are described in the next section.

## VIII. OPEN RESEARCH DIRECTIONS

In this section, we identify lines of research, which according to the authors' understanding, still require further efforts to aid increasing the energy efficiency of 5G and future networks.

### A. multi-cell Energy Efficiency Theoretical Modelling

As discussed throughout the survey, serving the end-users' QoS requirements with the minimum power consumption is key to energy savings, and while the bounds and trade-offs to drive

such optimisation in a single-cell case may be well understood, the fundamental understanding of energy efficiency in multi-cell networks is still limited, due to complexity issues.

Large-scale multi-cell networks are intricate to model (see Section V-B), and as a result, for tractability reasons, most current theoretical understanding of energy efficiency for wide-area networks have been derived based on, for example, the performance of the average UE in uniform networks with simplistic channel, operational and BS power consumption models [129] [130]. These models do not generally capture, however, relevant features, such as BS and UE distributions, NLoS and LoS transmissions, directional channels, antenna correlations. Novel theoretical analyses embracing such complexities are thus required to characterise still unknown energy efficiency trade-offs, which may exist and allow further technology breakthroughs in real deployments.

In this line, the work in [198]–[200] have represented a step forward, accounting for non-uniform BS and UE distributions, while being able to estimate local performance, i.e., not only the performance of the average UE, but also its distribution. On the same note, the work in [201] has characterised the cell load distribution for a given traffic density, and studied how this affect the network performance. These frameworks, however, are still in their infancy, and have been mostly applied, up to now, to the analysis of simpler single-antenna small cell networks. Further research is needed for their application to more complex networks and features, such as mMIMO.

With regard to channel models, to give another example, it is widely accepted that most mMIMO performance bounds used today work well when the useful signal coefficients behave almost deterministically, i.e., they have a non-zero mean and a small variance. However, the research in [202] has recently proven that under highly directional channels, for instance, the channel hardening effect does not so clearly appear, and that new bounds are thus required, in terms of both capacity and energy efficiency, for a more accurate performance evaluation in these more realistic setups.

It is also important to mention that there is a gap in the literature with respect to sophisticated energy efficiency performance analyses, via detailed numerical and/or system-level simulation tools, able to capture the complexity of large-scale multi-cell networks. Gaining understanding of the interplay among complex features such as mMIMO, CA, and coordinated transmissions, together with their power consumption, which is hard to derive through a pure theoretical analysis, can provide new road maps to fundamental network deployment and operation. The intuition gained via these tools can also lead to new theoretical research avenues.

### *B. Energy Efficiency-driven Network Planning Tools*

Deploying and operating a large-scale multi-cell network is expensive, and thus requires careful network dimensioning and planning to ensure an optimum radio resource utilisation, e.g., spectrum and bandwidth, number of BSs, their location, architecture and transmit power, number of antennas, and transceivers per BS, to cite a few [203], [204]. Importantly, network planning tools must ensure that the deployed system has a sufficient amount of radio resources, and can use it in an effective manner, to achieve the required level of network performance at the appropriate cost. Unfortunately, however, such tools are mostly network capacity-driven as of today, and not yet designed to derive optimal energy efficient deployments.

Once the network is planned and deployed, such implementation also imposes hard constraints on the future network performance and its energy consumption. It is thus of imperative importance to equip MNOs with sophisticated network planning tools for wide-area network design with energy efficiency at heart. For example, when should an MNO deploy less BSs and CCs with larger mMIMO arrays, or in contrast, use more BS and CCs with smaller mMIMO arrays? The applicability of optimisation algorithms in the network planning phase to find such type of practical answers is crucial, as the answer is local, and should rely on accurate topological descriptions of the deployment scenario, knowledge of current site deployments and performance, as well as UE and required traffic distributions and accurate BS power consumption models, among others [63].

It is also important to highlight that optimisation performance strictly depends on a reasonable trade-off between the channel and network functioning modelling accuracy with respect to complexity, and thus MNOs should choose their network models carefully on a per problem basis. This reinforces the need for flexible and efficient numerical radio propagation and system-level simulation tools and tailored optimization theories and algorithms for energy efficiency problems [205].

More developments in this area are needed at a professional level to make sure future networks are optimally dimensioned, and energy waste is avoided.

### *C. Multi-carrier and Heterogeneous Network Analysis*

In most scenarios, new 3GPP NR deployments will coexist with existing ones, e.g., 3GPP LTE. In some cases, these deployments may be orthogonal in frequency with, e.g., 3GPP NR in the 3.5 GHz band and 3GPP LTE in the 2 GHz one. In some other cases, due to the scarcity

of spectrum, 3GPP NR deployments will have to take place in the same spectrum already used by 3GPP LTE [32], [58]. In the latter case, the fundamental tool to enable such 3GPP NR/LTE spectrum coexistence is the dynamic time scheduling of both 3GPP NR and LTE, for which the 3GPP NR specification provides tools [206].

Given that 3GPP NR and LTE sites have very different characteristics (coverage, bandwidth, antennas, etc.), leading to distinct performance and energy consumption, it would also be desirable to inter-work and (de)activate these two technologies in a coordinated manner, while satisfying end-users' QoS requirements with the minimum energy consumption. In some cases, 3GPP LTE may operate at lower carrier frequencies than 3GPP NR, and thus be able to provide a better blanket coverage at smaller energy consumption. This may be the most energy efficient at low load periods. In contrast, at medium loads, 3GPP NR may be sufficient to provide the required capacity to the active UEs, and 3GPP LTE can be deactivated. If operated at different frequencies, at high loads, both technologies may be aggregated via dual connectivity [207].

In scenarios with the mentioned frequency imbalance, and because the BS can avail of larger transmit power than the UE, it may also make sense to simultaneously activate both technologies, and use downlink/uplink split [208], i.e., 3GPP NR for downlink transmissions and 3GPP LTE for the uplink [58]. However, this should only be done where and when necessary, under energy efficient conditions, avoiding potential energy waste due to having both technologies activated.

The optimisation of the inter-working between 3GPP NR and 3GPP LTE is also of high importance when 3GPP NR appears in the form of small cells [209] or millimetre wave [210] access points. These types of cells have a much smaller coverage radius, and can be (de)activated to provide boosted capacity where and when needed. Since some implementations of this type of cell, e.g., millimetre wave, may be power hungry, the usage of coordinated ASMs across a large number of this type of cells is critical. This can be facilitated through the separation of the data plane and control plane [211], where the latter is continuously provided by underlaying macro cells to ensure robust connectivity and mobility support, while capacity cells (i.e., small cells) allow for enhanced capacity and high rate data transmissions locally and on demand.

In general, there is a lack of studies covering the understanding and optimisation of these technology inter-working practical use cases from a energy efficiency point of view.



#### *D. Data-Driven Optimisation*

State-of-the-art data-driven approaches for network traffic prediction are mainly related to measurements biased by the observation point, i.e., the BSs, which usually does not report the effective traffic demand but rather the cell throughput or resource usage, which depend on the network deployment, interference, current RRM parameters, and running energy saving schemes. The use of this potentially biased measurements may be an issue when adopting prediction algorithms as enablers for improving the mobile network energy efficiency. In fact, the implementation of any energy saving scheme will impact the load distribution across the network, and make related forecasting unreliable. As a result, further research is encouraged with regard to the estimation and prediction of unbiased metrics, whose characterization is not affected by the algorithms implemented using these observations.

Moreover, there is currently a lack of understanding on how prediction errors, e.g. traffic forecasting errors, affect the gains provided by energy saving schemes. In this line, most of the current literature focuses on measuring the performance of the prediction in the metric space, (function of the difference between the predicted value and ground-truth, e.g., physical resource block (PRB) usage, throughput). However, it is generally not straightforward to derive how improvements in the prediction of such metrics help to minimise the network power consumption. It is thus recommended that prediction accuracy is investigated also in terms of energy savings when developing data-driven optimisation schemes [155].

As discussed in Section VII, there is also a lack of end-to-end ML frameworks that jointly use supervised learning and RL to characterise and optimise the 5G system. Specifically, supervised learning models can provide multi-step traffic predictions, achieving a comprehensive forecast of future status of the mobile network environment. Using this information can help RL algorithms to converge faster to optimal operational policies, and enhance the performance of the exploration phase, e.g., optimally deciding the moment to (de)activate BS functionalities without affecting network performance.

Importantly, it should be stressed that recent progresses in the areas of computational processing and data storage, as well as the increased availability of big data, have made the use of AI more practical than ever in many challenging fields. However, the acquisition of large datasets in wireless networks is currently challenging, and their processing energy demanding, which limits the opportunities for implement data-driven optimization in 5G systems. To address this

issue, the use of joint data-driven and model-based approaches is being widely explored [212], [213], and is becoming the foundation of new optimization mechanisms for large-scale multi-cell networks. Moreover, these techniques can be used for bootstrapping ML models, thus reducing their need for data, computational complexity, power consumption, and latency.

### *E. Green AI*

Most of the recent breakthroughs led by novel ML solutions have been possible thanks to the ever-increasing computational capacity of dedicated hardware platforms. The work in [214] has highlighted that, in the last decade, while ML models evolved from AlexNet—an image recognition DNN presented in 2012 [215]—to AlphaZero—a RL algorithm proposed in 2018 [216]—, the associated computational cost trend increased by 300,000x. In this line, the work in [217] has also analyzed the energy consumption issues arising from the need of exponentially larger computational resources to continue marginally increasing the model accuracy, and has estimated that the carbon footprint of the current brute force trend is environmentally unfriendly.

The training of DNNs on mobile devices in a distributed, computationally and energy efficient manner is also an ongoing research topic, which can brake down the aforementioned complexity. Collaborative learning schemes, such as federated learning [218], should be considered to mitigate the energy inefficiencies resulting from traditional, centralised ML approaches. Moreover, notable efforts are being made towards hardware design and software accelerators, which make possible to also move part of the ML process to the UE itself to reduce the overall energy consumption (see [219], [220] and references therein). In addition, tailored *early stopping* can also be used to terminate the training process when a near-optimal solution has been found thus reducing the required number of iterations—and the associated energy consumption—needed to train the ML model [221].

However, to pave the way for the successful integration of ML in 5G systems and beyond, it is key to consider computational and energy consumption aspects also during the design phase of data-driven optimisation algorithms. To achieve this goal, while evaluating an ML model, in addition to accuracy and optimisation-related metrics, computational efficiency and energy consumption must also be considered. Using these metrics, ML architectures that converge faster and/or need to be updated less frequently can be designed, prioritising energy consumption over model accuracy. One possible approach towards this goal is to investigate yet undiscovered ML paradigms. For instance, as discussed in [212], [213], model-based RL solutions, which exploit

a-priori expert knowledge to characterise physically/mathematically the system evolution can be integrated with model-free RL architectures, which interact with the environment to identify the optimal policy. Similarly, as explained in Section VII-B, RL can leverage information about the future status of the system obtained by supervised learning forecasting to speed up the training speed and converge towards improved operating conditions.

#### *F. Renewable Energy Sources*

In the last years, the use of renewable energy sources for supplying network elements has attracted the attention of the research community and industry, due to the increased efficiency and the decreasing costs of energy harvesters and storage devices. Gathering environmental energy through dedicated harvesting hardware to supply 5G BSs will translate into operational expenditure (OPEX) savings and a reduction of the environmental footprint of mobile networks [222].

The adoption of renewable energy sources, however, entails a higher management complexity. In fact, environmental energy, such as solar and wind, is inherently erratic and intermittent, which may cause fluctuating energy inflow and produce service outage. A proper optimisation of how the energy is drained and balanced across network elements is thus necessary for a self-sustainable network design.

Operational policies for sustainable mobile networks can be found by solving optimisation problems, which have the objective of maximizing the end-users' QoS, while dealing with the constraints coming with the adoption of renewables. In particular, traditional approaches assuming infinitely backlogged data buffers and unlimited energy storage cannot be adopted since they would provide unrealistic results [223].

Literature works focus on two classes of algorithms: offline and online. Offline algorithms enable computing optimal operational policies by adopting tools from optimisation theory, such as dynamic programming, when the meaningful processes (e.g., energy arrivals, CSI, data traffic) are known [224], [225]. However, using such tools in a real scenario is generally impracticable due to the high complexity of these approaches, and the optimal solutions obtained by offline algorithms are generally adopted as a benchmark to measure the optimality of online algorithms. On the contrary, online algorithms are designed to derive sub-optimal policies without needing any *a priori* information. In particular, ML approaches have been widely developed as a tool to solve these optimisation problems [226], [227].

In general, most of the literature relies on simplistic assumption. For instance, there is a lack of accurate models for batteries, whose capacity reduces with time, affecting the overall energy efficiency and costs [228]. Moreover, batteries cannot store all the harvested energy in particular periods of the year. Therefore, research targeting architectures and algorithms enabling an efficient use of the exceeding harvested energy is needed.

## IX. CONCLUSIONS

In this paper, we have provided an overview of the state-of-the-art on the fundamental understanding and practical considerations of the energy efficiency challenge in 5G networks. We have surveyed in detail the available BS power consumption models and metrics for the optimization of the energy efficiency. We have also reviewed the impact on energy efficiency of four 3GPP NR key features, i.e., mMIMO, the lean carrier design, ASMs, and ML, presenting the findings in the literature with respect to their available bounds, trade-offs and/or practical achievable energy savings. Importantly, we have highlighted the need for adapting the network resources to meet the end-users' QoS demands, while minimizing network power consumption, and have surveyed the related research differentiating among different algorithm time scales and classes (i.e. micro-sleeps, carrier and channel shutdown). We have also stressed the role that spatio-temporal predictions and online optimisation via ML will play in the previous network power consumption minimization task, and discussed state-of-the-art ML related approaches in such energy efficiency field. To conclude, we have also provided discussion around the lines of research that need further work to make 5G networks greener.

As a final note, given the enabling effect of that telecommunications systems and the impact that they can have in meeting the requirements for a sustainable development, we encourage the research community to continue making progress toward a sustainable communication system.

## REFERENCES

- [1] D. Kaufman, N. McKay, C. Routson *et al.*, "Holocene global mean surface temperature, a multi-method reconstruction approach," *Sci Data*, vol. 7, no. 21, Jun. 2020.
- [2] J. Rifkin, *The Third Industrial Revolution: How Lateral Power Is Transforming Energy, the Economy, and the World*, 1st ed. St. Martin's Press, Sep. 2011.
- [3] S. R. Weart, *The Discovery of Global Warming: Revised and Expanded Edition*, 2nd ed. Harvard University Press, Oct. 2008.
- [4] Worldometer, "Current world population," Available at <https://www.worldometers.info/world-population/> (2020/10/27).

- [5] NASA, “Global climate change: Vital signs of the planet,” Available at <https://climate.nasa.gov/vital-signs/carbon-dioxide/> (2020/10/27).
- [6] United Nations Environment Programme, “UN Emissions Gap Report 2019,” Tech. Rep., Nov. 2019. [Online]. Available: <https://wedocs.unep.org/bitstream/handle/20.500.11822/30797/EGR2019.pdf>
- [7] Secretariat of the United Nations Conference on Trade and Development, “UN Trade and Development report 2019,” Tech. Rep., Aug. 2019. [Online]. Available: [https://unctad.org/en/PublicationsLibrary/tdr2019\\_en.pdf](https://unctad.org/en/PublicationsLibrary/tdr2019_en.pdf)
- [8] T. F. Stocker *et al.*, “Climate Change 2013. The Physical Science Basis. Working Group I Contribution to the Fifth Assessment Report of the Intergovernmental Panel on Climate Change - Abstract for decision-makers,” Tech. Rep., Oct. 2013. [Online]. Available: <https://www.osti.gov/etdweb/biblio/22221318>
- [9] NASA Goddard Institute for Space Studies, GISTEMP Team, “GISS Surface Temperature Analysis (GISTEMP), version 4,” Available at [data.giss.nasa.gov/gistemp/](https://data.giss.nasa.gov/gistemp/) (2020/10/27).
- [10] N. Lenssen, G. Schmidt, J. Hansen, M. Menne, A. Persin, R. Ruedy, and D. Zyss, “Improvements in the GISTEMP uncertainty model,” *J. Geophys. Res. Atmos.*, vol. 124, no. 12, 2019.
- [11] A. Cazenave, “How fast are the ice sheets melting?” *Science*, vol. 314, no. 5803, pp. 1250–1252, Nov. 2006.
- [12] R. Seager, M. Ting, I. Held, Y. Kushnir, J. Lu, G. Vecchi, H. Huang *et al.*, “Model projections of an imminent transition to a more arid climate in Southwestern North America,” *Science*, vol. 316, no. 5828, pp. 1181–1184, Nov. 2007.
- [13] G. B. Bonan, “Forests and climate Change: Forcings, feedbacks, and the climate benefits of forests,” *Science*, vol. 320, no. 5882, pp. 1444–1449, Jun. 2008.
- [14] A. Clement, R. Burgman, and J. Norris, “Observational and model evidence for positive low-level cloud feedback,” *Science*, vol. 325, no. 5939, pp. 460–464, Jul. 2009.
- [15] GSMA, “2019 Mobile Industry SDG Impact Report,” Tech. Rep., Sep. 2019. [Online]. Available: <https://www.gsma.com/betterfuture/wp-content/uploads/2019/10/2019-09-24-a60d6541465e86561f37f0f77ebee0f7-1.pdf>
- [16] —, “The Enablement Effect: The impact of mobile communications technologies on carbon emission reductions,” Tech. Rep., Feb. 2020. [Online]. Available: [https://www.gsma.com/betterfuture/wp-content/uploads/2019/12/GSMA\\_Enablement\\_Effect.pdf](https://www.gsma.com/betterfuture/wp-content/uploads/2019/12/GSMA_Enablement_Effect.pdf)
- [17] Huawei Technologies Co., Ltd., “Green 5G: Building a sustainable world,” Tech. Rep., Aug. 2020. [Online]. Available: <https://www.huawei.com/en/public-policy/green-5g-building-a-sustainable-world>
- [18] I.-R. M.2083, “Framework and overall objectives of the future development of IMT for 2020 and beyond,” Tech. Rep., Sep. 2015. [Online]. Available: <https://www.itu.int/rec/R-REC-M.2083>
- [19] ITU-T, “Summary of SMART 2020 Report,” Tech. Rep., Aug. 2008. [Online]. Available: <https://www.itu.int/md/T05-FG.ICT-C-0004/en>
- [20] —, “Sustainable ICT in corporate organizations,” Tech. Rep., 2012. [Online]. Available: [https://www.itu.int/dms\\_pub/itu-t/opb/tut/T-TUT-ICT-2012-10-PDF-E.pdf](https://www.itu.int/dms_pub/itu-t/opb/tut/T-TUT-ICT-2012-10-PDF-E.pdf)
- [21] C40, “Carbon emissions are already falling in 30 cities,” Available at <https://www.bloomberg.com/news/articles/2019-10-09/c40-the-cities-where> (2019/10/09).
- [22] C.-L. I, S. Han, and S. Bian, “Energy-efficient 5G for a greener future,” *Nat Electron*, vol. 3, pp. 182–184, 2020.
- [23] G. Kouropoulos, “A predictive model for the estimation of carbon dioxide emissions of magnetic resonance imaging units and computed tomography scanners,” *Journal of Urban and Environmental Engineering*, vol. 12, no. 2, 2018.
- [24] SMARTer2030, “ICT Solutions for 21st Century Challenges,” Tech. Rep., 2015. [Online]. Available: [http://smarter2030.gesi.org/downloads/Full\\_report.pdf](http://smarter2030.gesi.org/downloads/Full_report.pdf)
- [25] GSMA, “Energy Efficiency,” Tech. Rep., May 2019. [Online]. Available: <https://www.gsma.com/futurenetworks/wiki/energy-efficiency-2/>

- [26] A. Abrol and R. K. Jha, "Power Optimization in 5G Networks: A Step Towards Green Communication," *IEEE Access*, vol. 4, pp. 1355–1374, 2016.
- [27] M. Usama and M. Erol-Kantarci, "A Survey on Recent Trends and Open Issues in Energy Efficiency of 5G," *Sensors (Basel)*, vol. 19, no. 14, Jul. 2019.
- [28] J. Lorincz, A. Capone, and J. Wu, "Greener, Energy-Efficient and Sustainable Networks: State-Of-The-Art and New Trends," *Sensors (Basel)*, vol. 19, no. 22, Nov. 2019.
- [29] X. Cao, L. Liu, Y. Cheng, and X. Shen, "Towards energy-efficient wireless networking in the big data era: A survey," *IEEE Communications Surveys Tutorials*, vol. 20, no. 1, pp. 303–332, 2018.
- [30] L. Pierucci, "The quality of experience perspective toward 5G technology," *IEEE Wireless Comm.*, vol. 22, no. 4, pp. 10–16, 2015.
- [31] 3GPP, "3gpp specification series: 38 series."
- [32] E. Dahlman, S. Parkvall, and J. Skold, *5G NR: The Next Generation Wireless Access Technology*. Academic Press, Aug. 2018.
- [33] J. Wu, S. Guo, H. Huang, W. Liu, and Y. Xiang, "Information and communications technologies for sustainable development goals: State-of-the-art, needs and perspectives," *IEEE Communications Surveys Tutorials*, vol. 20, no. 3, pp. 2389–2406, 2018.
- [34] R. Mahapatra, Y. Nijssure, G. Kaddoum, N. Ul Hassan, and C. Yuen, "Energy efficiency tradeoff mechanism towards wireless green communication: A survey," *IEEE Communications Surveys Tutorials*, vol. 18, no. 1, pp. 686–705, 2016.
- [35] Y. Chen, S. Zhang, S. Xu, and G. Y. Li, "Fundamental trade-offs on green wireless networks," *IEEE Communications Magazine*, vol. 49, no. 6, pp. 30–37, 2011.
- [36] G. Y. Li, Z. Xu, C. Xiong, C. Yang, S. Zhang, Y. Chen, and S. Xu, "Energy-efficient wireless communications: tutorial, survey, and open issues," *IEEE Wireless Communications*, vol. 18, no. 6, pp. 28–35, 2011.
- [37] Z. Hasan, H. Boostanimehr, and V. K. Bhargava, "Green cellular networks: A survey, some research issues and challenges," *IEEE Communications Surveys Tutorials*, vol. 13, no. 4, pp. 524–540, 2011.
- [38] D. Feng, C. Jiang, G. Lim, L. J. Cimini, G. Feng, and G. Y. Li, "A survey of energy-efficient wireless communications," *IEEE Communications Surveys and Tutorials*, vol. 15, no. 1, pp. 167–178, 2013.
- [39] A. De Domenico, E. Calvanese Strinati, and A. Capone, "Green cellular networks: A survey, some research issues and challenges," *Computer Communications*, vol. 37, pp. 5–24, 2014.
- [40] L. Budzisz, F. Ganji, G. Rizzo, M. Ajmone Marsan, M. Meo, Y. Zhang, G. Koutitas, L. Tassiulas, S. Lambert, B. Lannoo, M. Pickavet, A. Conte, I. Haratcherev, and A. Wolisz, "Dynamic resource provisioning for energy efficiency in wireless access networks: A survey and an outlook," *IEEE Communications Surveys Tutorials*, vol. 16, no. 4, pp. 2259–2285, 2014.
- [41] C.-L. I, C. Rowell, S. Han, Z. Xu, G. Li, and Z. Pan, "Toward green and soft: a 5g perspective," *IEEE Communications Magazine*, vol. 52, no. 2, pp. 66–73, 2014.
- [42] Q. Wu, G. Y. Li, W. Chen, D. W. K. Ng, and R. Schober, "An overview of sustainable green 5g networks," *IEEE Wireless Communications*, vol. 24, no. 4, pp. 72–80, 2017.
- [43] S. Zhang, Q. Wu, S. Xu, and G. Y. Li, "Fundamental green tradeoffs: Progresses, challenges, and impacts on 5g networks," *IEEE Communications Surveys and Tutorials*, vol. 19, no. 1, pp. 33–56, 2017.
- [44] A. Mughees, M. Tahir, M. A. Sheikh, and A. Ahad, "Towards energy efficient 5g networks using machine learning: Taxonomy, research challenges, and future research directions," *IEEE Access*, vol. 8, pp. 187 498–187 522, 2020.
- [45] Y. R. Li, M. Chen, J. Xu, L. Tian, and K. Huang, "Power saving techniques for 5g and beyond," *IEEE Access*, vol. 8, pp. 108 675–108 690, 2020.

- [46] Q. Nadeem, A. Kammoun, and M. Alouini, "Elevation Beamforming With Full Dimension MIMO Architectures in 5G Systems: A Tutorial," *IEEE Communications Surveys Tutorials*, vol. 21, no. 4, pp. 3238–3273, 2019.
- [47] F. Rusek *et al.*, "Scaling up MIMO: Opportunities and challenges with very large arrays," *IEEE Signal Process. Mag.*, vol. 30, no. 1, pp. 40–60, Jan. 2013.
- [48] X. Lin, J. Li, R. Baldemair, J. T. Cheng, S. Parkvall, D. C. Larsson, H. Koorapaty, M. Frenne, S. Falahati, A. Grovlen, and K. Werner, "5G New Radio: Unveiling the Essentials of the Next Generation Wireless Access Technology," *IEEE Communications Standards Magazine*, vol. 3, no. 3, pp. 30–37, 2019.
- [49] M. Fuentes, J. L. Carcel, C. Dietrich, L. Yu, E. Garro, V. Pauli, F. I. Lazarakis, O. Grøndalen, O. Bulakci, J. Yu, W. Mohr, and D. Gomez-Barquero, "5g new radio evaluation against imt-2020 key performance indicators," *IEEE Access*, vol. 8, pp. 110 880–110 896, 2020.
- [50] D. C. Nguyen *et al.*, "Wireless AI: Enabling an AI-Governed Data Life Cycle," *IEEE Commun. Surveys Tutorials*, 2020.
- [51] R. Ferrús, O. Sallent, and J. Perez-Romero, "Data Analytics Architectural Framework for Smarter Radio Resource Management in 5G Radio Access Networks," *IEEE Communications Magazine*, vol. 58, no. 5, pp. 98–104, 2020.
- [52] E. Pateromichelakis, F. Moggio, C. Mannweiler, P. Arnold, M. Shariat, M. Einhaus, Q. Wei, O. Bulakci, and A. De Domenico, "End-to-End Data Analytics Framework for 5G Architecture," *IEEE Access*, vol. 7, pp. 40 295–40 312, 2019.
- [53] M. Paolini, Senza Fili, "AI and machine learning: Why now? Network optimization in the age of 5G," 2019. Accessed on 18/10/2020. [Online]. Available: <https://www.intel.com/content/dam/www/public/us/en/documents/reports/ai-and-5g-report.pdf>
- [54] T. L. Marzetta, "Noncooperative Cellular Wireless with Unlimited Numbers of Base Station Antennas," *IEEE Transactions on Wireless Communications*, vol. 9, no. 11, pp. 3590–3600, 2010.
- [55] T. L. Marzetta, E. G. Larsson, H. Yang, and H. Q. Ngo, *Fundamentals of Massive MIMO*. Cambridge University Press, 2016.
- [56] E. Björnson, J. Hoydis, and L. Sanguinetti, "Massive mimo networks: Spectral, energy, and hardware efficiency," *Foundations and Trends® in Signal Processing*, vol. 11, no. 3-4, pp. 154–655, 2017.
- [57] C. Oestges and B. Clerckx, *MIMO Wireless Communications: From Real-World Propagation to Space-Time Code Design*. Academic Press, 2007.
- [58] H. Holma, D. A. Toskala, and T. Nakamura, *5G Technology : 3GPP New Radio*. John Wiley & Sons Ltd., Feb. 2020.
- [59] K. Zheng *et al.*, "Survey of large-scale MIMO systems," *IEEE Commun. Surveys Tutorials*, vol. 17, no. 3, pp. 1738–1760, Apr. 2015.
- [60] E. Dahlman, S. Parkvall, and J. Skold, *4G: LTE/LTE-Advanced for Mobile Broadband*. Academic Press, Oct. 2013.
- [61] P. Frenger, P. Moberg, J. Malmodin, Y. Jading, and I. Godor, "Reducing energy consumption in lte with cell dtx," in *2011 IEEE 73rd Vehicular Technology Conference (VTC Spring)*, 2011, pp. 1–5.
- [62] O. Blume, D. Zeller, and U. Barth, "Approaches to energy efficient wireless access networks," in *2010 4th International Symposium on Communications, Control and Signal Processing (ISCCSP)*, 2010, pp. 1–5.
- [63] Ajay R. Mishra, *Fundamentals of Network Planning and Optimisation 2G/3G/4G: Evolution to 5G*, 2nd ed. John Wiley & Sons Ltd., Jul. 2018.
- [64] P. Frenger and R. Tano, "More Capacity and Less Power: How 5G NR Can Reduce Network Energy Consumption," in *2019 IEEE 89th Vehicular Technology Conference (VTC2019-Spring)*, 2019, pp. 1–5.
- [65] Z. Niu, "TANGO: traffic-aware network planning and green operation," *IEEE Wireless Communications*, vol. 18, no. 5, pp. 25–29, 2011.
- [66] E. Oh, K. Son, and B. Krishnamachari, "Dynamic base station switching-on/off strategies for green cellular networks," *IEEE Transactions on Wireless Communications*, vol. 12, no. 5, pp. 2126–2136, 2013.

- [67] N. C. Luong, D. T. Hoang, S. Gong, D. Niyato, P. Wang, Y. Liang, and D. I. Kim, "Applications of deep reinforcement learning in communications and networking: A survey," *IEEE Communications Surveys Tutorials*, vol. 21, no. 4, pp. 3133–3174, 2019.
- [68] S. Hu, Y. Ouyang, Y. Yao, M. H. Fallah, and W. Lu, "A study of lte network performance based on data analytics and statistical modeling," in *2014 23rd Wireless and Optical Communication Conference (WOCC)*, 2014, pp. 1–6.
- [69] R. S. Sutton and A. G. Barto, *Reinforcement Learning: An Introduction*, 2nd ed. The MIT Press, 2018. [Online]. Available: <http://incompleteideas.net/book/the-book-2nd.html>
- [70] N. C. Thompson, K. Greenewald, K. Lee, and G. F. Manso, "The computational limits of deep learning," 2020.
- [71] 3GPP TSG RAN, "TR 38.801, Study on self evaluation towards IMT-2020 submission," *V16.1.0*, Sept. 2010.
- [72] 3GPP TSG SA, "TR 32.972, Telecommunication management; Study on system and functional aspects of energy efficiency in 5G networks," *V16.1.0*, Sept. 2019.
- [73] G. Auer, V. Giannini, C. Desset, I. Godor, P. Skillermark, M. Olsson, M. A. Imran, D. Sabella, M. J. Gonzalez, O. Blume, and A. Fehske, "How much energy is needed to run a wireless network?" *IEEE Wireless Communications*, vol. 18, no. 5, pp. 40–49, 2011.
- [74] D. López-Pérez, M. Ding, H. Claussen, and A. H. Jafari, "Towards 1 Gbps/UE in Cellular Systems: Understanding Ultra-Dense Small Cell Deployments," *IEEE Communications Surveys & Tutorials*, vol. 17, no. 4, pp. 2078–2101, 2015.
- [75] B. Chen, J. Chen, Y. Gao, and J. Zhang, "Coexistence of lte-laa and wi-fi on 5 ghz with corresponding deployment scenarios: A survey," *IEEE Communications Surveys Tutorials*, vol. 19, no. 1, pp. 7–32, 2017.
- [76] Hua Wang, C. Rosa, and K. I. Pedersen, "Dedicated carrier deployment in heterogeneous networks with inter-site carrier aggregation," in *2013 IEEE Wireless Communications and Networking Conference (WCNC)*, 2013, pp. 756–760.
- [77] C. Rosa, K. Pedersen, H. Wang, P. Michaelsen, S. Barbera, E. Malkamäki, T. Henttonen, and B. Sébire, "Dual connectivity for lte small cell evolution: functionality and performance aspects," *IEEE Communications Magazine*, vol. 54, no. 6, pp. 137–143, 2016.
- [78] K. I. Pedersen, F. Frederiksen, C. Rosa, H. Nguyen, L. G. U. Garcia, and Y. Wang, "Carrier aggregation for LTE-advanced: functionality and performance aspects," *IEEE Communications Magazine*, vol. 49, no. 6, pp. 89–95, 2011.
- [79] G. Yu, Q. Chen, R. Yin, H. Zhang, and G. Y. Li, "Joint Downlink and Uplink Resource Allocation for Energy-Efficient Carrier Aggregation," *IEEE Transactions on Wireless Communications*, vol. 14, no. 6, pp. 3207–3218, 2015.
- [80] S. Tombaz, P. Frenger, F. Athley, E. Semaan, C. Tidestav, and A. Furuskar, "Energy Performance of 5G-NX Wireless Access Utilizing Massive Beamforming and an Ultra-Lean System Design," in *2015 IEEE Global Communications Conference (GLOBECOM)*, 2015, pp. 1–7.
- [81] A. De Domenico, R. Gerzaguët, N. Cassiau, A. Clemente, R. D'Errico, C. Dehos, J. L. Gonzalez, D. Ktenas, L. Manat, V. Savin, and A. Siligaris, "Making 5g millimeter-wave communications a reality [industry perspectives]," *IEEE Wireless Communications*, vol. 24, no. 4, pp. 4–9, 2017.
- [82] E. Björnson, L. Sanguinetti, J. Hoydis, and M. Debbah, "Optimal design of energy-efficient multi-user mimo systems: Is massive mimo the answer?" *IEEE Transactions on Wireless Communications*, vol. 14, no. 6, pp. 3059–3075, 2015.
- [83] M. M. A. Hossain, C. Cavdar, E. Björnson, and R. Jäntti, "Energy Saving Game for Massive MIMO: Coping With Daily Load Variation," *IEEE Transactions on Vehicular Technology*, vol. 67, no. 3, pp. 2301–2313, 2018.
- [84] E. Björnson, L. Sanguinetti, J. Hoydis, and M. Debbah, "Designing multi-user mimo for energy efficiency: When is massive mimo the answer?" in *2014 IEEE Wireless Communications and Networking Conference (WCNC)*, 2014, pp. 242–247.
- [85] M. Fiorani, S. Tombaz, J. Martensson, B. Skubic, L. Wosinska, and P. Monti, "Modeling energy performance of C-RAN



- with optical transport in 5G network scenarios,” *IEEE/OSA Journal of Optical Communications and Networking*, vol. 8, no. 11, pp. B21–B34, 2016.
- [86] C. Rowell and Rohde & Schwarz, “Pillars of 5G: Spectral & Energy Efficiency,” *Microwave Journal*, pp. 182–184, 2020.
- [87] N. Nikaein, E. Schiller, R. Favraud, R. Knopp, I. Alyafawi, and T. Braun, *Towards a Cloud-Native Radio Access Network*. Cham: Springer International Publishing, 2017, pp. 171–202.
- [88] T. Sigwele, A. S. Alam, P. Pillai, and Y. F. Hu, “Energy-efficient cloud radio access networks by cloud based workload consolidation for 5g,” *Journal of Network and Computer Applications*, vol. 78, pp. 1 – 8, 2017.
- [89] A. Younis, T. X. Tran, and D. Pompili, “Bandwidth and Energy-Aware Resource Allocation for Cloud Radio Access Networks,” *IEEE Transactions on Wireless Communications*, vol. 17, no. 10, pp. 6487–6500, 2018.
- [90] D. Sabella, A. De Domenico, E. Katranaras, M. A. Imran, M. di Girolamo, U. Salim, M. Lalam, K. Samdanis, and A. Maeder, “Energy Efficiency Benefits of RAN-as-a-Service Concept for a Cloud-Based 5G Mobile Network Infrastructure,” *IEEE Access*, vol. 2, pp. 1586–1597, 2014.
- [91] J. K. Chaudhary, A. Kumar, J. Bartelt, and G. Fettweis, “C-ran employing xran functional split: Complexity analysis for 5g nr remote radio unit,” in *2019 European Conference on Networks and Communications (EuCNC)*, 2019, pp. 580–585.
- [92] S. Khatibi, K. Shah, and M. Roshdi, “Modelling of computational resources for 5G RAN,” in *Proc. EuCNC*, June 2018, pp. 1–5.
- [93] M. Fiorani, S. Tombaz, J. Mårtensson, B. Skubic, L. Wosinska, and P. Monti, “Energy performance of C-RAN with 5G-NX radio networks and optical transport,” in *IEEE International Conference on Communications (ICC)*, 2016, pp. 1–6.
- [94] A. Zappone and E. Jorswieck, “Energy efficiency in wireless networks via fractional programming theory,” *Foundations and Trends® in Communications and Information Theory*, vol. 11, no. 3-4, pp. 185–396, 2015.
- [95] ETSI TC EE, “ES 203 228, Environmental Engineering (EE); Assessment of mobile network energy efficiency,” *V1.3.1*, Oct. 2020.
- [96] 3GPP TSG RAN, “TR 38.913, Study on Scenarios and Requirements for Next Generation Access Technologies,” *V16.0.0*, July 2020.
- [97] 3GPP TSG SA, “TR 21.866, Study on Energy Efficiency Aspects of 3GPP Standards,” *V15.0.0*, June 2017.
- [98] Z. Yan, M. Peng, and C. Wang, “Economical Energy Efficiency: An Advanced Performance Metric for 5G Systems,” *IEEE Wireless Communications*, vol. 24, no. 1, pp. 32–37, 2017.
- [99] H. Peters, “Axiomatic bargaining game theory,” *Mathematical Programming and Operations Research*, W. Leinfellner and G. Eberlein, Eds. Kluwer Academic Publishers, vol. 9, 1992.
- [100] EU FP7 EARTH, “Deliverable D2.4, Most suitable efficiency metrics and utility functions,” Jan. 2012. Accessed on 18/10/2020. [Online]. Available: <https://cordis.europa.eu/docs/projects/cnect/3/247733/080/deliverables/001-EARTHWP2D24.pdf>
- [101] E. Björnson and E. G. Larsson, “How energy-efficient can a wireless communication system become?” in *2018 52nd Asilomar Conference on Signals, Systems, and Computers*. IEEE, 2018, pp. 1252–1256.
- [102] H. Q. Ngo, E. G. Larsson, and T. L. Marzetta, “Energy and spectral efficiency of very large multiuser mimo systems,” *IEEE Transactions on Communications*, vol. 61, no. 4, pp. 1436–1449, 2013.
- [103] E. Björnson, J. Hoydis, M. Kountouris, and M. Debbah, “Massive mimo systems with non-ideal hardware: Energy efficiency, estimation, and capacity limits,” *IEEE Transactions on Information Theory*, vol. 60, no. 11, pp. 7112–7139, 2014.

- [104] J. Hoydis, S. ten Brink, and M. Debbah, "Massive mimo in the ul/dl of cellular networks: How many antennas do we need?" *IEEE Journal on Selected Areas in Communications*, vol. 31, no. 2, pp. 160–171, 2013.
- [105] J. Tang, D. K. C. So, E. Alsusa, and K. A. Hamdi, "Resource efficiency: A new paradigm on energy efficiency and spectral efficiency tradeoff," *IEEE Transactions on Wireless Communications*, vol. 13, no. 8, pp. 4656–4669, 2014.
- [106] Y. Hao, Q. Ni, H. Li, and S. Hou, "Energy and spectral efficiency tradeoff with user association and power coordination in massive mimo enabled hetnets," *IEEE Communications Letters*, vol. 20, no. 10, pp. 2091–2094, 2016.
- [107] Y. Huang, S. He, J. Wang, and J. Zhu, "Spectral and energy efficiency tradeoff for massive mimo," *IEEE Transactions on Vehicular Technology*, vol. 67, no. 8, pp. 6991–7002, 2018.
- [108] L. You, J. Xiong, A. Zappone, W. Wang, and X. Gao, "Spectral efficiency and energy efficiency tradeoff in massive mimo downlink transmission with statistical csit," *IEEE Transactions on Signal Processing*, vol. 68, pp. 2645–2659, 2020.
- [109] Z. Liu, W. Du, and D. Sun, "Energy and spectral efficiency tradeoff for massive mimo systems with transmit antenna selection," *IEEE Transactions on Vehicular Technology*, vol. 66, no. 5, pp. 4453–4457, 2017.
- [110] J. Choi, D. J. Love, and P. Bidigare, "Downlink training techniques for fdd massive mimo systems: Open-loop and closed-loop training with memory," *IEEE Journal of Selected Topics in Signal Processing*, vol. 8, no. 5, pp. 802–814, 2014.
- [111] X. Gao, B. Jiang, X. Li, A. B. Gershman, and M. R. McKay, "Statistical eigenmode transmission over jointly correlated mimo channels," *IEEE Transactions on Information Theory*, vol. 55, no. 8, pp. 3735–3750, 2009.
- [112] E. V. Belmega and S. Lasaulce, "Energy-efficient precoding for multiple-antenna terminals," *IEEE Transactions on Signal Processing*, vol. 59, no. 1, pp. 329–340, 2011.
- [113] V. S. Varma, S. Lasaulce, M. Debbah, and S. E. Elayoubi, "an energy-efficient framework for the analysis of mimo slow fading channels," *IEEE Transactions on Signal Processing*.
- [114] L. Liu, G. Miao, and J. Zhang, "Energy-efficient scheduling for downlink multi-user mimo," in *2012 IEEE International Conference on Communications (ICC)*, 2012, pp. 4394–4394.
- [115] J. Mao, J. Gao, Y. Liu, and G. Xie, "Simplified semi-orthogonal user selection for mu-mimo systems with zfbf," *IEEE Wireless Communications Letters*, vol. 1, no. 1, pp. 42–45, 2012.
- [116] X. Zhang, S. Zhou, Z. Niu, and X. Lin, "An energy-efficient user scheduling scheme for multiuser mimo systems with rf chain sleeping," in *2013 IEEE Wireless Communications and Networking Conference (WCNC)*, 2013, pp. 169–174.
- [117] H. Li, H. Zhang, D. Li, Y. Liu, and A. Nallanathan, "Joint antenna selection and user scheduling in downlink multi-user mimo systems," in *2018 IEEE 4th International Conference on Computer and Communications (ICCC)*, 2018, pp. 1072–1076.
- [118] H. Lee and A. Paulraj, "Mimo systems based on modulation diversity," *IEEE Transactions on Communications*, vol. 58, no. 12, pp. 3405–3409, 2010.
- [119] A. He, S. Srikanteswara, K. K. Bae, T. R. Newman, J. H. Reed, W. H. Tranter, M. Sajadieh, and M. Verhelst, "Power consumption minimization for mimo systems — a cognitive radio approach," *IEEE Journal on Selected Areas in Communications*, vol. 29, no. 2, pp. 469–479, 2011.
- [120] M. Di Renzo, H. Haas, A. Ghayeb, S. Sugiura, and L. Hanzo, "Spatial modulation for generalized mimo: Challenges, opportunities, and implementation," *Proceedings of the IEEE*, vol. 102, no. 1, pp. 56–103, 2014.
- [121] M. Haenggi, *Stochastic geometry for wireless networks*. Cambridge University Press, 2012.
- [122] J. Andrews, F. Baccelli, and R. Ganti, "A tractable approach to coverage and rate in cellular networks," *IEEE Transactions on Communications*, vol. 59, no. 11, pp. 3122–3134, Nov. 2011.
- [123] H. Dhillon, R. Ganti, F. Baccelli, and J. Andrews, "Modeling and analysis of K-tier downlink heterogeneous cellular networks," *IEEE Journal on Selected Areas in Communications*, vol. 30, no. 3, pp. 550–560, Apr. 2012.

- [124] T. Bai and R. W. Heath, "Coverage and Rate Analysis for Millimeter-Wave Cellular Networks," *IEEE Transactions on Wireless Communications*, vol. 14, no. 2, pp. 1100–1114, Feb. 2015.
- [125] M. Ding, P. Wang, D. López-Pérez, G. Mao, and Z. Lin, "Performance impact of LoS and NLoS transmissions in dense cellular networks," *IEEE Transactions on Wireless Communications*, vol. 15, no. 3, pp. 2365–2380, Mar. 2016.
- [126] T. Bai and R. W. Heath, "Analyzing uplink sinr and rate in massive mimo systems using stochastic geometry," *IEEE Transactions on Communications*, vol. 64, no. 11, pp. 4592–4606, 2016.
- [127] Q. Zhang, H. H. Yang, T. Q. S. Quek, and J. Lee, "Heterogeneous cellular networks with los and nlos transmissions—the role of massive mimo and small cells," *IEEE Transactions on Wireless Communications*, vol. 16, no. 12, pp. 7996–8010, 2017.
- [128] P. Parida and H. S. Dhillon, "Stochastic geometry-based uplink analysis of massive mimo systems with fractional pilot reuse," *IEEE Transactions on Wireless Communications*, vol. 18, no. 3, pp. 1651–1668, 2019.
- [129] E. Björnson, L. Sanguinetti, and M. Kountouris, "Deploying dense networks for maximal energy efficiency: Small cells meet massive mimo," *IEEE Journal on Selected Areas in Communications*, vol. 34, no. 4, pp. 832–847, 2016.
- [130] Y. Xin, D. Wang, J. Li, H. Zhu, J. Wang, and X. You, "Area Spectral Efficiency and Area Energy Efficiency of Massive MIMO Cellular Systems," *IEEE Transactions on Vehicular Technology*, vol. 65, no. 5, pp. 3243–3254, 2016.
- [131] E. Björnson, L. Sanguinetti, and M. Kountouris, "Designing wireless broadband access for energy efficiency: Are small cells the only answer?" in *2015 IEEE International Conference on Communication Workshop (ICCW)*, 2015, pp. 136–141.
- [132] A. Zappone, L. Sanguinetti, G. Bacci, E. Jorswieck, and M. Debbah, "Energy-efficient power control: A look at 5g wireless technologies," *IEEE Transactions on Signal Processing*, vol. 64, no. 7, pp. 1668–1683, 2016.
- [133] A. Zappone, E. Björnson, L. Sanguinetti, and E. Jorswieck, "Globally optimal energy-efficient power control and receiver design in wireless networks," *IEEE Transactions on Signal Processing*, vol. 65, no. 11, pp. 2844–2859, 2017.
- [134] 3GPP TSG RAN, "TR 37.910, Study on new radio access technology: Radio access architecture and interfaces," *V14.0.0*, Mar. 2017.
- [135] W. Yang, K. Lin, and H. Wei, "5g on-demand si acquisition framework and performance evaluation," *IEEE Access*, vol. 7, pp. 163 245–163 261, 2019.
- [136] B. Debaillie, C. Desset, and F. Louagie, "A flexible and future-proof power model for cellular base stations," in *IEEE 81st Vehicular Technology Conference (VTC Spring)*, 2015, pp. 1–7.
- [137] F. E. Salem, T. Chahed, Z. Altman, and A. Gati, "Traffic-aware Advanced Sleep Modes management in 5G networks," in *2019 IEEE Wireless Communications and Networking Conference (WCNC)*, 2019, pp. 1–6.
- [138] F. E. Salem, "Management of advanced sleep modes for energy-efficient 5G networks," Theses, Institut Polytechnique de Paris, Dec. 2019. [Online]. Available: <https://tel.archives-ouvertes.fr/tel-02500618>
- [139] S. Tombaz, P. Frenger, M. Olsson, and A. Nilsson, "Energy performance of 5g-nx radio access at country level," in *2016 IEEE 12th International Conference on Wireless and Mobile Computing, Networking and Communications (WiMob)*, 2016, pp. 1–6.
- [140] F. E. Salem, A. Gati, Z. Altman, and T. Chahed, "Advanced Sleep Modes and Their Impact on Flow-Level Performance of 5G Networks," in *2017 IEEE 86th Vehicular Technology Conference (VTC-Fall)*, 2017, pp. 1–7.
- [141] R. Tano, M. Tran, and P. Frenger, "KPI Impact on 5G NR Deep Sleep State Adaption," in *IEEE 90th Vehicular Technology Conference (VTC2019-Fall)*, 2019, pp. 1–5.
- [142] Orange, "RP-190326, NR enhancements for Advanced Sleep Modes," *3GPP RAN #83*, Mar. 2019.
- [143] 3GPP TSG RAN, "TR 36.927, Potential solutions for energy saving for E-UTRAN," *V16.0.0*, July 2020.
- [144] T. Beitelmal, S. S. Szyszkowicz, D. G. González, and H. Yanikomeroglu, "Sector and site switch-off regular patterns

- for energy saving in cellular networks,” *IEEE Transactions on Wireless Communications*, vol. 17, no. 5, pp. 2932–2945, 2018.
- [145] X. Lin, D. Yu, and H. Wiemann, “A primer on bandwidth parts in 5g new radio,” *arXiv preprint arXiv:2004.00761*, 2020.
  - [146] T. Kim, Y. Kim, Q. Lin, F. Sun, J. Fu, Y. Kim, A. Papasakellariou, H. Ji, and J. Lee, “Evolution of Power Saving Technologies for 5G New Radio,” *IEEE Access*, vol. 8, pp. 198 912–198 924, 2020.
  - [147] M. Feng, S. Mao, and T. Jiang, “Base Station ON-OFF Switching in 5G Wireless Networks: Approaches and Challenges,” *IEEE Wireless Communications*, vol. 24, no. 4, pp. 46–54, 2017.
  - [148] —, “BOOST: Base Station on-off Switching Strategy for Green Massive MIMO HetNets,” *IEEE Transactions on Wireless Communications*, vol. 16, no. 11, pp. 7319–7332, 2017.
  - [149] L. Chiaraviglio, F. Cuomo, M. Listanti, E. Manzia, and M. Santucci, “Fatigue-Aware Management of Cellular Networks Infrastructure with Sleep Modes,” *IEEE Transactions on Mobile Computing*, vol. 16, no. 11, pp. 3028–3041, 2017.
  - [150] H. Celebi, Y. Yapici, I. Guvenç, and H. Schulzrinne, “Load-Based On/Off Scheduling for Energy-Efficient Delay-Tolerant 5G Networks,” *IEEE Transactions on Green Communications and Networking*, vol. 3, no. 4, pp. 955–970, 2019.
  - [151] N. Saxena, A. Roy, and H. Kim, “Traffic-Aware Cloud RAN: A Key for Green 5G Networks,” *IEEE Journal on Selected Areas in Communications*, vol. 34, no. 4, pp. 1010–1021, 2016.
  - [152] Z. Niu, Y. Wu, J. Gong, and Z. Yang, “Cell zooming for cost-efficient green cellular networks,” *IEEE Communications Magazine*, vol. 48, no. 11, pp. 74–79, 2010.
  - [153] A. Conte, A. Feki, L. Chiaraviglio, D. Ciullo, M. Meo, and M. A. Marsan, “Cell wilting and blossoming for energy efficiency,” *IEEE Wireless Communications*, vol. 18, no. 5, pp. 50–57, 2011.
  - [154] H. Jiang, S. Yi, L. Wu, H. Leung, Y. Wang, X. Zhou, Y. Chen, and L. Yang, “Data-Driven Cell Zooming for Large-Scale Mobile Networks,” *IEEE Transactions on Network and Service Management*, vol. 15, no. 1, pp. 156–168, 2018.
  - [155] G. Vallero, D. Renga, M. Meo, and M. A. Marsan, “Greener RAN Operation Through Machine Learning,” *IEEE Transactions on Network and Service Management*, vol. 16, no. 3, pp. 896–908, 2019.
  - [156] 3GPP TSG SA, “TS 28.310, Management and orchestration; Energy efficiency of 5G ,” *V16.2.0*, Sept. 2020.
  - [157] 3GPP TSG RAN, “TR 37.816, Study on RAN-centric data collection and utilization for LTE and NR,” *V16.0.0*, July 2019.
  - [158] K. N. R. S. V. Prasad, E. Hossain, and V. K. Bhargava, “Energy efficiency in massive mimo-based 5g networks: Opportunities and challenges,” *IEEE Wireless Communications*, vol. 24, no. 3, pp. 86–94, 2017.
  - [159] S. Asaad, A. M. Rabiei, and R. R. Müller, “Massive MIMO With Antenna Selection: Fundamental Limits and Applications,” *IEEE Transactions on Wireless Communications*, vol. 17, no. 12, pp. 8502–8516, 2018.
  - [160] X. Gao, O. Edfors, J. Liu, and F. Tufvesson, “Antenna selection in measured massive MIMO channels using convex optimization,” in *IEEE Globecom Workshops (GC Wkshps)*, 2013, pp. 129–134.
  - [161] J. Xu and L. Qiu, “Energy efficiency optimization for mimo broadcast channels,” *IEEE Transactions on Wireless Communications*, vol. 12, no. 2, pp. 690–701, 2013.
  - [162] N. P. Le, F. Safaei, and L. C. Tran, “Antenna selection strategies for mimo-ofdm wireless systems: An energy efficiency perspective,” *IEEE Transactions on Vehicular Technology*, vol. 65, no. 4, pp. 2048–2062, 2016.
  - [163] B. Makki, A. Ide, T. Svensson, T. Eriksson, and M. Alouini, “A genetic algorithm-based antenna selection approach for large-but-finite mimo networks,” *IEEE Transactions on Vehicular Technology*, vol. 66, no. 7, pp. 6591–6595, 2017.
  - [164] B.-J. Lee, S.-L. Ju, N.-I. Kim, and K.-S. Kim, “Enhanced Transmit-Antenna Selection Schemes for Multiuser Massive MIMO Systems,” *Wireless Communications and Mobile Computing*, Jun. 2017.
  - [165] M. Arash, E. Yazdian, Mohammad, S. Fazel, G. Brante, and M. A. Imran, “Employing antenna selection to improve energy-efficiency in massive MIMO systems,” *Wireless Communications and Mobile Computing*, Aug. 2017.

- [166] K. Senel, E. Björnson, and E. G. Larsson, "Joint Transmit and Circuit Power Minimization in Massive MIMO With Downlink SINR Constraints: When to Turn on Massive MIMO?" *IEEE Transactions on Wireless Communications*, vol. 18, no. 3, pp. 1834–1846, 2019.
- [167] W. Pramudito, E. Alsusa, A. Al-Dweik, K. A. Hamdi, D. K. C. So, and T. L. Marzetta, "Load-Aware Energy Efficient Adaptive Large Scale Antenna System," *IEEE Access*, vol. 8, pp. 82 592–82 606, 2020.
- [168] Y. Li, "Deep Reinforcement Learning," *CoRR*, vol. abs/1810.06339, October 2018. [Online]. Available: <http://arxiv.org/abs/1810.06339>
- [169] T. O'Shea and J. Hoydis, "An introduction to deep learning for the physical layer," *IEEE Transactions on Cognitive Communications and Networking*, vol. 3, no. 4, pp. 563–575, 2017.
- [170] D. L. Jagerman, B. Melamed, and W. Willinger, "Stochastic modeling of traffic processes," *Frontiers in queueing*, pp. 271–370, 1997.
- [171] R. J. Hyndman and G. Athanasopoulos, *Forecasting: principles and practice*. OTexts, 2018.
- [172] A. Azari, P. Papapetrou, S. Denic, and G. Peters, "Cellular traffic prediction and classification: A comparative evaluation of lstm and arima," in *Discovery Science*, P. Kralj Novak, T. Šmuc, and S. Džeroski, Eds. Springer International Publishing, 2019, pp. 129–144.
- [173] F. Martínez, M. P. Frías, M. D. Pérez, and A. J. Rivera, "A methodology for applying k-nearest neighbor to time series forecasting," *Artificial Intelligence Review*, vol. 52, no. 3, 2019.
- [174] C.-H. Wu, J.-M. Ho, and D.-T. Lee, "Travel-time prediction with support vector regression," *IEEE transactions on intelligent transportation systems*, vol. 5, no. 4, pp. 276–281, 2004.
- [175] S. Hochreiter and J. Schmidhuber, "Long short-term memory," *Neural computation*, vol. 9, no. 8, pp. 1735–1780, 1997.
- [176] X. Zhang and J. You, "A gated dilated causal convolution based encoder-decoder for network traffic forecasting," *IEEE Access*, vol. 8, pp. 6087–6097, 2020.
- [177] A. Vaswani, N. Shazeer, N. Parmar, J. Uszkoreit, L. Jones, A. N. Gomez, u. Kaiser, and I. Polosukhin, "Attention is all you need," ser. NIPS'17. Red Hook, NY, USA: Curran Associates Inc., 2017, p. 6000–6010.
- [178] X. Wang, Z. Zhou, F. Xiao, K. Xing, Z. Yang, Y. Liu, and C. Peng, "Spatio-temporal analysis and prediction of cellular traffic in metropolis," *IEEE Transactions on Mobile Computing*, vol. 18, no. 9, pp. 2190–2202, 2019.
- [179] M. S. Hossain and G. Muhammad, "A deep-tree-model-based radio resource distribution for 5g networks," *IEEE Wireless Communications*, vol. 27, no. 1, pp. 62–67, 2020.
- [180] J. Wang, J. Tang, Z. Xu, Y. Wang, G. Xue, X. Zhang, and D. Yang, "Spatiotemporal modeling and prediction in cellular networks: A big data enabled deep learning approach," in *IEEE INFOCOM 2017 - IEEE Conference on Computer Communications*, 2017, pp. 1–9.
- [181] I. Goodfellow, Y. Bengio, A. Courville, and Y. Bengio, *Deep learning*. MIT press Cambridge, 2016, vol. 1, no. 2.
- [182] X. Shi, Z. Chen, H. Wang, D.-Y. Yeung, W.-K. Wong, and W.-c. Woo, "Convolutional lstm network: A machine learning approach for precipitation nowcasting," *Advances in neural information processing systems*, vol. 28, pp. 802–810, 2015.
- [183] C. Zhang, H. Zhang, D. Yuan, and M. Zhang, "Citywide cellular traffic prediction based on densely connected convolutional neural networks," *IEEE Communications Letters*, vol. 22, no. 8, pp. 1656–1659, 2018.
- [184] C. Zhang and P. Patras, "Long-term mobile traffic forecasting using deep spatio-temporal neural networks," in *Proceedings of the Eighteenth ACM International Symposium on Mobile Ad Hoc Networking and Computing*. New York, NY, USA: Association for Computing Machinery, 2018, p. 231–240. [Online]. Available: <https://doi.org/10.1145/3209582.3209606>
- [185] F. Xu, Y. Li, H. Wang, P. Zhang, and D. Jin, "Understanding mobile traffic patterns of large scale cellular towers in urban environment," *IEEE/ACM Transactions on Networking*, vol. 25, no. 2, pp. 1147–1161, 2017.

- [186] C. Zhang, H. Zhang, J. Qiao, D. Yuan, and M. Zhang, "Deep transfer learning for intelligent cellular traffic prediction based on cross-domain big data," *IEEE Journal on Selected Areas in Communications*, vol. 37, no. 6, pp. 1389–1401, 2019.
- [187] X. Wang, T. Yang, Y. Cui, Y. Jin, and H. Wang, "Bsenet: A data-driven spatio-temporal representation learning for base station embedding," *IEEE Access*, vol. 8, pp. 51 674–51 683, 2020.
- [188] P. V. Klaine, M. A. Imran, O. Onireti, and R. D. Souza, "A survey of machine learning techniques applied to self-organizing cellular networks," *IEEE Communications Surveys Tutorials*, vol. 19, no. 4, pp. 2392–2431, 2017.
- [189] K. Arulkumaran, M. P. Deisenroth, M. Brundage, and A. A. Bharath, "Deep Reinforcement Learning: A Brief Survey," *IEEE Signal Processing Magazine*, vol. 34, no. 6, pp. 26–38, 2017.
- [190] T. Jaakkola, M. I. Jordan, and S. P. Singh, "On the convergence of stochastic iterative dynamic programming algorithms," *Neural Computation*, vol. 6, no. 6, pp. 1185–1201, 1994.
- [191] A. De Domenico and D. Kténas, "Reinforcement learning for interference-aware cell dtx in heterogeneous networks," in *2018 IEEE Wireless Communications and Networking Conference (WCNC)*, 2018, pp. 1–6.
- [192] L. Zadeh, "The concept of a linguistic variable and its application to approximate reasoning—i," *Information Sciences*, vol. 8, no. 3, pp. 199 – 249, 1975.
- [193] V. Mnih, K. Kavukcuoglu, D. Silver, A. A. Rusu, J. Veness, M. G. Bellemare, A. Graves, M. Riedmiller, A. K. Fidjeland, G. Ostrovski, S. Petersen, C. Beattie, A. Sadik, I. Antonoglou, H. King, D. Kumaran, D. Wierstra, S. Legg, and D. Hassabis, "Human-level control through deep reinforcement learning," *Nature*, vol. 518, no. 7540, pp. 529–533, 2015.
- [194] J. Liu, B. Krishnamachari, S. Zhou, and Z. Niu, "DeepNap: Data-Driven Base Station Sleeping Operations Through Deep Reinforcement Learning," *IEEE Internet of Things Journal*, vol. 5, no. 6, pp. 4273–4282, 2018.
- [195] T. Schaul, J. Quan, I. Antonoglou, and D. Silver, "Prioritized experience replay," in *International Conference on Learning Representations*, Puerto Rico, 2016.
- [196] J. Ye and Y. J. A. Zhang, "Drag: Deep reinforcement learning based base station activation in heterogeneous networks," *IEEE Transactions on Mobile Computing*, vol. 19, no. 9, pp. 2076–2087, 2020.
- [197] T. P. Lillicrap, J. J. Hunt, A. Pritzel, N. Heess, T. Erez, Y. Tassa, D. Silver, and D. Wierstra, "Continuous control with deep reinforcement learning," 2019.
- [198] M. Di Renzo, S. Wang, and X. Xi, "Inhomogeneous double thinning—modeling and analysis of cellular networks by using inhomogeneous poisson point processes," *IEEE Transactions on Wireless Communications*, vol. 17, no. 8, pp. 5162–5182, 2018.
- [199] Q. Cui, X. Yu, Y. Wang, and M. Haenggi, "The sir meta distribution in poisson cellular networks with base station cooperation," *IEEE Transactions on Communications*, vol. 66, no. 3, pp. 1234–1249, 2018.
- [200] S. Wang and M. Di Renzo, "On the mean interference-to-signal ratio in spatially correlated cellular networks," *IEEE Wireless Communications Letters*, vol. 9, no. 3, pp. 358–362, 2020.
- [201] G. Ghatak, A. De Domenico, and M. Coupechoux, "Coverage analysis and load balancing in hetnets with millimeter wave multi-rat small cells," *IEEE Transactions on Wireless Communications*, vol. 17, no. 5, pp. 3154–3169, 2018.
- [202] G. Caire, "On the ergodic rate lower bounds with applications to massive mimo," *IEEE Transactions on Wireless Communications*, vol. 17, no. 5, pp. 3258–3268, 2018.
- [203] M. J. Nawrocki, M. Dohler, and A. H. Aghvami, *Understanding UMTS Radio Network Modelling, Planning and Automated Optimisation: Theory and Practice*, 1st ed. John Wiley & Sons Ltd., Apr. 2006.
- [204] J. Laiho, A. Wacker, and T. Novosad, *Radio Network Planning and Optimisation for UMTS*, 2nd ed. John Wiley & Sons Ltd., Feb. 2006.
- [205] J. T. J. Penttinen, *5G Network Planning and Optimization*, 2019, pp. 255–269.

- [206] L. Wan, Z. Guo, and X. Chen, "Enabling efficient 5g nr and 4g lte coexistence," *IEEE Wireless Communications*, vol. 26, no. 1, pp. 6–8, 2019.
- [207] O. N. C. Yilmaz, O. Teyeb, and A. Orsino, "Overview of lte-nr dual connectivity," *IEEE Communications Magazine*, vol. 57, no. 6, pp. 138–144, 2019.
- [208] D. López-Pérez, J. Ling, B. H. Kim, V. Subramanian, S. Kanugovi, and M. Ding, "Boosted wifi through lte small cells: The solution for an all-wireless enterprise," in *2016 IEEE 27th Annual International Symposium on Personal, Indoor, and Mobile Radio Communications (PIMRC)*, 2016, pp. 1–6.
- [209] D. López-Pérez, M. Ding, H. Claussen, and A. H. Jafari, "Towards 1 gbps/ue in cellular systems: Understanding ultra-dense small cell deployments," *IEEE Communications Surveys Tutorials*, vol. 17, no. 4, pp. 2078–2101, 2015.
- [210] M. Giordani, M. Polese, A. Roy, D. Castor, and M. Zorzi, "A tutorial on beam management for 3gpp nr at mmwave frequencies," *IEEE Communications Surveys Tutorials*, vol. 21, no. 1, pp. 173–196, 2019.
- [211] A. Mohamed, O. Onireti, M. A. Imran, A. Imran, and R. Tafazolli, "Control-data separation architecture for cellular radio access networks: A survey and outlook," *IEEE Communications Surveys Tutorials*, vol. 18, no. 1, pp. 446–465, 2016.
- [212] N. Shlezinger, J. Whang, Y. C. Eldar, and A. G. Dimakis, "Model-based deep learning," 2020.
- [213] A. Zappone, M. Di Renzo, and M. Debbah, "Wireless networks design in the era of deep learning: Model-based, ai-based, or both?" *IEEE Transactions on Communications*, vol. 67, no. 10, pp. 7331–7376, 2019.
- [214] R. Schwartz, J. Dodge, N. A. Smith, and O. Etzioni, "Green ai," *Commun. ACM*, vol. 63, no. 12, p. 54–63, Nov. 2020. [Online]. Available: <https://doi.org/10.1145/3381831>
- [215] A. Krizhevsky, I. Sutskever, and G. E. Hinton, "Imagenet classification with deep convolutional neural networks," in *Advances in Neural Information Processing Systems*, F. Pereira, C. J. C. Burges, L. Bottou, and K. Q. Weinberger, Eds., vol. 25. Curran Associates, Inc., 2012, pp. 1097–1105. [Online]. Available: <https://proceedings.neurips.cc/paper/2012/file/c399862d3b9d6b76c8436e924a68c45b-Paper.pdf>
- [216] D. Silver, T. Hubert, J. Schrittwieser, I. Antonoglou, M. Lai, A. Guez, M. Lanctot, L. Sifre, D. Kumaran, T. Graepel *et al.*, "A general reinforcement learning algorithm that masters chess, shogi, and go through self-play," *Science*, vol. 362, no. 6419, pp. 1140–1144, 2018.
- [217] E. Strubell, A. Ganesh, and A. McCallum, "Energy and policy considerations for deep learning in NLP," in *Proceedings of the 57th Annual Meeting of the Association for Computational Linguistics*. Florence, Italy: Association for Computational Linguistics, Jul. 2019, pp. 3645–3650. [Online]. Available: <https://www.aclweb.org/anthology/P19-1355>
- [218] P. Kairouz and H. B. McMahan, "Advances and open problems in federated learning," *Foundations and Trends® in Machine Learning*, vol. 14, no. 1, pp. –, 2021. [Online]. Available: <http://dx.doi.org/10.1561/22000000083>
- [219] Y. Deng, "Deep Learning on Mobile Devices: a Review," in *Mobile Multimedia/Image Processing, Security, and Applications*, vol. 10993. International Society for Optics and Photonics, 2019, p. 109930A.
- [220] J. Lee, N. Chirkov, E. Ignasheva, Y. Pisarchyk, M. Shieh, F. Riccardi, R. Sarokin, A. Kulik, and M. Grundmann, "On-device Neural Net Inference with Mobile GPUs," *arXiv preprint arXiv:1907.01989*, 2019.
- [221] L. Prechelt, *Early Stopping — But When?* Berlin, Heidelberg: Springer Berlin Heidelberg, 2012, pp. 53–67.
- [222] N. Piovesan, A. F. Gambin, M. Miozzo, M. Rossi, and P. Dini, "Energy sustainable paradigms and methods for future mobile networks: A survey," *Computer Communications*, vol. 119, pp. 101–117, 2018.
- [223] Q. Wu, G. Y. Li, W. Chen, D. W. K. Ng, and R. Schober, "An overview of sustainable green 5g networks," *IEEE Wireless Communications*, vol. 24, no. 4, pp. 72–80, 2017.
- [224] N. Piovesan and P. Dini, "Optimal direct load control of renewable powered small cells: A shortest path approach," *Internet Technology Letters*, vol. 1, no. 1, p. e7, 2018.

- [225] J. Gong, J. S. Thompson, S. Zhou, and Z. Niu, "Base station sleeping and resource allocation in renewable energy powered cellular networks," *IEEE Transactions on Communications*, vol. 62, no. 11, pp. 3801–3813, 2014.
- [226] N. Piovesan, D. López-Pérez, M. Miozzo, and P. Dini, "Joint load control and energy sharing for renewable powered small base stations: a machine learning approach," *IEEE Transactions on Green Communications and Networking*, pp. 1–1, 2020.
- [227] H. Li, H. Gao, T. Lv, and Y. Lu, "Deep q-learning based dynamic resource allocation for self-powered ultra-dense networks," in *2018 IEEE International Conference on Communications Workshops (ICC Workshops)*. IEEE, 2018, pp. 1–6.
- [228] M. Mendil, A. De Domenico, V. Heiries, R. Caire, and N. Hadjsaid, "Battery-aware optimization of green small cells: Sizing and energy management," *IEEE Transactions on Green Communications and Networking*, vol. 2, no. 3, pp. 635–651, 2018.